Cold In-Place Recycling Project Selection and Guidance for Iowa Roadways

Final Report
July 2023

IOWA STATE UNIVERSITY
Institute for Transportation

Sponsored by
Iowa Highway Research Board
(IHRB Project TR-774)
Iowa Department of Transportation
(InTrans Project 19-695)

About the Asphalt Materials and Pavements Program

The Asphalt Materials and Pavements Program (AMPP) at InTrans specializes in improving asphalt materials and pavements through research and technology transfer and in developing students' technical skills in asphalt.

About the Institute for Transportation

The mission of the Institute for Transportation (InTrans) at Iowa State University is to save lives and improve economic vitality through discovery, research innovation, outreach, and the implementation of bold ideas.

Iowa State University Nondiscrimination Statement

Iowa State University does not discriminate on the basis of race, color, age, ethnicity, religion, national origin, pregnancy, sexual orientation, gender identity, genetic information, sex, marital status, disability, or status as a US veteran. Inquiries regarding nondiscrimination policies may be directed to the Office of Equal Opportunity, 3410 Beardshear Hall, 515 Morrill Road, Ames, Iowa 50011, telephone: 515-294-7612, hotline: 515-294-1222, email: eooffice@iastate.edu.

Disclaimer Notice

The contents of this report reflect the views of the authors, who are responsible for the facts and the accuracy of the information presented herein. The opinions, findings and conclusions expressed in this publication are those of the authors and not necessarily those of the sponsors.

The sponsors assume no liability for the contents or use of the information contained in this document. This report does not constitute a standard, specification, or regulation.

The sponsors do not endorse products or manufacturers. Trademarks or manufacturers' names appear in this report only because they are considered essential to the objective of the document.

Iowa DOT Statements

Federal and state laws prohibit employment and/or public accommodation discrimination on the basis of age, color, creed, disability, gender identity, national origin, pregnancy, race, religion, sex, sexual orientation or veteran's status. If you believe you have been discriminated against, please contact the Iowa Civil Rights Commission at 800-457-4416 or the Iowa Department of Transportation affirmative action officer. If you need accommodations because of a disability to access the Iowa Department of Transportation's services, contact the agency's affirmative action officer at 800-262-0003.

The preparation of this report was financed in part through funds provided by the Iowa Department of Transportation through its "Second Revised Agreement for the Management of Research Conducted by Iowa State University for the Iowa Department of Transportation" and its amendments.

The opinions, findings, and conclusions expressed in this publication are those of the authors and not necessarily those of the Iowa Department of Transportation.

Technical Report Documentation Page

1. Report No.	2. Government Accession No.	3. Recipient's Catalog No.	
IHRB Project TR-774			
4. Title and Subtitle Cold In-Place Recycling Project Selection and Guidance for Iowa Roadways		**5. Report Date** July 2023 6. Performing Organization Code	
7. Author(s) Ashley Buss (orcid.org/0000-0002-8563-9553), Irvin Pinto (orcid.org/0000-0003-0311-4049), Hosin "David" Lee (orcid.org/0000-0001-9766-1232), Byungkyu Moon (orcid.org/0000-0002-4213-0773), Charles T. Jahren (orcid.org/0000-0003-2828-8483), Yuhan Zhang (orcid.org/0000-0002-7892-0689), and Xinyu Hu (orcid.org/0009-0000-1440-715X)		**8. Performing Organization Report No.** InTrans Project 19-695	
9. Performing Organization Name and Address Institute for Transportation Iowa State University 2711 South Loop Drive, Suite 4700 Ames, IA 50010-8664		**10. Work Unit No. (TRAIS)** **11. Contract or Grant No.**	
12. Sponsoring Organization Name and Address Iowa Highway Research Board Iowa Department of Transportation 800 Lincoln Way Ames, IA 50010		**13. Type of Report and Period Covered** Final Report **14. Sponsoring Agency Code** IHRB Project TR-774	
15. Supplementary Notes Visit https://intrans.iastate.edu for color pdfs of this and other research reports.			

16. Abstract

Cold in-place recycling (CIR) involves cold milling 3 to 4 in. of a deteriorated asphalt pavement, processing and stabilizing the millings, and relaying, compacting, curing, and covering with a hot-mix asphalt (HMA) overlay or (rarely in Iowa) a bituminous surface treatment. This report documents an investigation of CIR projects in Iowa with the objective of understanding CIR pavement deterioration processes so that improvements can be made in project selection, design, construction, and maintenance. Multiple research methods were used, including a literature review, a meta-analysis of the literature, database analysis, recovery of field pavement cores and milling samples, laboratory testing, and development of conclusions and recommendations.

Analysis of 44 CIR pavement projects from the Iowa Pavement Management Information System database showed that rutting was the distress that triggered performance concerns first, followed by longitudinal wheel path cracking and transverse cracking. Pavement distress indices typically dropped below trigger values 10 to 15 years after CIR rehabilitation, and thicker CIR and HMA layers were associated with better performance outcomes.

Laboratory testing of field cores recovered from an Iowa CIR pavement with performance issues confirmed that the flexibility of the CIR pavement layers was greater than that of the overlaid HMA layers. Since CIR layers have a relatively high air void ratio, a possible deterioration process was postulated where heavy wheel loads cause compaction rutting in the CIR layer, which in turn causes the less flexible HMA layer to longitudinally crack in the wheel path after it is forced to conform to the rutted CIR cross section. Resulting recommendations are to specify a more flexible HMA overlay, use rut filling treatments after ruts appear, and avoid selecting CIR for roads that experience many heavy wheel loads.

This report also documents a forensic case study of two low-volume roads that did not meet performance expectations and a comparison of asphalt milling gradations from CIR versus hot in-place recycling (HIR) projects. The forensic study showed that pavement thicknesses were less than planned, the pavement structure was insufficient for typical local subgrade strengths, and gradations were finer than expected. In the gradation comparison, HIR millings were confirmed to be coarser than CIR millings.

17. Key Words		18. Distribution Statement	
cold in-place recycling (CIR)—hot-mix asphalt—pavement distress		No restrictions.	
19. Security Classification (of this report)	**20. Security Classification (of this page)**	**21. No. of Pages**	**22. Price**
Unclassified.	Unclassified.	108	NA

Form DOT F 1700.7 (8-72) **Reproduction of completed page authorized**

COLD IN-PLACE RECYCLING PROJECT SELECTION AND GUIDANCE FOR IOWA ROADWAYS

Final Report
July 2023

Principal Investigator
Charles T. Jahren, Ph.D., P.E., (Minnesota), Emeritus Morrill Professor
Institute for Transportation, Iowa State University

Co-Principal Investigator
Hosin "David" Lee, Ph.D., P.E., Professor
Iowa Technology Institute, University of Iowa

Research Assistants
Irvin Pinto and Yuhan Zhang, Iowa State University
Byungkyu Moon and Xinyu Hu, University of Iowa

Authors
Ashley Buss, Irvin Pinto, Hosin "David" Lee, Byungkyu Moon,
Charles T. Jahren, Yuhan Zhang, and Xinyu Hu

Sponsored by
Iowa Highway Research Board and
Iowa Department of Transportation
(IHRB Project TR-774)

Preparation of this report was financed in part
through funds provided by the Iowa Department of Transportation
through its Research Management Agreement with the
Institute for Transportation
(InTrans Project 19-695)

A report from
Institute for Transportation
Iowa State University
2711 South Loop Drive, Suite 4700
Ames, IA 50010-8664
Phone: 515-294-8103 / Fax: 515-294-0467
https://intrans.iastate.edu

TABLE OF CONTENTS

LIST OF FIGURES

LIST OF TABLES

ACKNOWLEDGMENTS

The authors would like to thank the Iowa Department of Transportation (DOT) and the Iowa Highway Research Board (IHRB) for sponsoring this research. The Technical Advisory Committee members included Jeff DeVries, Iowa DOT; Royce Fitchner, Iowa Asphalt Paving Association; and Brian Moore, Iowa County Engineers Service Bureau.

The field pavement cores described in Chapter 3 were extracted by Iowa DOT Special Investigations staff, with Brent Terry as lead technician. L.L. Pelling Co. performed the burn-off tests described in Chapter 3. The field pavement cores described Chapter 4 were provided by the Iowa Asphalt Paving Association. Several Iowa DOT, local jurisdiction, and Institute for Transportation (InTrans) staff aided the research team in accessing databases, plans, and other necessary data and information. The authors are grateful for all assistance and support provided throughout this project.

Ashley Buss, currently an Iowa DOT Bituminous Engineer, wrote the original proposal for this project with co-principal investigators Hosin "David" Lee of the University of Iowa and Charles T. Jahren of Iowa State University. As an Iowa State University faculty member, Ashly Buss served as principal investigator for this project from its inception until May 15, 2021, when she accepted her current position at the Iowa DOT. Since then, she has provided considerable guidance and advice to the research team. Charles T. Jahren has served as principal investigator for this project since May 16, 2021.

Iowa State University researchers were primarily responsible for Chapters 1, 2, and 4 of this report. This research team, in addition to Ashley Buss and Charles T. Jahren, included post-doctoral research associate Irvin Pinto and graduate research assistant Yuhan Zhang. University of Iowa Researchers were primarily responsible for Chapters 3 and 5 of this report. This research team, in addition to Hosin "David" Lee, included graduate research associates Byunkyu Moon and Xinyu Hu.

EXECUTIVE SUMMARY

Cold in-place recycling (CIR) is an asphalt pavement recycling method that involves cold milling 3 to 4 in. of the top layers of an existing pavement section; processing the millings by screening, crushing, and adding stabilizing agents; and then relaying the milled and processed materials with an asphalt paver. Subsequently, the material is compacted, cured, and covered with a bituminous surface treatment (rarely in Iowa) or one or two lifts of hot-mix asphalt (HMA, with two lifts typical in Iowa). Stabilizing agents include asphalt emulsion and foamed asphalt in some cases, with additives such as lime and cementitious materials.

CIR is typically used on lower traffic volume roads, defined as roads with annual average daily traffic (AADT) volumes of less than 5,000 in general and less than 2,000 in Iowa, but its successful use has been occasionally documented on higher volume roads, such as the Interstate system, outside of Iowa. Because the treatment adds little to the structure of the pavement section and the processing equipment requires considerable subgrade support, it is not recommended for roads with poor subgrades or pavement sections that are so thin that after milling the remaining pavement will not support the processing equipment.

CIR has several benefits. It has been successful in addressing distresses such as raveling, bleeding (flushing), rutting, and roughness and is especially effective in addressing cracking, as there is evidence in the literature that it serves as a stress relieving layer that mitigates the propagation of reflective cracks. Furthermore, CIR has several environmental benefits, such as reducing the need to use virgin materials and reducing fuel use for trucking and materials processing.

The research team conducted this investigation using several methods, including a literature review, database analysis using both descriptive statistics and statistical modeling, field activities including the collection of pavement cores and milling samples, laboratory testing and analysis of the cores and milling samples, and development of conclusions and recommendations.

The Iowa Pavement Management Information System (PMIS) database, which contains data for the primary and Interstate highway systems in Iowa from 1998 to the present, was reviewed through 2019 to identify projects that included CIR pavement layers. Forty-four projects were identified that met data completeness and other criteria for analysis. A subset of the projects was subjected to descriptive statistical analysis to allow researchers an initial understanding to the database contents. Initial findings were that noticeable pavement deterioration often became evident from 10 to 15 years after the road was recycled and that rutting and cracking distresses were often the first distress types to compromise performance. Statistical modeling confirmed that rutting was the earliest distress type to compromise performance, followed by longitudinal wheel path and transverse cracking. Thicker CIR and HMA overlay layers were found to perform better than compared to thinner layers.

Based on the aforementioned analysis, CIR/HMA overlay sections on US 34 in Mills and Wapello Counties were selected for more in-depth investigation. These CIR projects were experiencing challenges in terms of traffic volume and pavement deterioration. Cores were

recovered from the right wheel path and quarter point (between wheel paths) at eight locations. The cores were cut into discs to isolate the pavement layers, and the discs were fabricated into semicircular bending test specimens. The output of this test is used to calculate the flexibility index, which serves as an indication of the flexibility of a pavement layer. The CIR pavement layers were found to be more flexible in comparison to the HMA layers. This corroborates assertions in the literature that CIR layers are highly flexible, which allows them to serve as a stress relieving layer and mitigate reflective cracking. The literature also provides evidence that CIR layers have higher air void ratios in comparison to typical HMA layers, which is likely correlated to the CIR layers' flexibility.

Based on the forgoing results, a possible deterioration process is proposed that, although it cannot be confirmed with certainty, is consistent with the aforementioned evidence. It is postulated that when subjected to heavy wheel loads, the CIR layer undergoes compaction rutting due to its relatively high air void ratio. The less flexible HMA overlay layer is forced to conform to the rutted cross section of the CIR layer and, with repeated loadings, cracks longitudinally at the bottom of the wheel paths. When conducting windshield observations of CIR pavements, research team members noticed distresses consistent with this proposed deterioration process, especially at locations where end-of-load segregation of the surface course was evident.

Two other studies are documented within this report. One was a forensic investigation of two low-volume roads that did not meet performance expectations. A laboratory investigation of field cores showed that many of the pavement layers were thinner than what was required by the plans and that the CIR aggregate gradations were finer than those that are typically recommended for CIR projects in Iowa. Analysis of falling weight deflectometer data indicated that the pavement structure was insufficient for typical subgrade strengths. The second study compared the gradations of millings obtained from a recent hot in-place recycling (HIR) project on IA 22 to those of CIR millings obtained from previous projects conducted in nine counties in Iowa. The HIR gradations were confirmed to be coarser than the CIR gradations.

Several recommendations are made based on the investigations detailed in this report. Considerable effort was expended in data preparation when using the PMIS database, including removing values that were reported for years when no measurement was taken, resolving differences in metric versus imperial measurements, and excluding obvious outliers. Data preparation efforts for future PMIS database analyses could be reduced if users could agree on what data preparation steps would benefit most users, which would reduce the need for each user to prepare data independently. Changes to project selection, design, construction, and maintenance processes could be considered to address the proposed deterioration process. Such changes could include providing a more flexible overlay for CIR projects to reduce the tendency for wheel path cracking, using rut filling treatments and overlays when ruts do develop, and avoiding the selection of CIR methods on roads that experience many heavy wheel loads.

1. INTRODUCTION AND LITERATURE REVIEW

1.1. Introduction

Cold in-place recycling (CIR) is a pavement rehabilitation technique used to extend the life of asphalt concrete pavements. CIR involves milling off approximately 2 to 4 in. of the existing hot-mix asphalt (HMA) surface layer, mixing it with a stabilizing agent or a combination of agents, and compacting the recycled material into a new base layer. The recycled layer is then covered with an asphalt overlay, a thin HMA overlay, or a bituminous surface treatment to protect it from traffic and environmental factors. The use of CIR in the United States dates to the 1960s, and it continues to be used for the mitigation of distresses such as thermal cracking, raveling, and minor rutting.

Studies have shown that the use of recycled materials can be both a cost-effective and environmentally friendly solution (Thomas and Kadrmas 2003). Given the dwindling supply of quality aggregates and the overall good performance of CIR in Iowa, CIR is a much-needed sustainable alternative as a pavement rehabilitation technique. The stabilizing agents transform the milled asphalt pavement into a base layer that can mitigate future distress and extend pavement life. Asphalt emulsions and foamed asphalt are two popular bituminous materials that are used as stabilizing agents for CIR, along with portland cement and lime. Each agent has its own advantages and drawbacks. While bitumen-based stabilizers provide flexibility to the CIR layer, they tend to be more susceptible to rutting, while portland cement tends to mitigate rutting by stiffening the CIR layer, but it also makes that layer more prone to cracking (Cox and Howard 2016).

The existing literature reveals that cold in-place recycling is most commonly used on low-volume roads (Jahren et al. 1999a, Kim et al. 2010); however, there are documented instances where projects with poor subgrade support and a relatively thin HMA layer thickness occasionally fail to withstand the weight of the CIR train, therefore leading to decreased post-construction performance (Stroup-Gardiner 2012). Some long-term performance studies have shown that CIR performed on projects with a poor subgrade showed premature failure and reoccurrence of distresses (Kim et al. 2010, Modarres et al. 2014). Cold in-place recycling has also been applied on major Interstate roadways with high traffic volumes (Diefenderfer and Apeagyei 2014). Post-completion studies of cold in-place recycling on I-81 in Virginia have shown that the pavement continues to perform as expected. Another study indicated that CIR tends to perform more poorly in cold or cold and wet climates (Stroup-Gardiner 2012).

Iowa has a rich history of CIR. CIR research in Iowa has made Iowa a leader in CIR best practices, foamed asphalt CIR mixture design and validation, construction recommendations, and long-term performance tracking. Iowa researchers found that CIR pavements last on average 15 to 26 years on roadways with average daily traffic (ADT) volumes of less than 2,000 (Jahren et al. 1998), and later research extended the expected life to 21 to 25 years based on best fit regression (Jahren and Chen 2007, Chen et al. 2010, Kim et al. 2010). These studies also emphasized the importance of project selection and adequate subgrade support.

Performance studies of CIR pavements showed that the treatment effectively mitigates reflective cracking in Iowa pavements (Jahren et al. 1998, Jahren and Chen 2007, Buss et al. 2017). A survivability analysis of the performance of pavement treatments for reflective cracking found that Iowa CIR pavements outperformed alternative treatments, which included mill and fill, overlay, rubblization, and heater scarification (Chen et al. 2015). However, a challenge remains that not all roadways are good candidates for CIR, and the differences between good and poor candidates can be hard to identify.

Other important issues include how soon to allow traffic to temporarily use the recycled surface after recycling and before overlaying and when the CIR layer is sufficiently cured to allow the roadway to be overlaid. A relatively high moisture content in the CIR layer may indicate insufficient curing to allow an overlay. Research by Lee et al. (2009) and Kim et al. (2011) found that CIR moisture can be monitored using a capacitance moisture sensor. Another important finding from this research was that a Humboldt GeoGauge could be helpful in determining the stiffness of the CIR layer and the recommended timing of the overlay. Finally, the curing rate was found to be more influenced by temperature than by moisture content. Following the recommendations from this research, the Iowa Department of Transportation (DOT) increased the moisture content requirement before an HMA overlay could be applied from 1.5% to 3.5% (Iowa DOT 2022).

CIR mixture design is commonly used throughout the country to set initial binder and moisture rates during construction. In Iowa, Kim and Lee (2006) developed and validated a mixture design process for CIR made with foamed asphalt. The study investigated a section of US 20 near Manchester, Iowa, that had been recycled using foamed asphalt and engineered asphalt emulsion in 2002. It was found that when foamed asphalt is used, the half-life and the expansion ratios should be measured to optimize the foaming conditions of the asphalt. In a follow up study, Chen et al. (2010) found that the indirect tensile test (IDT) wet strength and the dynamic modulus of the CIR material were important mixture characteristics. This study showed that CIR pavements with lower stiffness and higher air void contents exhibit better performance; however, ensuring adequate pavement density is also pivotal to better performance. This indicates that there is a window of optimal material properties for a CIR mixture (Chen et al. 2010). Engineered emulsions and additives for CIR have changed considerably over the past 20 years. Kim and Lee (2012) evaluated mixture design properties for CIR made with asphalt emulsion and showed that optimal emulsion content helped reduce the mixture's susceptibility to raveling under traffic. Both of these mixture design studies found value in performing traditional tests (IDT wet strength) and testing for more complex material properties such as dynamic modulus. The evolution of pavement design will require inputs for the more complex material properties.

1.2. Benefits of CIR

The rise in popularity of pavement life extension can be attributed to the rising cost and limited availability of virgin paving materials as well as the reduced environmental impact of recycling pavement materials. Cold in-place recycling ensures the reuse of existing materials in extending the life of the current pavement. The benefits of using cold in-place recycling pavements are described in the following sections.

1.2.1. Reuse of a Nonrenewable Natural Resource through Reuse of the Aggregates in the Pavement Layer

A key advantage of cold in-place recycling is the reuse of the existing asphalt pavement as a pavement layer with enhanced material properties. Between 3 and 4 in. of the existing asphalt pavement are milled off and mixed with stabilizers and laid down as a fresh flexible base layer. This results in the reuse of materials and more sustainable construction practices (Cox and Howard 2015). Off-site hauling is reduced, while the application of foamed asphalt and asphalt emulsions lead to reduced heating costs (Alkins et al. 2008).

1.2.2. Reduced Instances of Reflective Cracking

A cold in-place recycled layer is often used as an intermediate base layer between the old asphalt pavement below the milling depth and the surface layer that carries traffic. Because of its flexible nature, the CIR layer acts as a stress relieving layer and hence reduces the amount and severity of cracks reflected to the surface from the old pavement (Chen et al. 2010). A study by Buss et. al. (2017) on the performance of cold in-place recycled pavements in Iowa showed that CIR treatments in Iowa helped reduce transverse cracking in pavements.

1.2.3. Historically Good Performance in Iowa with Significant Cost Savings

There have been extensive studies on the performance of CIR in Iowa, and the consensus from the available literature indicates that CIR works well on pavements with ADT volumes of less than 2,000 where sufficient subgrade support is available for the CIR train and where the structural capacity of the pavement is not compromised (Jahren et al. 1998, Kim et al. 2010, Jahren et al. 1999b).

1.3. CIR Project Selection Guidelines

Cold in-place recycling has seen an increase in use over the last few years due to increased interest in treatments using recycled asphalt (Kim and Lee 2006, Buss et al. 2017). However, the final performance of CIR can vary depending on the quality of the existing materials as well as subgrade, traffic, and climate conditions (Sebaaly et al. 2004), which makes project selection an important consideration in the use of CIR. This section highlights the various factors that play a role in choosing pavements for potential CIR treatment.

1.3.1. Traffic Loading

One of the factors that could influence the decision to use CIR for pavement rehabilitation is traffic loading. A review of CIR in Iowa was conducted by Jahren et al. (1998), who noted that pavements with an annual average daily traffic (AADT) of less than 2,000 had an average life of about 15 to 20 years and showed retarded transverse cracking and a decreased occurrence of rutting, pointing to lower volume roads being favorable candidates for CIR. Rogge et al. (1990) suggested that CIR projects are best suited for cracked and broken pavements with an ADT of

5,000 or less. The authors also suggested that pavements with a rough surface or raveling and pavements in locations where native aggregate is poor or in short supply are other good candidates for CIR. A CIR design procedure by Sebaaly et al. (2004) that highlighted the need for lime treatment of the recycled base layer was carried out successfully on low- and medium-volume roads. A study on the effect of recycled materials on the long-term performance of CIR showed that CIR-rehabilitated roadways would wear out faster with traffic volumes higher than 800 vehicles per day. The study primarily indicated that a higher air void content significantly increased CIR performance on both high- and low-volume roads. Likewise, the Pennsylvania DOT restricts CIR projects to roadways with an ADT of 3,000 or less (Sebaaly et al. 2004).

On the other hand, a study by Stroup-Gardner (2012) showed that lower volume roads may not be good candidates for CIR given that these pavements had HMA thicknesses of 4 in. or less and inadequate base support for recycling equipment. This finding is backed up by a study by Jahren et al. (1999b), which showed that the heavy weight of the CIR train and other equipment could well exceed the supporting capacity of the pavement subgrade, especially on low-volume roads. The authors cautioned that care must be taken to ensure that there is adequate subgrade support for the weight of CIR construction equipment prior to rehabilitating the pavement. Sebaaly et al. (2004) noted that the flexibility of the CIR layer plays a major role in determining the amount of traffic it can carry; the CIR layer must have sufficient stability to carry traffic loads but enough flexibility to prevent the recurrence of reflective cracking. A review of the traffic information available in the literature showed that many CIR projects were undertaken on pavements with ADT volumes under 5,000. Although studies have shown that CIR could be successful on higher volume roads (Croteau and Davidson 2001), the available data show that it performs best on low-volume roads with a sufficiently strong subgrade to sustain the weight of the CIR construction equipment. Table 1-1 summarizes traffic loading recommendations based on the literature review.

Table 1-1. Traffic loading recommendations for CIR

Study No.	Author/Manuscript Reference	Location	Traffic Information/Recommendation
1	Wood et al. 1988	Pennsylvania	<3,000 ADT
2	Rogge et al. 1990	Oregon	<5,000 ADT
3	Sebaaly et al. 2004	Nevada	30–300 equivalent single axle loads (ESALS)/day
4	Forsberg et al. 2002	Minnesota	ADT approximately 580
5	Mallela et al. 2006	Arizona	ADT between 1,500 and 3,500 over 20 years of observation
6	Jahren et al. 1998, 1999a	Iowa	<2,000 ADT
7	Stroup-Gardner 2012	United States	5,000<AADT<30,000
8	Croteau and Davidson 2001	United States and Canada	State agencies currently removing the limit of a maximum ADT of 5,000
9	Scholz et al. 1991a	Oregon	Recommended ADT <5,000
10	Cross and Jakatimath 2007	Oklahoma	ADT of 1,700 on test sections

1.3.2. Subgrade Conditions

A review of numerous peer-reviewed papers on CIR performance revealed that subgrade conditions can be a determining factor in the success or failure of a CIR project. Modarres et al. (2014) noted that rutted pavements with a high asphalt content and pavements that failed due to unstable bases and underlying soils are poor candidates for CIR. Chen et al. (2010) noted that the predicted service life of CIR test sections that had good subgrade support was much higher than that of CIR test sections with poor subgrade support. Flexible pavements with fair subgrades and pavement condition index (PCI) values of 40 to 55 were recommended as viable candidates for CIR. Studies have shown that in order for a pavement to be considered a good candidate for CIR, the existing pavement cross-section must be free from excessive permanent deformation indicative of a weak subgrade (Croteau and Davidson 2001).

Studies have also shown that prior testing must be done to ensure that the subgrade is strong enough to support the load of the CIR equipment (Jahren et al. 1998, Jahren et al. 1999b, Stroup-Gardiner 2012, Croteau and Davidson 2001, Scholz et al. 1991a). This is an important point to note because CIR is not a structural rehabilitation technique and does not enhance the load bearing capacity of the pavement (Croteau and Davidson 2001). To determine the quality of the subgrade, pretesting is recommended on pavement sections that are under consideration for CIR treatment (Scholz et al. 1991b). This can include nondestructive testing with a falling weight deflectometer (FWD) or extraction of cores for laboratory testing (Hunsucker et al. 2017).

In a study sponsored by the Minnesota Local Road Research Board, Jahren et al. (2016) found CIR and FDR to be cost-effective; however, recycled materials have historically lacked well-defined engineering parameters, which has led to inconsistency in their performance (Forsberg et al. 2002).

Subgrade support has been shown to be an important factor in long-term performance for CIR roadways. Jahren et al. (1998 and 1999b) developed a constructability test for CIR roadways in Iowa to determine whether a roadway's subgrade support would be too soft or unstable during CIR construction. Several examples of Iowa CIR projects with major constructability issues due to a soft subgrade were given. The studies showed that dynamic cone penetrometer (DCP) blow counts above six indicated probable success and that blow counts below 4 indicated probable failure, with mixed results in the 4 to 6 blow count range. It should be noted that the piece of DCP equipment used in these studies, which was developed by the U.S. Army Corps of Engineers, was larger and heavier than equipment typically in current use. Prather and Weilinski (2016) recommended that the structural capacity of the pavement should be at least 75% of the design capacity of the HMA to ensure the success of CIR. In a study on the construction of CIR pavements over glacial till in Saskatchewan, cementitious waste products were found to be helpful in stabilizing the subgrade to allow for rehabilitation in situations where the existing subgrade is unsuitable for CIR construction (Berthelot and Gerbrandt 2002).

1.3.3. Climate, Moisture, and Temperature

Climate and temperature play an important role in the performance of CIR pavements. The air temperature can significantly affect the breaking of asphalt emulsions and hence affect the curing of the CIR mat (Moore et al. 2017). While high temperatures increase the rate of emulsion breakage, cold temperatures can significantly slow the breaking process. Scholz et al. (1991a) recommended that CIR should not be performed late in the fall or early in the winter since the CIR mat needs several nights of warm weather to cure properly. At air temperatures below 10°C, it is recommended to use more emulsion or use an emulsion with a high solvent content due to the inherent stiffness of aged asphalt (Croteau and Davidson 2001).

A detailed study of moisture susceptibility for CIR pavements showed that the early-age strength and stability of CIR are a function of moisture content, curing time, and cement content (Lee et al. 2009). A tool based on moisture loss index and in situ stiffness was developed for determining the optimal timing of HMA overlay placement on the CIR layer (Woods et al. 2012). Excess water, if not removed, will hinder compaction of the mixture, but mixtures with insufficient water are unworkable, leading to instability during compaction and decreased fatigue life (Scholtz et al. 1991b). Some concerns that contractors have mentioned are (1) challenges in scheduling the placement of the HMA layer and (2) shallow water table depths. The latter can be problematic because vibrations associated with construction can cause capillary water to rise, which can weaken the subgrade and possibly soak the CIR and underlying layers in the pavement section.

Compaction of recycled materials is critical to long-term performance; however, overcompaction should be avoided to prevent flushing. Other factors that influence curing are ambient temperature, humidity, construction methods, and material properties. Coarse gradations invite segregation, dragging, the formation of excess voids, and problems with laydown, and finer gradations are more sensitive to changes in water and emulsion contents (Scholtz et al. 1991b). Most public agencies have various requirements for the curing time of the CIR mat and specify a certain number of days after which an overlay or surface treatment can be placed over the CIR layer. However, inclement weather can often make it necessary to modify these standards. A study by Kim et al. (2011) explored technically sound methods of determining how curing time and moisture content affect the strength of the CIR layer by using indirect tensile strength and dynamic modulus data. Results showed that strength gain was dependent on the stabilizer type, with CIR samples made from foamed asphalt exhibiting greater strength gain and lower moisture contents than samples made from emulsified asphalt for the same curing duration. Results also showed that much of the strength gain occurs during the later stages of CIR curing. Because of the importance of curing on the strength gain of the recycled mat, CIR requires reasonably good weather conditions during the construction season. Extremely hot or cold weather can adversely affect the curing and moisture levels of the CIR mat and affect strength gain and the ability of the roadway to be opened to traffic in a timely manner (Prather and Wielinski 2016).

1.3.4. Drainage

Good pavement drainage is important for adequate subgrade support and, it follows, the success of CIR. Therefore, the presence of curbs, gutters, ditches, and drainage tiles is essential for a road to be considered for CIR.

1.4. Pavement Distresses Addressed by CIR

According to Prather and Wielinski (2016), CIR addresses raveling in the surface layer, reflective cracking, edge and block cracking, top-down cracking, potholes, and stripping. An evaluation of CIR rehabilitation on US 412 by Cross and Jakatimath (2007) showed a reduced recurrence of the original transverse cracking, though longitudinal wheel path cracking continued to occur. Morian et al. (2004) showed that CIR can be a cost-effective rehabilitation technique for mitigating reflective cracking in pavements with concrete bases.

1.5. CIR Mix Design and Laboratory Testing

The variable nature of CIR mixes in the field highlights the importance of a well-defined inspection and testing strategy for agencies. Many state agencies have their own CIR mix design processes, which makes comparing CIR performance among states difficult, while the use of various stabilizing agents adds further complications.

Foamed asphalt and emulsified asphalt are the two bituminous stabilizing agents used in CIR. Foamed asphalt is generated by combining asphalt and cold water and has proved useful in creating mixes with both virgin and recycled aggregate (Castedo et al. 1983). Kim and Lee (2006) determined mix design parameters for cold in-place recycled pavements using foamed asphalt with the help of the Marshall stability test and the indirect tensile test for 13 combinations of foamed asphalt content and water content along with 3 different gradations. The authors recommended that the indirect tensile test be used to determine the optimum foamed asphalt content, with the results of the study indicating an optimum foamed asphalt content between 2% and 2.5% for the given gradations. Studies in Kansas (Cross 1999) showed that adding hydrated lime slurry along with asphalt emulsions to CIR mixes improved performance. Cores from test projects were tested for tensile strength, moisture susceptibility, and resilient modulus and showed improved material properties irrespective of the emulsion used.

1.6. CIR Project Case Studies

This section reviews case studies of CIR performance across the United States and globally that compare pavement performance before and after treatment, with the factors that led to the success or failure of the project highlighted. The results of the case studies are distilled into a series of recommendations for future projects.

A study by Sanjeevan et al. (2014) of the effect of surface treatments and finishing courses on CIR pavements in Nevada revealed that CIR with a surface treatment performed much better on

higher volume roads compared to lower volume roads. A study of post-construction performance showed that transverse and longitudinal cracking were the two major distresses observed in pavements with a CIR layer. The authors noted that the use of CIR with both an HMA overlay and a surface treatment was the most effective strategy to prevent early post-construction distresses; in contrast, the use of only an HMA overlay or a surface treatment over a CIR layer was less effective (Sanjeevan et al. 2014).

An improved CIR design process in Minnesota developed by Forsberg et al. (2002) showed superior performance when compared to the conventional CIR design process used by the Minnesota DOT. The new design process focused on a better quality control and quality assurance plan, which ensured that laboratory testing mirrored field conditions through the creation of mix designs for each of the gradations present in the field. An improved asphalt emulsion was also used in the mix design that provided better early strength gain and higher residual binder content. This ensured a quicker opening to traffic. Although the new design process was 10% more expensive than the conventional CIR design methodology, the authors noted that the new design process was expected to provide better long-term performance (Forsberg et al. 2002).

A study by Chen et al. (2010) of 24 pavements in Iowa that were rehabilitated with CIR showed that higher air void contents and lower CIR modulus values correlated with better CIR performance. The authors used FWD data to characterize the performance of the 24 pavement sections and compared these results to the results of laboratory tests. The results support the theory that the CIR layer acts as a stress relieving layer and prevents the propagation of cracks in the lower layers of the pavement from reaching the surface. This study further underlines the importance of the material properties of the CIR layer and the need for making provisions in the design process to ensure that these physical properties are met (Chen et al. 2010).

A study by Cross and Jakatimath (2007) of two pavement sections in Oklahoma exhibiting transverse and longitudinal cracking revealed that while CIR did reduce the recurrence of transverse cracks (thermally induced), longitudinal cracking (fatigue induced) reoccurred two years after treatment in one of the test sections. Both test sections had a traffic count of 1,700 ADT. While one of the sections had 4 in. of CIR thickness (Section A), the second section had 3 in. of CIR thickness (Section B). Both sections were treated with fly ash slurry to seal cracks before the sections were milled. Section B also had existing transverse cracks sealed off with precoated fabric membrane strips. A pre-rehabilitation survey showed that Section A had more distress than Section B, while Section B did not have excessive transverse or longitudinal wheel path cracking but had significant longitudinal joint cracking. Two years after treatment, the amount of transverse cracking was lower in Section A than in Section B, probably due to the extra inch of milling depth. However, the authors blame the stiff HMA layer placed over the CIR layer, made from a PG 76-28 binder, as being responsible for the recurrence of longitudinal cracking in Section A; this once again highlights that CIR is not a structural fix and that a thin, stiff HMA layer placed over a softer CIR layer could have led to the recurrence of longitudinal cracking in this case, which was suspected to be top-down fatigue cracking. The authors also suspected that poor workmanship while placing the HMA layer could have caused a recurrence of longitudinal cracking in test Section A (Cross and Jakatimath 2007).

A study by Jahren et al. (1999b) of a CIR project in Iowa highlights the problem with unstable subgrades. The CIR test section was built on subgrades with varying levels of instability. The study used DCP testing to determine subgrade stability along the project after CIR equipment caused severe rutting in some sections. DCP tests were conducted at 31 different locations along the project, which included areas where CIR was successful and areas of unstable subgrade. Results of DCP testing were analyzed against pavement distress at various testing points, and the analysis showed that the blow counts required in severely distressed areas were significantly lower than those required in areas where CIR was completed successfully. The authors recommended that CIR be performed on pavements where the recycling train has at least 1 to 2 in. of existing asphalt pavement below the milled surface and that the subgrade consist of natural soil or an engineered aggregate base to ensure that the soil can sustain the load from the CIR equipment (Jahren et al. 1999b).

2. IOWA PMIS DATA COLLECTION AND ANALYSIS

2.1. Introduction

The Iowa Pavement Management Information System (PMIS) contains performance, traffic, and structural data on Iowa's major pavement systems from 1998 to present. The PMIS was used to gather data on the performance of CIR projects across the state of Iowa from 1998 to 2019, and these data were supplemented with plan sets available from the Iowa DOT's digital repository. With various types of rehabilitation and construction projects in the PMIS, two identifiers were used to filter and shortlist the sections needed for analysis. These two identifiers are the project number and the project origin key.

Each project in Iowa is identified by a project number, which is associated with the project from conception to construction. A typical project number is made up of a system prefix letter code, a route number, a milepost (MP) number, and a two-digit county number, all of which can be used to help pinpoint a particular project to a specific location. An example of a project number description is given in Table 2-1.

Table 2-1. Example of project number description for project IM-35-5(87)111--13-85

Number/Code	Designation/Purpose
IM	System prefix letter code
35	Route number
5	Federal control section number
(87)	Paren number
111	Milepost number
13	Alpha-numeric system prefix
85	Two-digit county code

Iowa's major pavements are divided into various origin keys, which are largely consistent with location but tend to change over the years as modifications are made to the pavement system. Among other information, each origin key contains the start and end mileposts of the section it describes, which is useful in determining the section's precise location. Origin keys are set up similar to project numbers, with numbers representing the route, system, direction, mileposts, and county. An example of an origin key description is shown in Table 2-2.

Table 2-2. Example of origin key description for 04431074 78078 6439

Number/Code	Designation/Purpose
044	Route number
3	System number
1	Direction
074.78	Beginning milepost
078.46	Ending milepost
39	Two-digit county code

2.2. Data Collection

Data for the various CIR sections in Iowa were collected from a list of known CIR projects based on previous research. It was assumed that the list was a random sample and contained a mixture of both well performing and poorly performing sections. The process for data collection from the PMIS consisted of the following steps.

2.2.1. Consolidate Data from All PMIS Years into a Master Worksheet

The PMIS data used in this project were extracted from several worksheets of PMIS data for the years 1998 through 2019. There were inconsistencies in the system of units used in the PMIS, with the years 1998 through 2010 using metric units and the years 2011 through 2019 switching to imperial units, as well as inconsistencies in the data columns among various PMIS years. To remedy this, it was necessary to take the following steps.

2.2.2. Obtain Plan Sets for the Projects Listed

Plan sets were obtained from the Iowa DOT digital repository based on the CIR project numbers in the list of CIR projects. The plan sets contain geographical information useful in pinpointing the exact location of each CIR project in the form of a map and the start and end mileposts of the project. The plan sets are also extremely useful in determining whether the design intent had indeed been followed by comparing the plan set requirements to the data available in the PMIS.

2.2.3. Locate the Origin Keys and Project Bounds for the CIR Projects from the Plan Sets and PMIS Database

Once the plan sets were downloaded, the origin keys for a particular project were verified by the project bounds on the plan set. The first step was to input the project number under the "PROJECT1" column of the PMIS using a data filter to filter all the entries in the PMIS associated with that particular project. The list of entries was then further filtered by county and route, both found within the project number. Using the beginning and ending mileposts, origin keys whose PMIS description fit the plan set location were selected.

2.2.4. Use Selected Origin Keys to Gather PMIS Data for Each Section

The origin keys were then input into a Microsoft Excel solver that matched the origin keys to their corresponding data in the PMIS. Each origin key was expected to have 21 rows of data for the 21 years from 1998 to 2019. However, there were instances where either a single origin key was broken into two different origin keys or two origin keys were merged into one, which could cause comparatively fewer data to be obtained. The obtained data were then copied into a separate Excel spreadsheet, with each origin key having its own sheet.

2.3. PMIS Metadata

Table 2-3 provides a list of PMIS variables used in this analysis and the metadata information for each variable.

Table 2-3. PMIS metadata

Variable Name	Units	Description	Values
ORIGKEY		Original origin (smart) key	String value (route, system, direction, begin post, end post, county)
DESCRIPT		Pavement management section description	String
AGE	year	Number of years since last resurface/construction	Numeric value (+/-)
PCI_2	index	Pavement condition index version 2.3	0–100
RUT_INDX	index	Rutting index rating	0–100
IRI_INDX	index	International roughness index rating	0–100
CRACK_INDX	index	All cracking combined index rating	0–100
IRI	in./mi	International roughness index	0–100
RUT	in.	Rut depth	Numeric value
T_INDX	index	Transverse cracking index rating	0–100
L_INDX	index	Longitudinal cracking index rating	0–100
LW_INDX	index	Longitudinal wheel path cracking index rating	0–100
TCRACKH TCRACKM TCRACKL	count/mi	High-, moderate-, and low-severity transverse cracks/mi	Numeric value
LCRACKH LCRACKM LCRACKL	ft/mi	High-, moderate-, and low-severity longitudinal cracks (ft/mi)	Numeric value
LCRACKWH LCRACKWM LCRACKWL	ft/mi	High-, moderate-, and low-severity longitudinal cracks – wheel path (ft/mi)	Numeric value
STRUC80		80% structural rating	0.00–15.00
STRUCAV		Average structural rating	0.50–15.00
AVEK	PSI/in.	Average “K” rating	Numeric value
AADT	count/day	AADT by direction	Numeric value
TRUCKS	count	ADT - trucks	Numeric value
PAVTHICK	in.	Pavement thickness	Numeric value
LAYR(1-8)		Layer year #(1–8)	1900–2019
PROJECT(1-8)		Project number #(1–8)	String
SURTHK(1-8)		Surface thickness #(1–8)	Numeric value
BASTHK(1-8)		Base thickness #(1–8)	Numeric value
SUBTHK(1-8)		Subbase (CIR) thickness #(1–8)	Numeric value

2.4. Data Analysis

Due to gaps and inconsistencies in the PMIS data, a total of 44 CIR projects were selected for survival analysis after the data were prepared. The average age of the pavements was calculated to be 9.5 years, with the mode and median age being 6 and 7, respectively. Since CIR in Iowa is typically designed to last 20 to 21 years, the failure thresholds for distresses were set at 70

instead of 60 because of the relatively low median age of the pavements. The pavement condition index (PCI_2) was used to classify pavements based on their performance after CIR construction. PCI_2 is a modified version of the pavement condition index equation for pavements in Iowa, and its calculation is shown below:

$$PCI_2 = 0.4 \times cracking\ index + 0.4 \times IRI + 0.2 \times rutting\ index \quad (2\text{-}1)$$

where the IRI is the international roughness index of the pavement.

Figure 2-1 shows the PCI_2 values of the 44 pavement sections over the years from 1998 to 2019. For each pavement, the negative age indicates the period before the pavement had undergone CIR treatment.

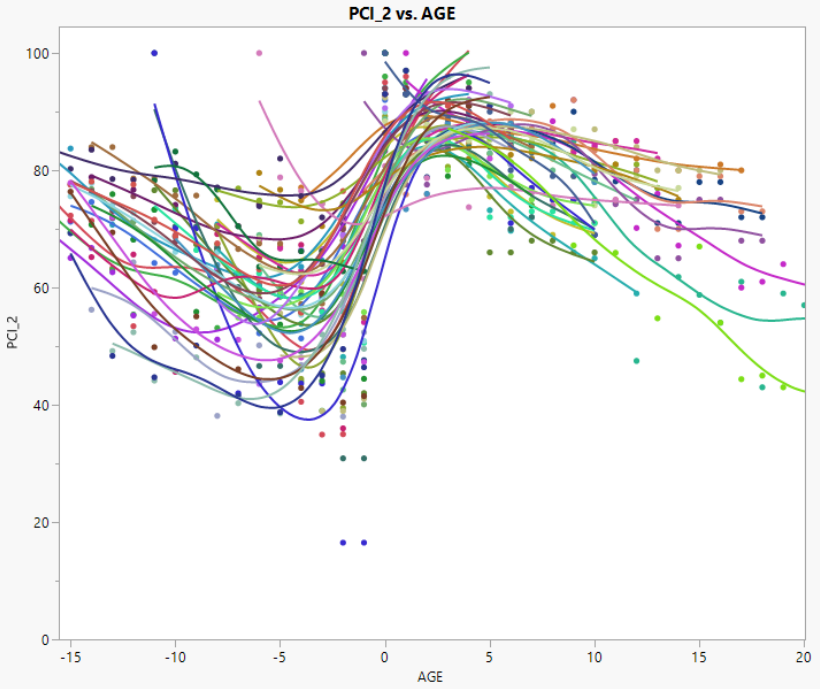

Figure 2-1. PCI_2 versus pavement age after CIR construction for 44 pavement sections

When analyzing pavement performance, the four commonly used parameters available in the PMIS are PCI_2, IRI_INDX, RUT_INDX, and CRACK_INDX. PCI_2 is a representation of the overall pavement condition index, and for asphalt concrete (AC) surfaces the PCI_2_{AC} is calculated as follows:

$$PCI\_2_{AC} = (0.40 \times CRACK\_INDX) + (0.40 \times IRI\_INDX) + (0.20 \times RUT\_INDX) \quad (2\text{-}2)$$

Note that the parameters are defined in Table 2-3. The cracking index is obtained by combining the sub-indices for the cracking data (T_INDX, L_INDX, LW_INDX, and A_INDX). The cracking index is calculated using the cracking sub-index weights shown in Table 2-4.

Table 2-4. Cracking sub-index weights

Sub-Index	Weight (%)	
	PCC	AC
Transverse	60	20
Longitudinal	40	10
Wheel path	—	30
Alligator	—	40

The international roughness index (IRI_INDX) is almost unanimously accepted as a roughness measurement. Although there is variation among agencies, an IRI below 1.5 m/km (95 in./mi) is generally considered to be smooth (or good and very good) and an IRI above 2.7 m/km (170 in./mi) is considered to be rough (poor and very poor). Thus, roughness index values above 65 can be taken as good or better and values below 35 can be taken as poor or worse.

2.5. CIR Data Preparation

The data in Table 2-5 come from the PMIS database and are used as an example in the description of the data preparation process below.

Table 2-5. Example data for PMIS preparation procedure

ORIG KEY 1	PCI_2	RUT_INDX	IRI_INDX	CRACK_INDX	AGE
03421011 94015 2365	75.03333	79.16666667	48	100	-8
03421011 94015 2365	75.03333	79.16666667	48	100	-7
03421011 94015 2365	64.89673	65	44.25	85.49181818	-6
03421011 94015 2365	64.89673	65	44.25	85.49181818	-5
03421011 94015 2365	60.979	60	40.5	81.9475	-4
03421011 94015 2365	60.979	60	40.5	81.9475	-3
03421011 94015 2365	60.62327	71.66666667	33.25	82.47484848	-2
03421011 94015 2365	60.62327	71.66666667	33.25	82.47484848	-1
03421011 94015 2365	100	100	100	100	0
03421011 94015 2365	100	100	100	100	1
03421011 94015 2365	85.964	80	77.25	97.66	2
03421011 94015 2365	85.92764	80	77.25	97.56909091	3
03421011 94015 2365	88	80	81	98	4
03421011 94015 2365	75.54721	64.16666667	70	54.29	5
03421011 94015 2365	72.95091	52.5	69.75	52.89	6
03421011 94015 2365	77	57	80	85	7
03421011 94015 2365	69	51	73	74	8
03421011 94015 2365	69	51	73	74	9
03421011 94015 2365	71	47	71	83	10
03421011 94015 2365	71	46	71	84	11
03421011 94015 2365	0	0	0	0	12
03421011 94015 2365	0	0	0	0	13

The original database includes many other columns, but for simplicity of explanation only six columns are shown here. The data preparation process must include all columns that are used in the analysis. The ORIG KEY 1 column in Table 2-5 is the original origin key for a project. Although this origin key is also sometimes designated as ORIGKEY and ORIG KEY in the PMIS, the concept is identical, despite the slight difference in designation. The components of an ORIG KEY value are provided in Table 2.2.

Based on the vales in the ORIG KEY 1 column, the pavement section described in Table 2-5 is located on US 34 starting from the east junction of US 275 and continuing east 8.0 mi to the western city limits of the municipality of Hastings. The values of PCI_2, RUT_INDX, IRI_INDX, and CRACK_INDX range from 0 to 100 depending on the pavement condition. Age is the number of years since CIR construction, with negative numbers indicating years before CIR construction.

To intuitively display the data in Table 2-5, Figure 2-2 through Figure 2-5, respectively, show age on the x-axis versus PCI_2, RUT_INDX, IRI_INDX, and CRACK_INDX on the y-axis; higher values of each index indicate better performance of the pavement. The line indicates a smoothed linear relationship as determined by the JMP software application that was used to create these figures. The shadow area denotes the width of the confidence interval. In the following examples, the shadow area only provides a trend because only one observation is reported over time.

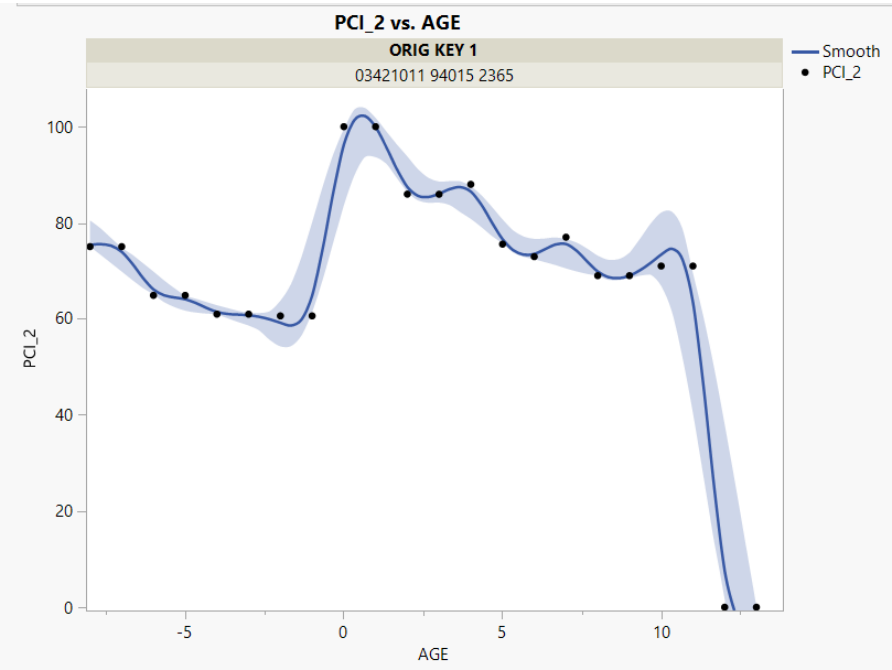

Figure 2-2. Initial PCI_2 versus AGE

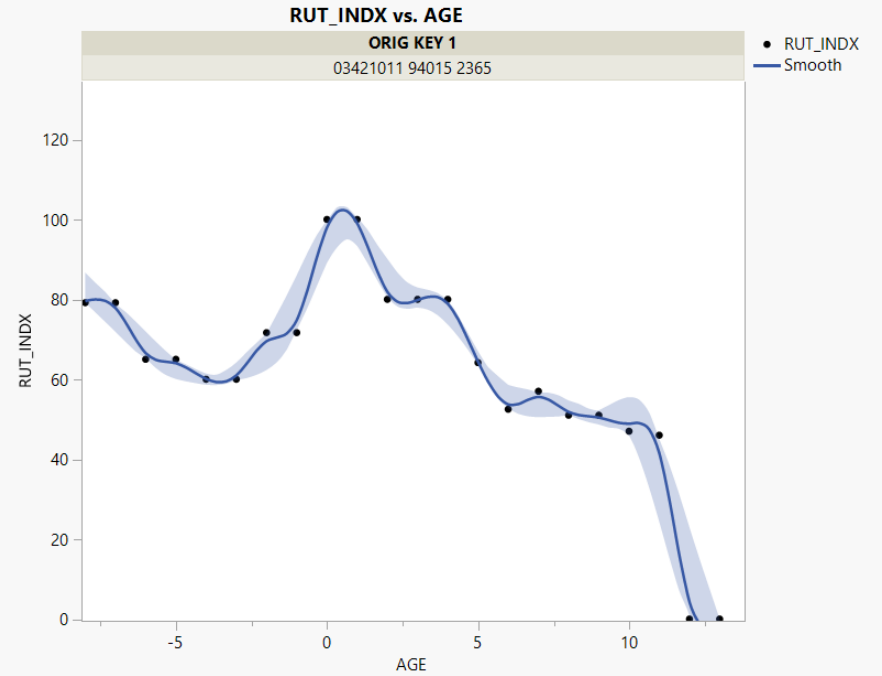

Figure 2-3. Initial RUT_INDX versus AGE

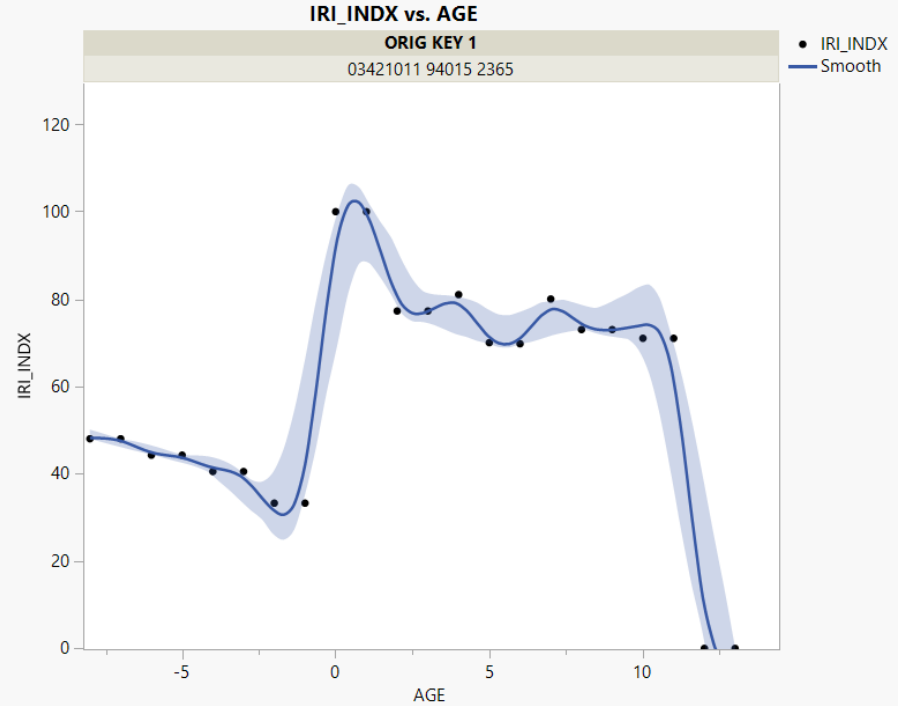

Figure 2-4. Initial IRI_INDX versus AGE

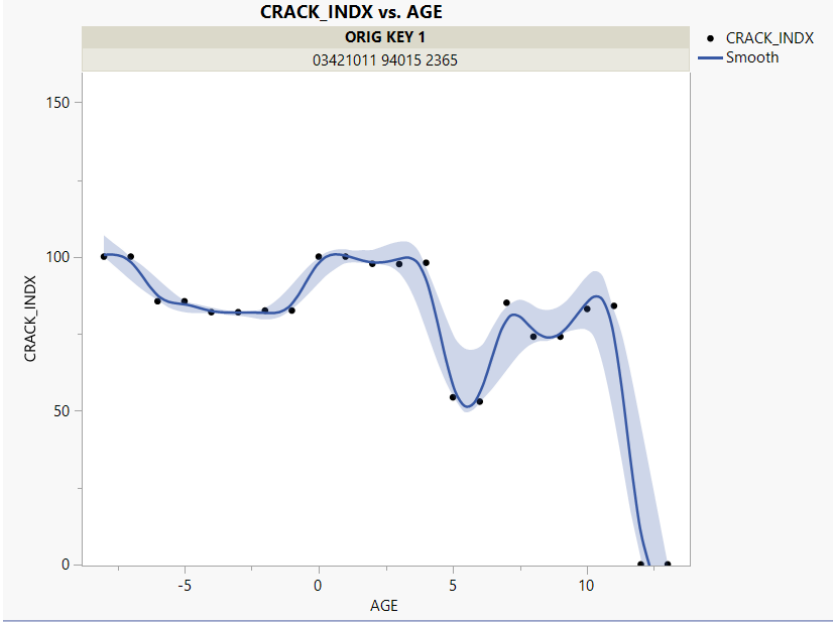

Figure 2-5. Initial CRACK_INDX versus AGE

2.5.1. Step 1

The goal in performing the data preparation is to use the prepared data to model typical pavement deterioration, since, for various reasons, unprepared data are not consistent with typical deterioration. However, note that the research team did not find any evidence of typical deterioration for any of these road segments. In the data preparation process, decisions are made to exclude certain data from analysis. Although some data are excluded from the analysis, the original data are retained in the original database and a rationale is provided for any exclusions.

By analyzing the data in Table 2-6, it is evident that cells B1=B2, B3=B4, B5=B6, B7=B8, B9=B10, B17=B18, and B19=B20, which is same across all columns and distress indices. This redundancy occurs because the Iowa DOT measures pavement performance every two years and the PMIS system automatically records data from the previous year for years where no data are recorded. To better analyze the performance of CIR projects, the redundant data are excluded from the analysis. Also, all data in the range of cells from B22 through E23 equal zero, which indicates that in those two years the pavement suddenly deteriorated to the worst condition; since such a circumstance is not typical, these zero values are excluded from the analysis. Since the goal of most pavement condition analyses is to model typical pavement deterioration, excluding such zero values from the analysis is appropriate. Visual observation by the research team members confirmed that sudden deterioration to the worst condition did not occur.

Table 2-6. Data preparation process Step 1 (redundancies and zero values highlighted)

ORIG KEY 1	PCI_2	RUT_INDX	IRI_INDX	CRACK_INDX	AGE
03421011 94015 2365	75.03333	79.16666667	48	100	-8
03421011 94015 2365	75.03333	79.16666667	48	100	-7
03421011 94015 2365	64.89673	65	44.25	85.49181818	-6
03421011 94015 2365	64.89673	65	44.25	85.49181818	-5
03421011 94015 2365	60.979	60	40.5	81.9475	-4
03421011 94015 2365	60.979	60	40.5	81.9475	-3
03421011 94015 2365	60.62327	71.66666667	33.25	82.47484848	-2
03421011 94015 2365	60.62327	71.66666667	33.25	82.47484848	-1
03421011 94015 2365	100	100	100	100	0
03421011 94015 2365	100	100	100	100	1
03421011 94015 2365	85.964	80	77.25	97.66	2
03421011 94015 2365	85.92764	80	77.25	97.56909091	3
03421011 94015 2365	88	80	81	98	4
03421011 94015 2365	75.54721	64.16666667	70	54.29	5
03421011 94015 2365	72.95091	52.5	69.75	52.89	6
03421011 94015 2365	77	57	80	85	7
03421011 94015 2365	69	51	73	74	8
03421011 94015 2365	69	51	73	74	9
03421011 94015 2365	71	47	71	83	10
03421011 94015 2365	71	46	71	84	11
03421011 94015 2365	0	0	0	0	12
03421011 94015 2365	0	0	0	0	13

With the redundant data and zero values excluded, the revised PMIS database is shown in Table 2-7.

Table 2-7. Data preparation process Step 1 (redundancies and zero values removed)

ORIG KEY 1	PCI_2	RUT_INDX	IRI_INDX	CRACK_INDX	AGE
03421011 94015 2365	75.03333333	79.16666667	48	100	-8
03421011 94015 2365					-7
03421011 94015 2365	64.89672727	65	44.25	85.49181818	-6
03421011 94015 2365					-5
03421011 94015 2365	60.979	60	40.5	81.9475	-4
03421011 94015 2365					-3
03421011 94015 2365	60.62327273	71.66666667	33.25	82.47484848	-2
03421011 94015 2365					-1
03421011 94015 2365	100	100	100	100	0
03421011 94015 2365					1
03421011 94015 2365	85.964	80	77.25	97.66	2
03421011 94015 2365	85.92763636			97.56909091	3
03421011 94015 2365	88		81	98	4
03421011 94015 2365	75.54721212	64.16666667	70	54.29	5
03421011 94015 2365	72.95090909	52.5	69.75	52.89	6
03421011 94015 2365	77	57	80	85	7
03421011 94015 2365	69	51	73	74	8
03421011 94015 2365					9
03421011 94015 2365	71	47	71	83	10
03421011 94015 2365		46		84	11
03421011 94015 2365					12
03421011 94015 2365					13

Figures 2-6 through 2-9 show AGE on the x-axis versus PCI_2, RUT_INDX, IRI_INDX, and CRACK_INDX, respectively, on the y-axis after Step 1 of the data preparation process.

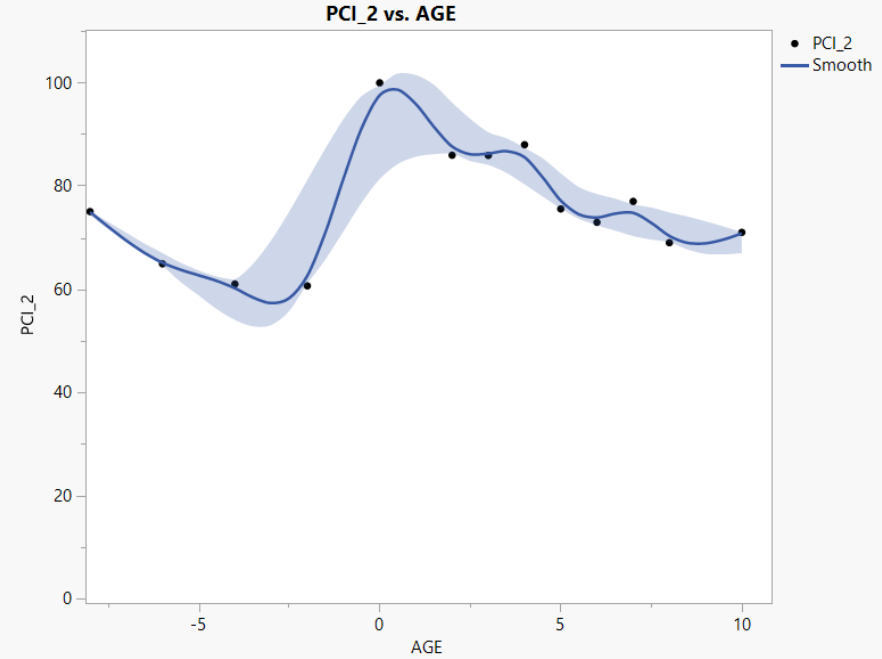

Figure 2-6. PCI_2 versus AGE after Step 1

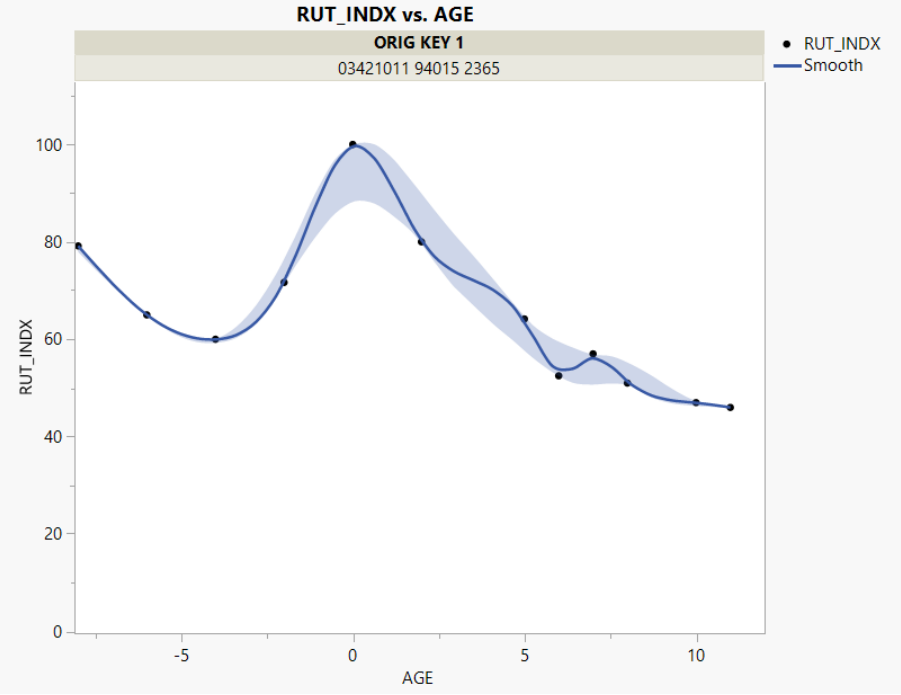

Figure 2-7. RUT_INDX versus AGE after Step 1

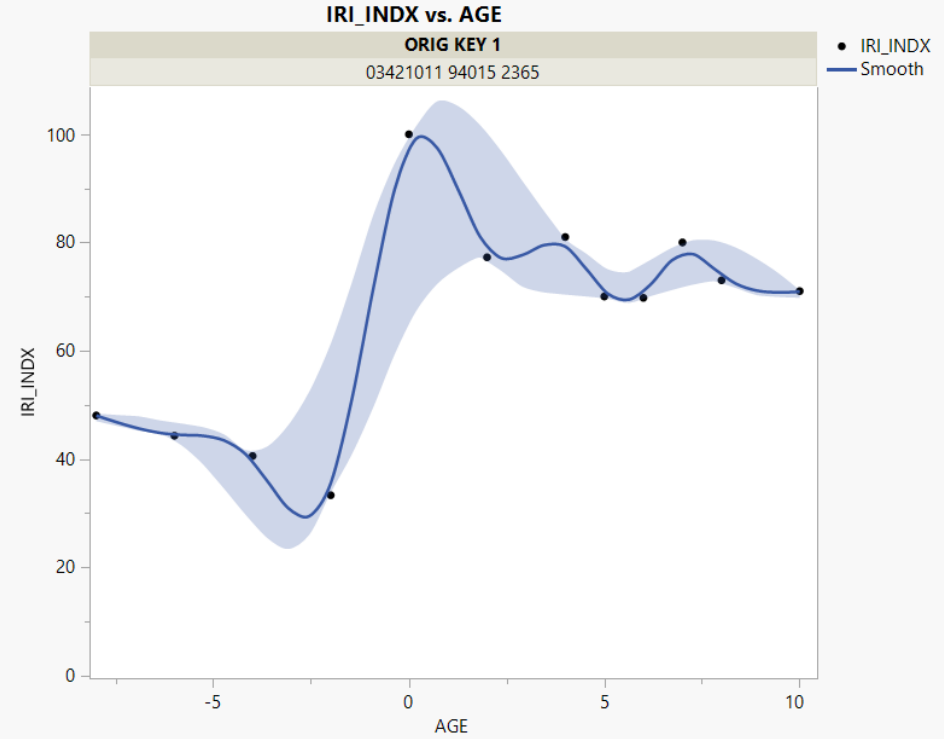

Figure 2-8. IRI_INDX versus AGE after Step 1

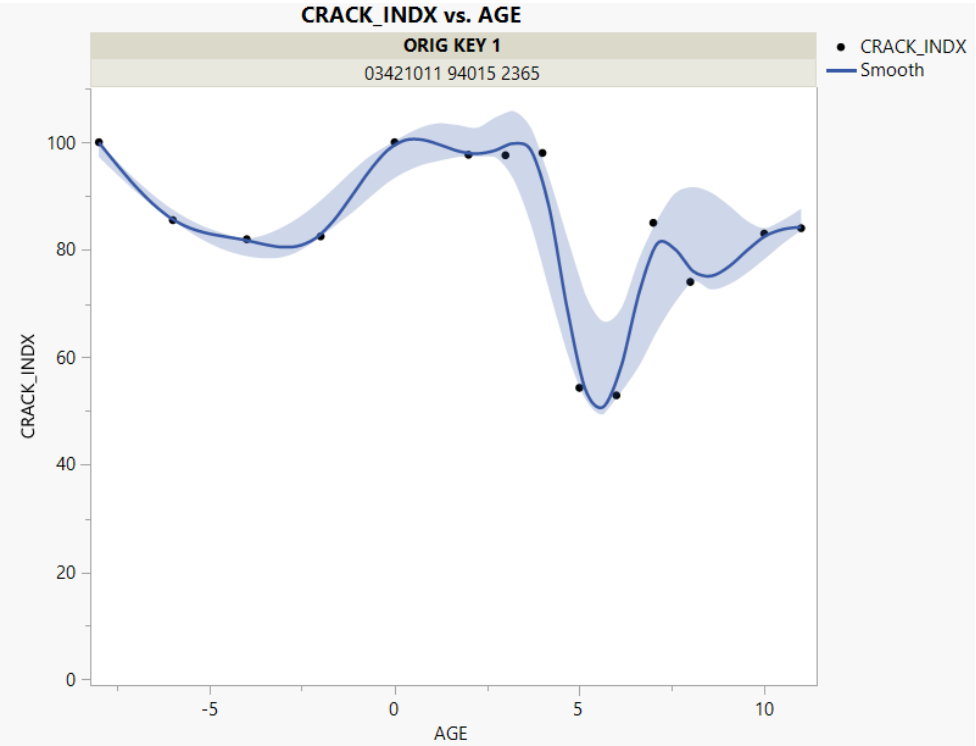

Figure 2-9. CRACK_INDX versus AGE after Step 1

2.5.2. Step 2

For the next step in the data preparation process, potential outliers are removed from the data. Outliers may include sudden large changes in index values that do not support the analysis of typical gradual deterioration relationships. A review of PCI_2, IRI_INDX, CRACK_INDX, and RUT_INDX versus AGE in Figures 2-6 to 2-9 shows that CRACK_INDX exhibits a sudden large change at the age of 5 and 6 years. This change is identified in Figure 2-10.

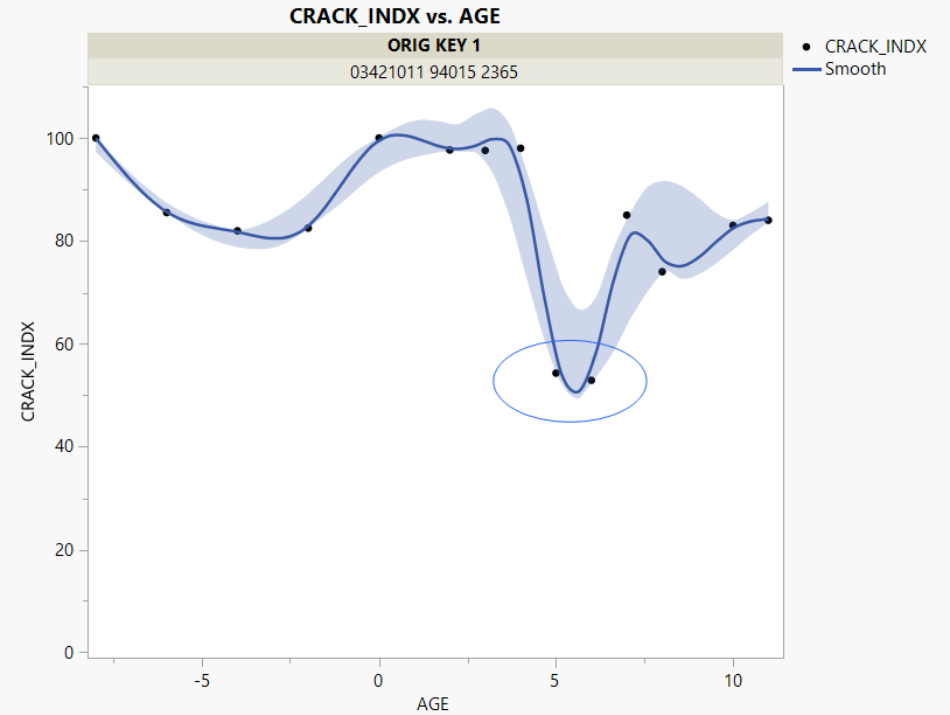

Figure 2-10. CRACK_INDX versus AGE after Step 1, with outlier values circled

As shown in Table 2-8, from AGE 4 to 6 the CRACK_INDX value drops from 98 to 52.89 for two years and increases back to 85 after two years, and from AGE 7 to 10 the CRACK_INDX value drops from 85 to 74 for one year and increases back to 83 after three years. Trends such as these are rarely seen on actual pavements. These outlier data (Table 2-8, red) are therefore excluded from the analysis. Table 2-9 shows the data after Step 2 is performed.

Table 2-8. Data preparation process Step 2 (outlier values highlighted)

ORIG KEY 1	PCI_2	RUT_INDX	IRI_INDX	CRACK_INDX	AGE
03421011 94015 2365	75.03333333	79.16666667	48	100	-8
03421011 94015 2365					-7
03421011 94015 2365	64.89672727	65	44.25	85.49181818	-6
03421011 94015 2365					-5
03421011 94015 2365	60.979	60	40.5	81.9475	-4
03421011 94015 2365					-3
03421011 94015 2365	60.62327273	71.66666667	33.25	82.47484848	-2
03421011 94015 2365					-1
03421011 94015 2365	100	100	100	100	0
03421011 94015 2365					1
03421011 94015 2365	85.964	80	77.25	97.66	2
03421011 94015 2365	85.92763636			97.56909091	3
03421011 94015 2365	88		81	98	4
03421011 94015 2365	75.54721212	64.16666667	70	54.29	5
03421011 94015 2365	72.95090909	52.5	69.75	52.89	6
03421011 94015 2365	77	57	80	85	7
03421011 94015 2365	69	51	73	74	8
03421011 94015 2365					9
03421011 94015 2365	71	47	71	83	10
03421011 94015 2365		46		84	11
03421011 94015 2365					12
03421011 94015 2365					13

Table 2-9. Data preparation process Step 2 (outlier values removed)

ORIG KEY 1	PCI_2	RUT_INDX	IRI_INDX	CRACK_INDX	AGE
03421011 94015 2365	75.03333333	79.16666667	48	100	-8
03421011 94015 2365					-7
03421011 94015 2365	64.89672727	65	44.25	85.49181818	-6
03421011 94015 2365					-5
03421011 94015 2365	60.979	60	40.5	81.9475	-4
03421011 94015 2365					-3
03421011 94015 2365	60.62327273	71.66666667	33.25	82.47484848	-2
03421011 94015 2365					-1
03421011 94015 2365	100	100	100	100	0
03421011 94015 2365					1
03421011 94015 2365	85.964	80	77.25	97.66	2
03421011 94015 2365	85.92763636			97.56909091	3
03421011 94015 2365	88		81	98	4
03421011 94015 2365	75.54721212	64.16666667	70		5
03421011 94015 2365	72.95090909	52.5	69.75		6
03421011 94015 2365	77	57	80	85	7
03421011 94015 2365	69	51	73		8
03421011 94015 2365					9
03421011 94015 2365	71	47	71	83	10
03421011 94015 2365		46		84	11
03421011 94015 2365					12
03421011 94015 2365					13

2.5.3. Step 3

Step 3 of the data preparation process is executed to focus the analysis on the pavement's performance after CIR construction. In Step 3, all data recorded before CIR construction are excluded from the analysis input, and the starting points for all graphs are set at AGE 0. Figures 2-11 through 2-14 show PCI_2, RUT_INDX, IRI_INDX, and CRACK_INDX on the y-axis, respectively, versus AGE on the x-axis, where 0 is the year when CIR construction occurred.

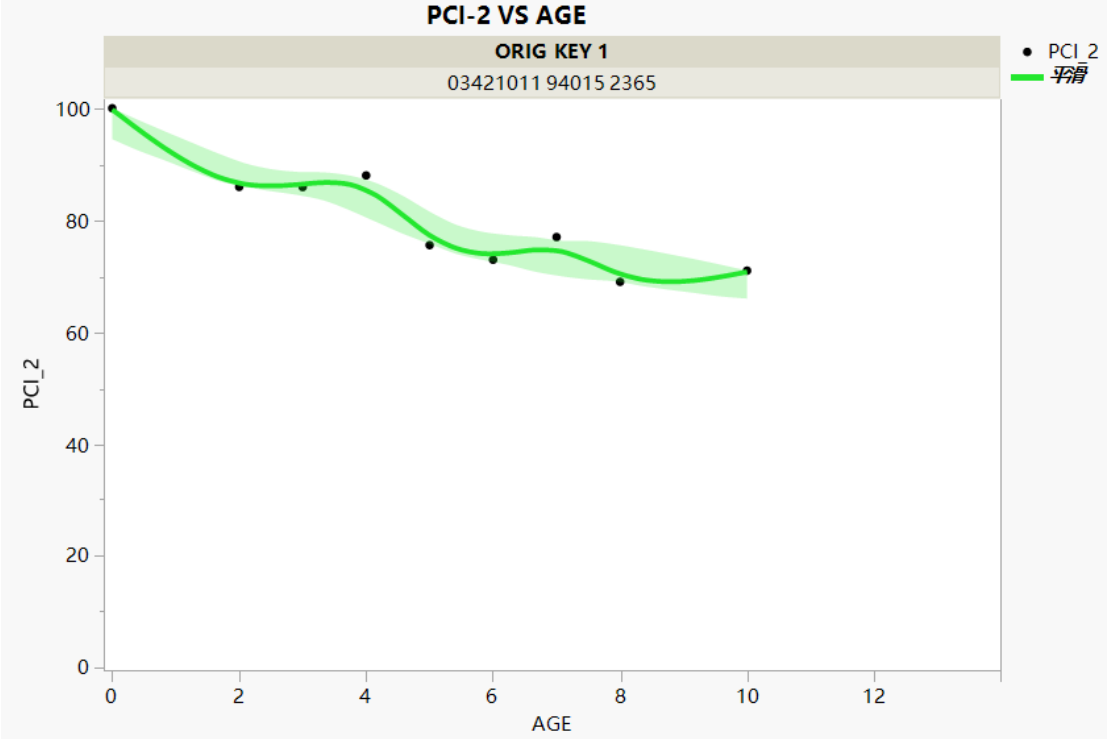

Figure 2-11. PCI_2 versus AGE after Step 3

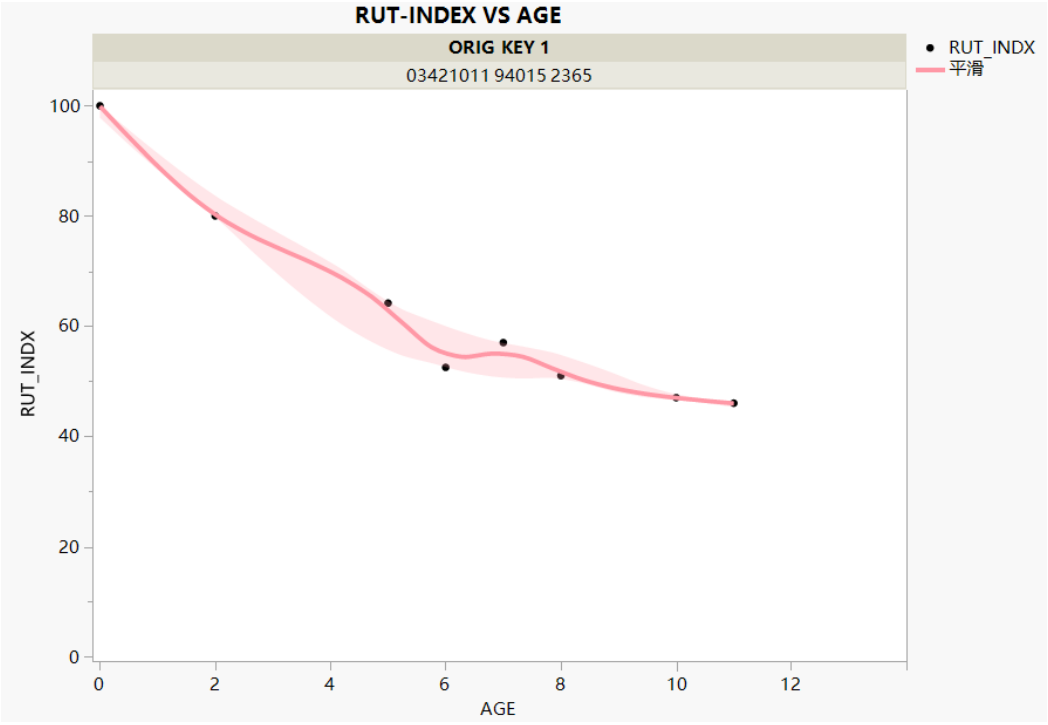

Figure 2-12. RUT_INDX versus AGE after Step 3

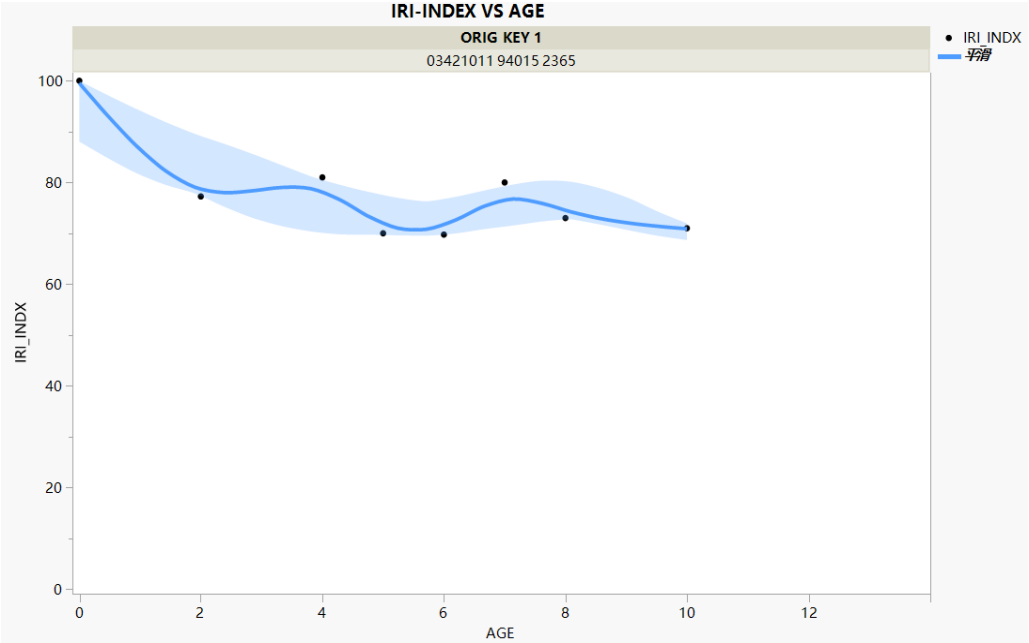

Figure 2-13. IRI_INDX versus AGE after Step 3

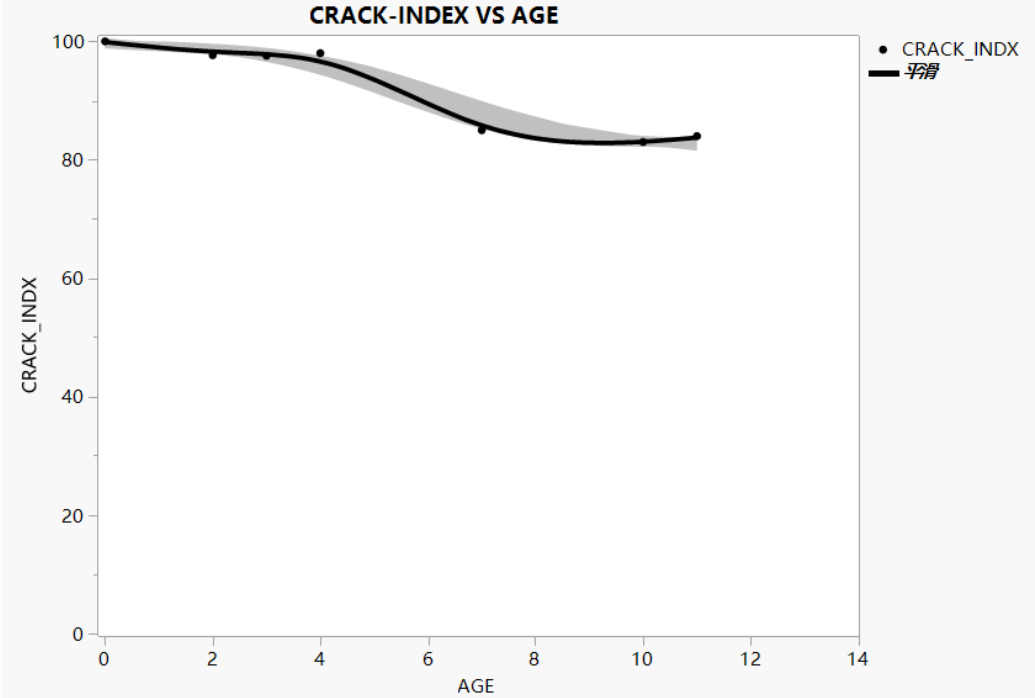

Figure 2-14. CRACK_INDX versus AGE after Step 3

When using the PMIS database, repeated data, unexpected zero values, and outliers can make the data difficult to analyze. After the data preparation process is performed, researchers can use the prepared data to analyze CIR performance by comparing the pavement performance parameters after CIR construction. The prepared data could also be used to develop long-term evaluations of

CIR performance and to carry out other CIR-related research. In the next section, prepared PMIS data are used in a series of case studies.

2.6. Initial Analysis of a Subset of the Prepared Data

Case studies using prepared PMIS data can help researchers assess how various parameters, including CIR layer thickness (inches), traffic volume (AADT), and other parameters, may influence the long-term performance of a pavement that includes a CIR layer.

For the analysis described in this section, 10 projects were selected and grouped based on their PCI_2 values (5 projects with good performance and 5 projects with poor performance), and case studies were performed by comparing these 10 projects. If a project's PCI_2 value was still above 70 after 10 years after CIR, that project was designated as having good performance. Otherwise, it was designated as having poor performance. The project ORIG KEYs for the selected pavements are shown in Table 2-9. The project locations designated by the last 4 digits of the ORIG KEYs are shown in Figure 2-15.

Table 2-9. Project information for case studies

ORIG KEY 1	Project Number	Good/Poor PCI_2
03421176 82181 4990	NHSX-034-7(139) --3H-90	Good
00231085 86091 3580	STP-002-4(41) --2C-80	Good
01531055 42063 7232	STP-15-4(10) --2C-32	Good
06921125 84127 3485	STP-069-5(92) --2C-85	Good
14131119 67122 6725	STP-141-5(15) --2C-39	Good
04431022 52028 9983	STP-44-2(42) --2C-83	Poor
03421015 23020 4165	NHSN-034-1(75) --2R-65	Poor
02531048 97057 0001	STPN-25-3(19) --2J-01	Poor
02531058 26071 2101	STPN-25-3(19) --2J-01	Poor
04431078 64088 7025	STP-44-4(40) --2C-39	Poor

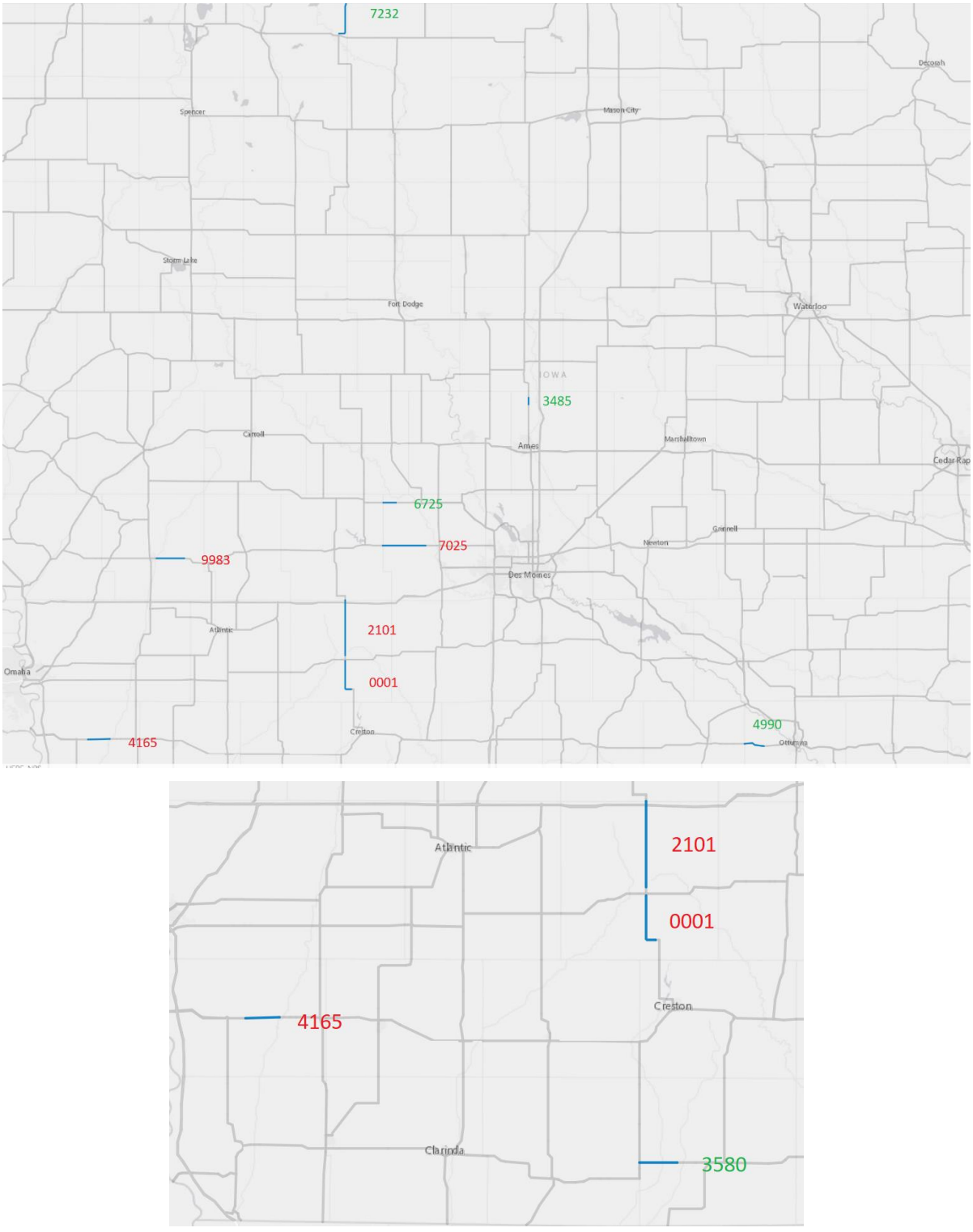

Figure 2-15. Project locations for case studies

The complete set of prepared PMIS data, including PCI_2, RUT_INDX, IRI_INDX, and CRACK_INDX, are provided in Appendix A for projects having good performance and Appendix B for projects having poor performance. Using this information, Figures 2-16 through

2-23 were developed with PCI_2, RUT_INDX, IRI_INDX, and CRACK_INDX, respectively, on the y-axis versus AGE on the x-axis for both projects having good performance and projects having poor performance.

Projects having good performance are illustrated in Figures 2-16 through 2-19.

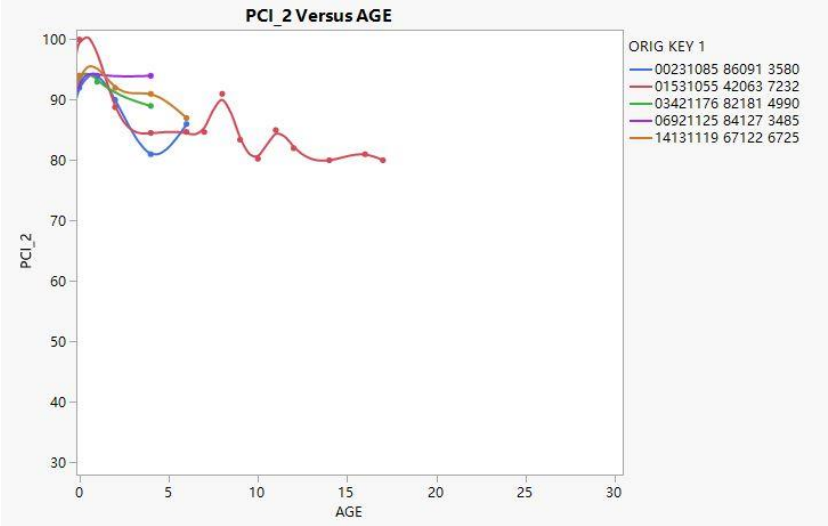

Figure 2-16. PCI_2 versus AGE for projects having good performance

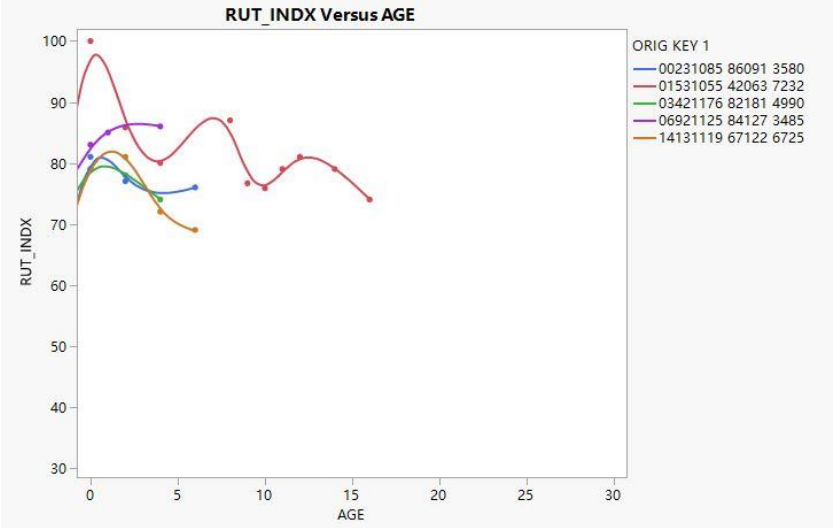

Figure 2-17. RUT_INDX versus AGE for projects having good performance

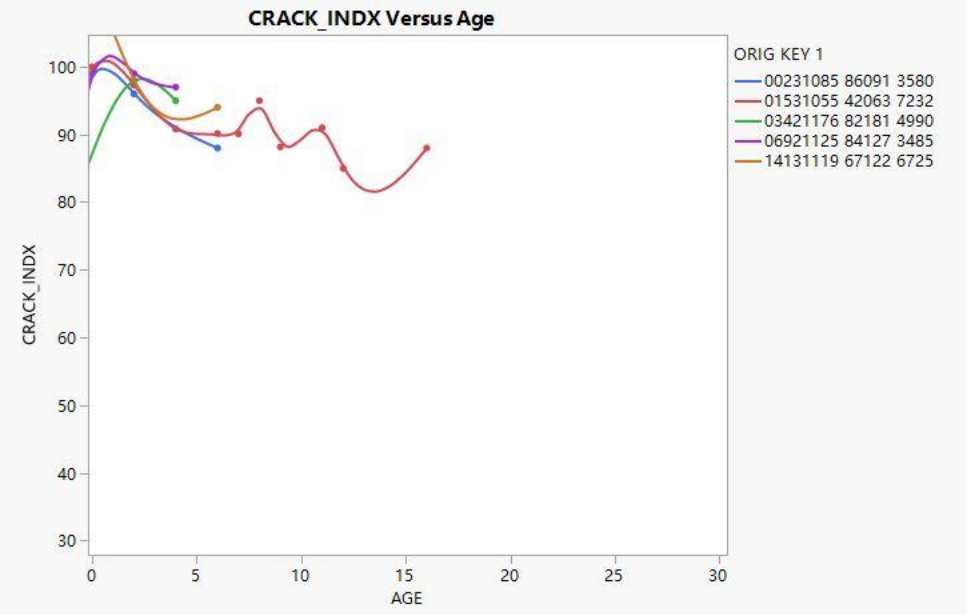

Figure 2-18. CRACK_INDX versus AGE for projects having good performance

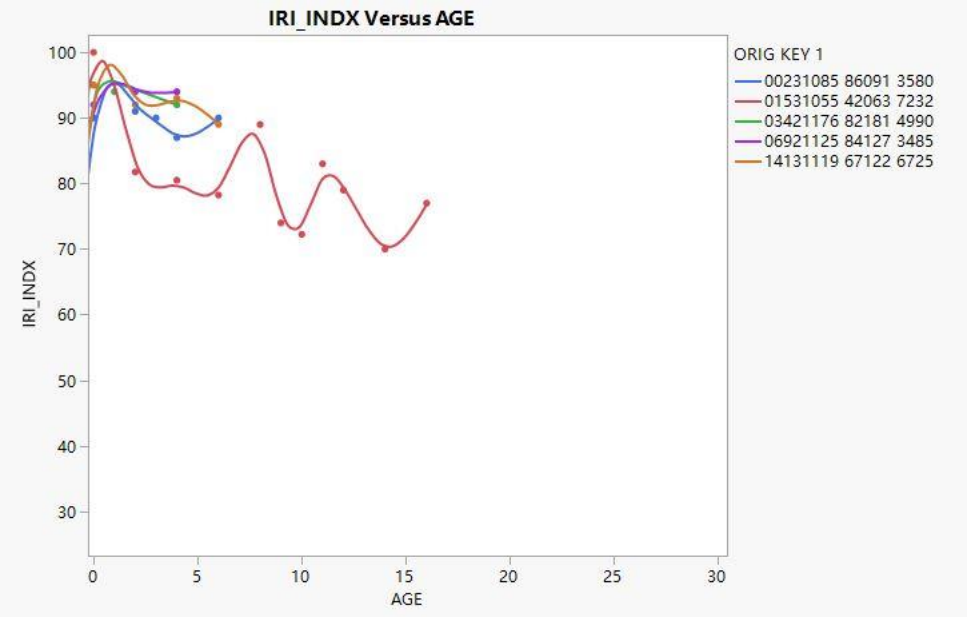

Figure 2-19. IRI_INDX versus AGE for projects having good performance

Projects having poor performance are illustrated in Figures 2-20 through 2-22.

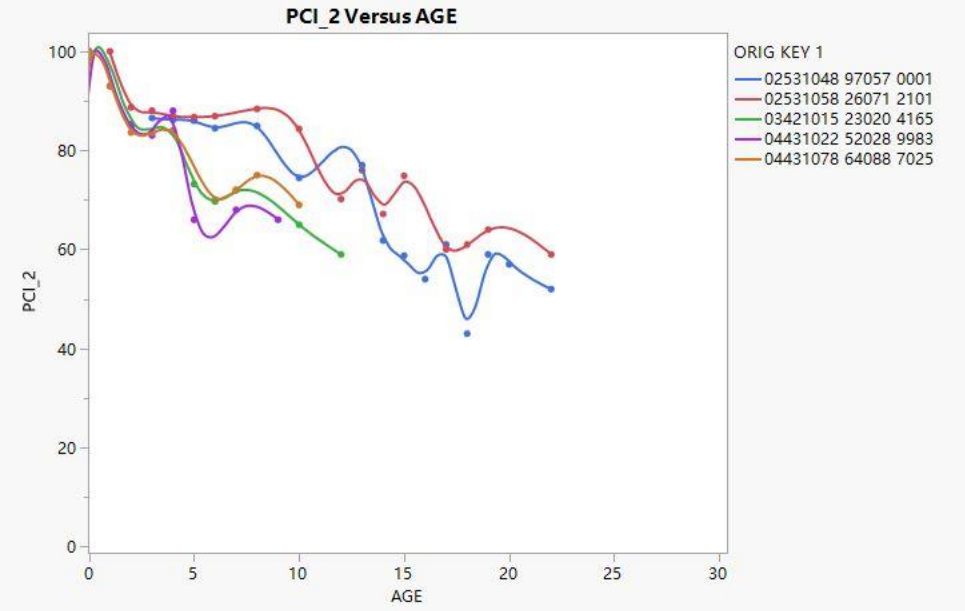

Figure 2-20. PCI_2 versus AGE for projects having poor performance

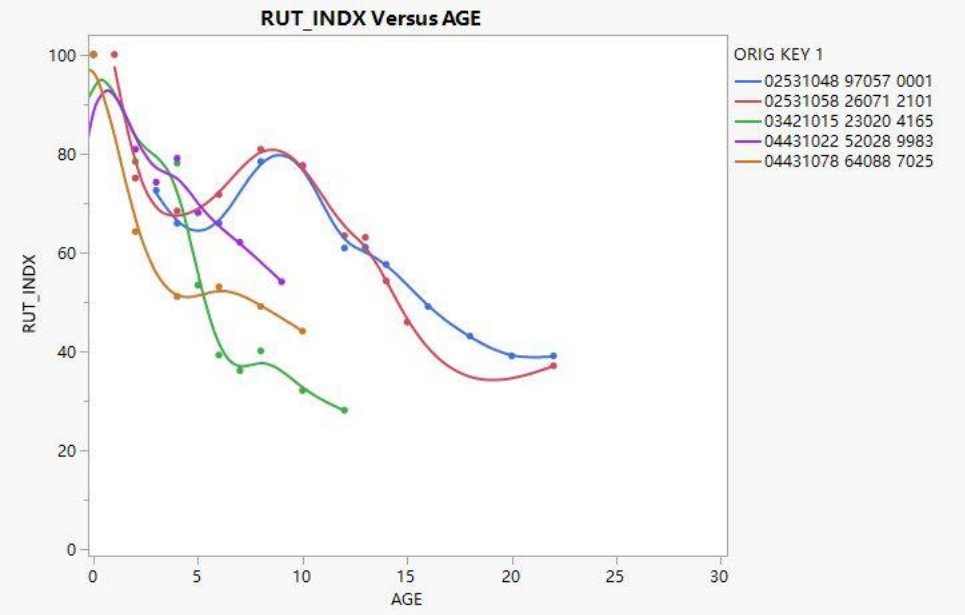

Figure 2-21. RUT_INDX versus AGE for projects having poor performance

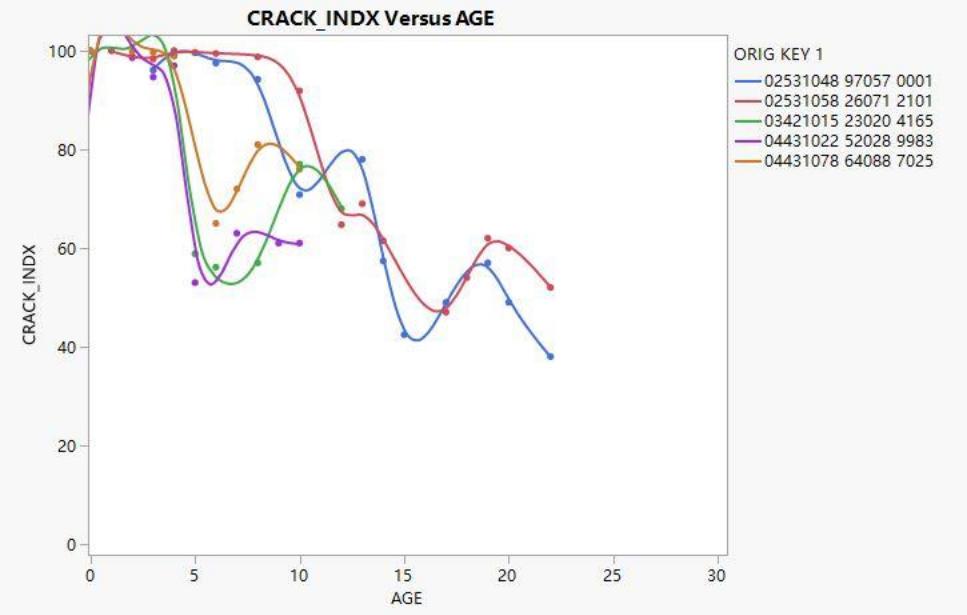

Figure 2-22. CRACK_INDX versus AGE for projects having poor performance

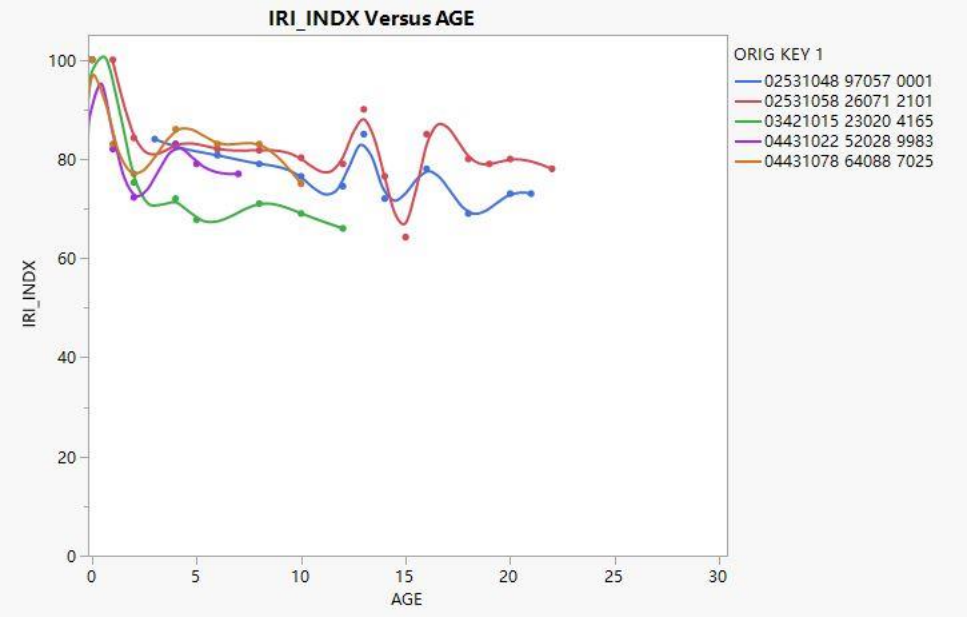

Figure 2-23. IRI_INDX versus AGE for projects having poor performance

For Figures 2-16 to 2-23, all data end in 2019. The age of the pavement since recycling occurred depends on the year when recycling occurred, with shortened data streams indicating that recycling occurred more recently. Even though the PMIS data were prepared, some fluctuations in index values are evident. The possible causes are differences in how the measurement equipment is calibrated and set up from year to year, unrecorded maintenance efforts that result in temporary improvement for one or two measurement cycles, and sudden pavement deterioration that was detected in one measurement cycle and corrected shortly after.

After comparing RUT_INDX, IRI_INDX, and CRACK_INDX versus AGE in Figures 2-16 to 2-23 for projects having good performance and projects having poor performance, RUT_INDX appears noticeably lower than IRI_INDX and CRACK_INDX, which indicates that rutting appears to be the parameter that contributes most to declining pavement performance.

2.7. Analysis of Projects with CIR Age Greater than 10 Years

Since most of the selected projects that exhibit good performance do not have an AGE over 10 years, six additional projects with an AGE over 10 years were selected to better analyze performance, including three projects with good performance and three projects with poor performance. These projects were added because the short-lived projects exhibiting good performance have not proved that they can remain in good condition over a longer timeframe. Figures 2-24 to 2-27 show PCI_2, RUT_INDX, IRI_INDX, and CRACK_INDX, respectively, on the y-axis versus AGE on the x-axis.

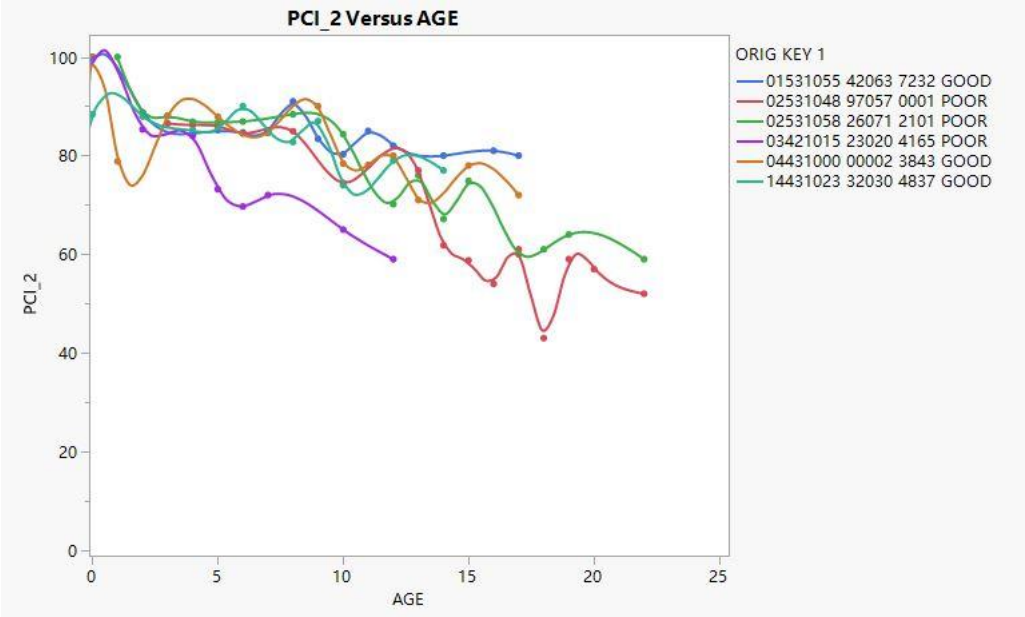

Figure 2-24. PCI_2 versus AGE for six additional projects

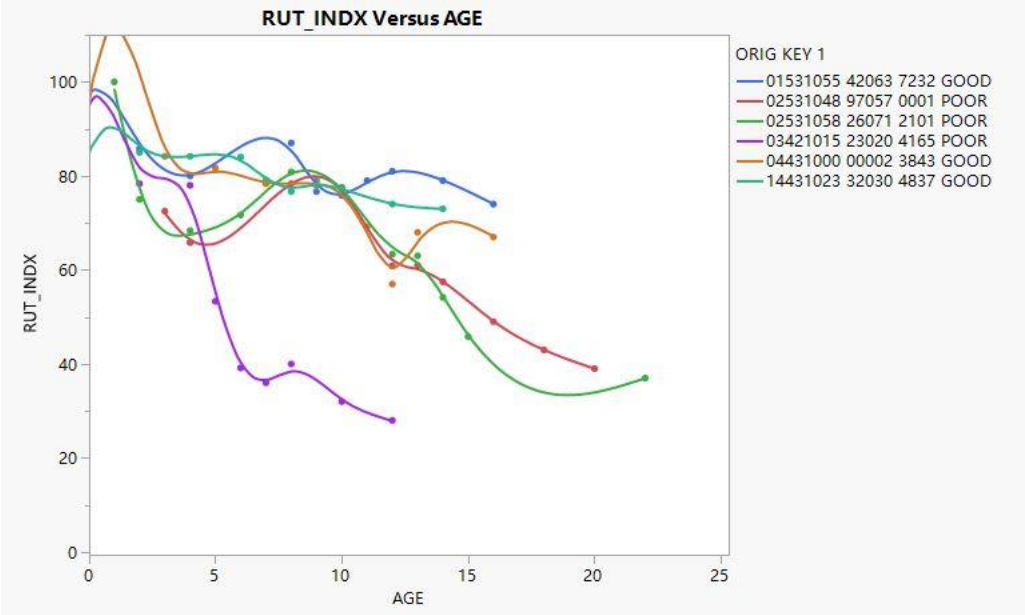

Figure 2-25. RUT_INDX versus AGE for six additional projects

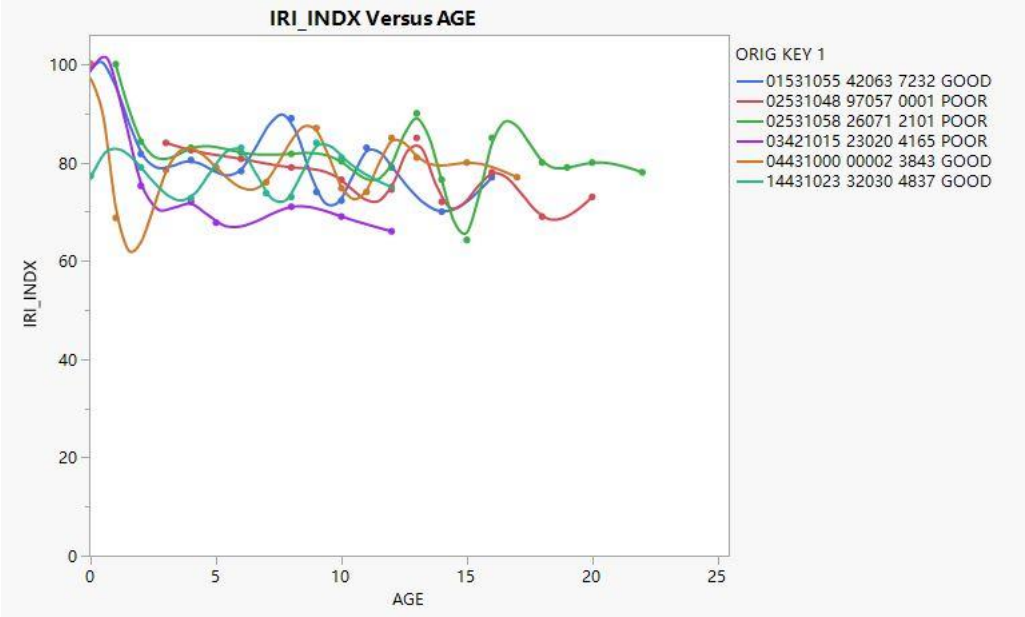

Figure 2-26. IRI_INDX versus AGE for six additional projects

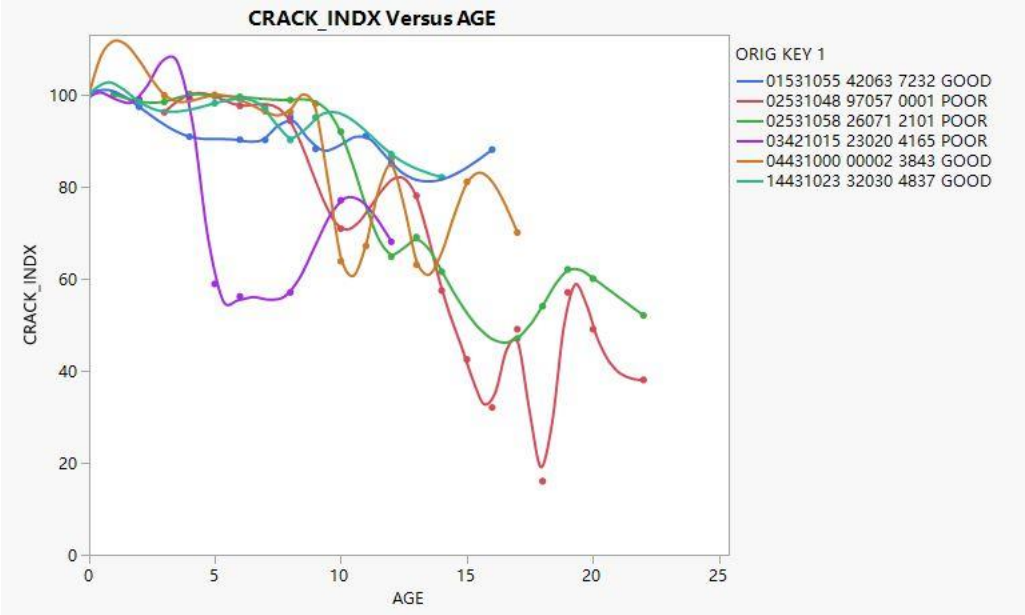

Figure 2-27. CRACK_INDX versus AGE for six additional projects

In Figures 2-24 to 2-27, the largest decrease occurred from an AGE of 10 to 15 years, which suggests that for CIR projects that are similar to those selected, noticeable pavement distress is most likely to occur 10 to 15 years after CIR is performed.

2.8. Analysis of Traffic Volume

Traffic volume, especially heavy (truck) traffic volume, could be another parameter that would affect long-term pavement performance. The AADT and the heavy (truck) traffic volume (TRUCKS) are defined in the metadata (Table 2-3) for the projects shown in Figures 2-28 to 2-31. The data used to develop these figures are provided in Appendix C.

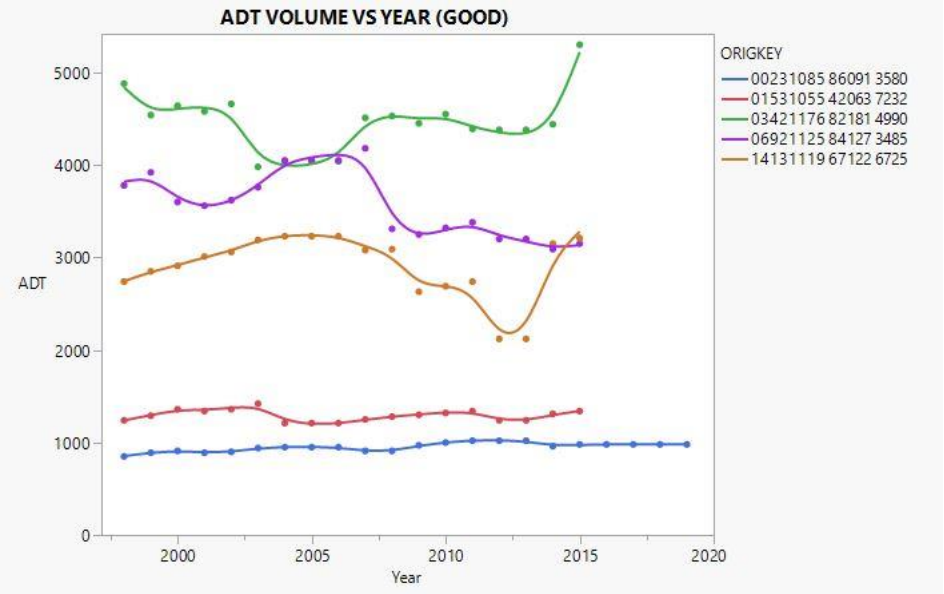

Figure 2-28. ADT VOLUME versus YEAR for projects having good performance

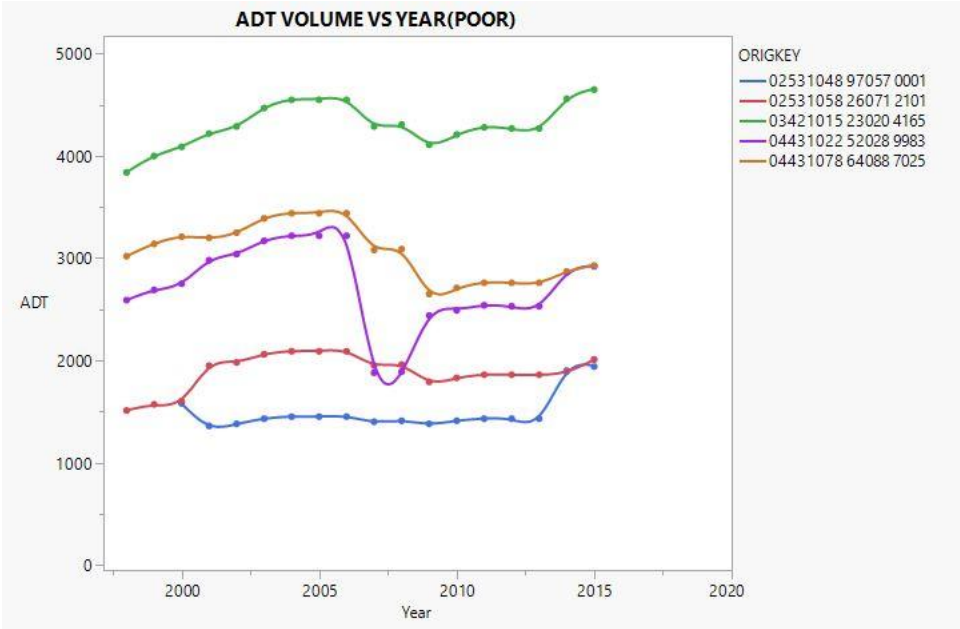

Figure 2-29. ADT VOLUME versus YEAR for projects having poor performance

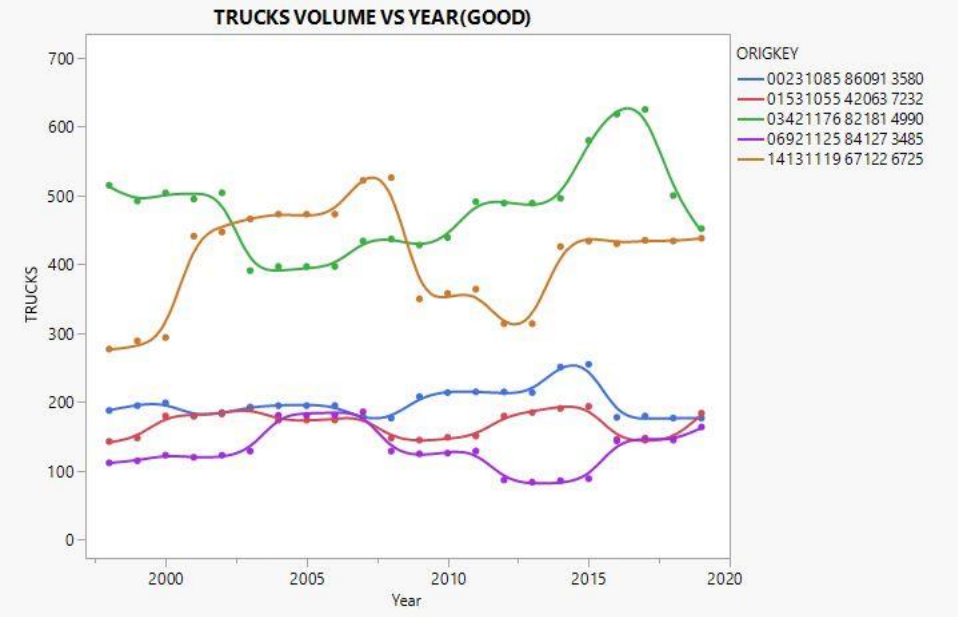

Figure 2-30. TRUCK VOLUME versus YEAR for projects having good performance

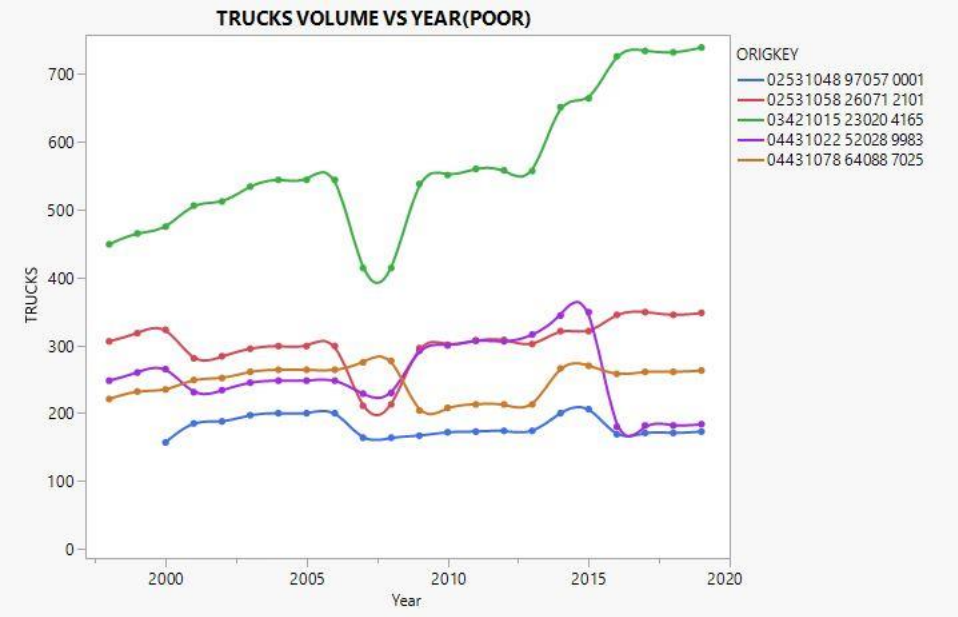

Figure 2-31. TRUCK VOLUME versus YEAR for projects having poor performance

In the figures, the ADT volume is on the y-axis and the corresponding year is on the x-axis. A comparison of the ADT volume versus year for projects having good/poor performance indicates that ADT volume does not have a noticeable impact on the long-term performance of the pavement. A comparison of the actual ADT volume indicates that both projects having good performance and projects having poor performance had ADT volumes of 1,000 to 5,000. A comparison of the actual truck volume indicates that both projects having good performance and projects having poor performance had truck volumes of 200 to 600. In Figure 2-31, the section

with ORIGKEY 03421015 23020 4165 experienced the largest truck volume increase between the years 2000 and 2020. This increase may have contributed to the earlier pavement distress for this project.

When engineers design pavements, traffic volume, especially heavy (truck) traffic volume, is considered to be an important design factor, and therefore high ADT volumes and expected increases in traffic volume are accounted for in pavement design. An interesting circumstance can be discerned by observing Figures 2-28 to 2-31: For these roads, traffic volume and truck volume did not linearly increase, as a planner might typically assume. In fact, the traffic volume and truck volume fluctuated for various reasons.

2.9. Survival Analysis

A survival analysis was conducted to ascertain the performance of the CIR projects over their lifetimes regarding the distresses that were declared to cause failure.

The declared distresses included overall cracking, transverse cracking, longitudinal cracking, longitudinal wheel path cracking, roughness, rutting, and generally poor pavement performance. These were measured by the corresponding indices of CRACK_INDEX, TCRACK, LCRACK, LCRACKW, IRI_INDEX, RUT_INDEX, and PCI_2. In this analysis, failure was declared to occur when any of the previously mentioned indices fell below 70. Year zero was taken as the year that CIR construction occurred. Upon failure, the pavement was "censored," and the number of years that had elapsed since CIR construction and the cause of failure were noted. Any pavement that was not censored during the analysis period was deemed to have survived. A distribution of the various types of distress along with their censoring counts is shown in Figure 2-32.

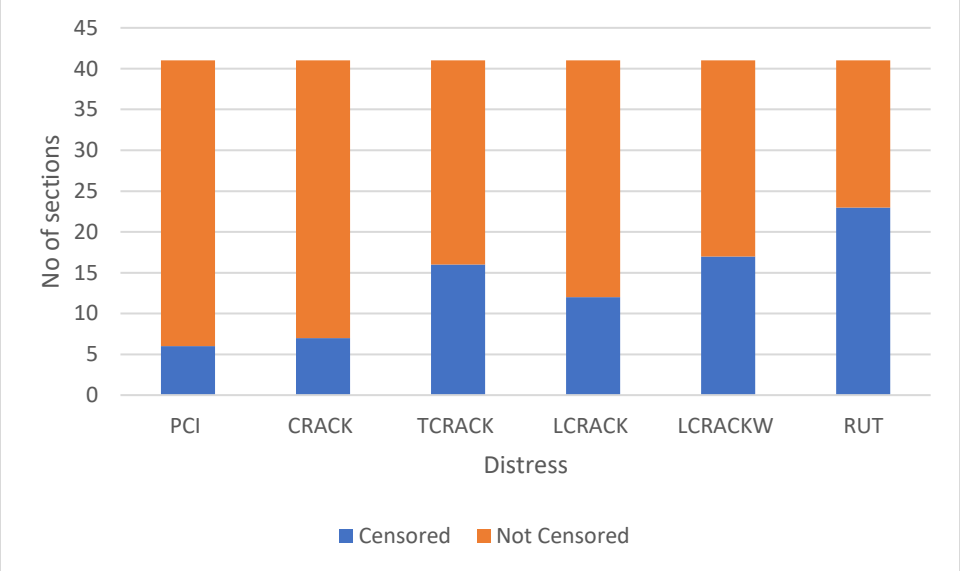

Figure 2-32. Censoring by distress type/pavement condition

Figure 2-32 shows that the highest number of failed (censored) sections were from rutting, followed by longitudinal wheel path and transverse cracking.

Figure 2-33 shows graphically which indices contribute to the pavement condition index (PCI_2) and the cracking index (CRACK_INDX).

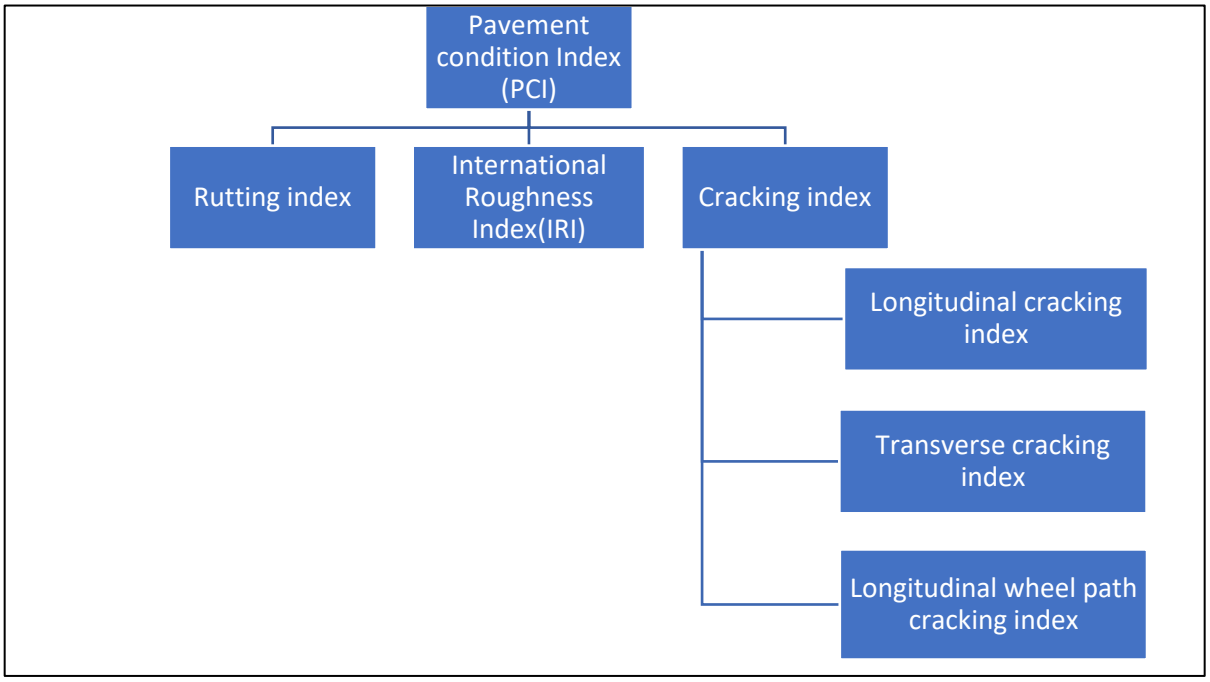

Figure 2-33. Relationship among distress indices

PCI_2 is calculated with contributions from CRACK_INDX, RUT_INDX, and IRI_INDX. If failure is considered in terms of PCI_2, failure can be declared on account of overall poor pavement performance as well as cracking, rutting, or roughness individually. Six pavement sections met the failure criteria on account of their PCI_2 values, which is the lowest number of failures attributed to any of the indices. The overall cracking index of the pavement is calculated with contributions from the individual cracking indices (T_INDX, L_INDX, and LW_INDX) according to Equation 2-2. If failure is considered in terms of CRACK_INDX, failure can be declared on account of overall poor cracking performance as well as each specific type of cracking individually.

Figure 2-34 shows a plot of the probability of survival versus pavement age. Survival is defined as a condition where the distress index under analysis does not fall below the threshold value of 70.

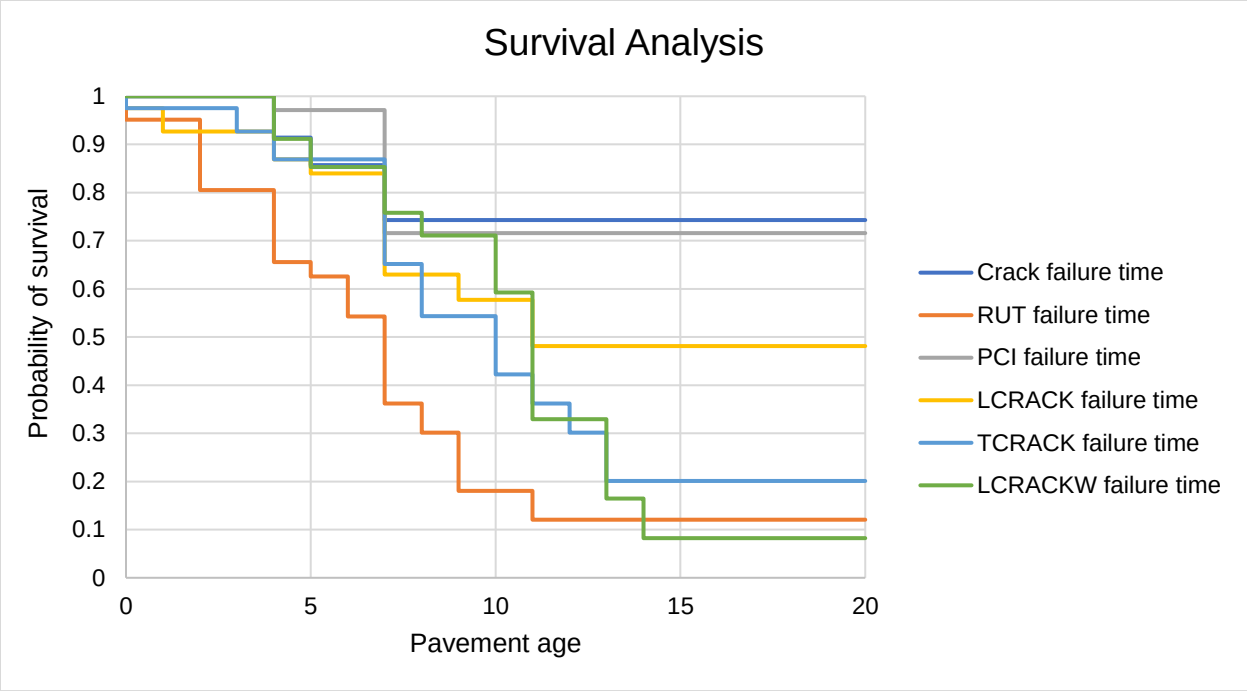

Figure 2-34. Survival time for CIR pavements by distress

Survival against rutting had the lowest probability among all of the indices analyzed. The various modes of cracking (i.e., longitudinal, longitudinal wheel path, and transverse cracking) all showed similar probabilities of survival for up to 10 years, with transverse and longitudinal wheel path cracking showing the lowest probability of survival at the end of the 20-year predicted CIR lifespan. Survival against rutting dropped below 50% at 7 years, compared to 10 to 11 years for the three cracking sub-indices. The probability of survival for CRACK_INDX and PCI_2 was above 50% throughout the 20-year analysis period. After 11 years of age, less than 50% of the pavements analyzed met the survival criteria for any of the individual cracking indices, with distresses like transverse cracking and longitudinal wheel path cracking having 20% and 9% probabilities of survival, respectively.

2.10. Multivariate Analysis

To identify the most important variables that affect CIR performance, a multivariate analysis was carried out on the data for the various CIR sections. The procedure involved in the multivariate analysis is explained below

2.10.1. Determining a Classification Metric for CIR Pavements

To differentiate between CIR sections with satisfactory and unsatisfactory performance, a metric summarizing each section's performance was required. While distress indicators like the pavement condition index (PCI_2), rutting index (RUT_INDX), and cracking index (CRACK_INDX) are useful performance metrics, these indices are age dependent and do not represent changes in the performance of a project over an observed period. However, the trends

observed for the various indices can be used as an indicator of changes in performance over a given period. For this study, the trend observed for PCI_2 was selected as the metric for classifying CIR section performance.

A linear model was used to fit the PCI_2 values of each CIR section versus time, and the slope of each fit was used as a performance indicator. Although pavement deterioration does not typically follow a linear trajectory, the purpose of a linear fit in this instance was only to calculate the slope of the relationship between PCI_2 and age and not to predict or forecast PCI_2 values over time. In other words, employing a linear fit to determine the slope of each pavement's PCI_2 values over time provided a metric for classifying the performance of each CIR project. Figure 2-35 shows the linear fits of PCI_2 versus age for various CIR sections.

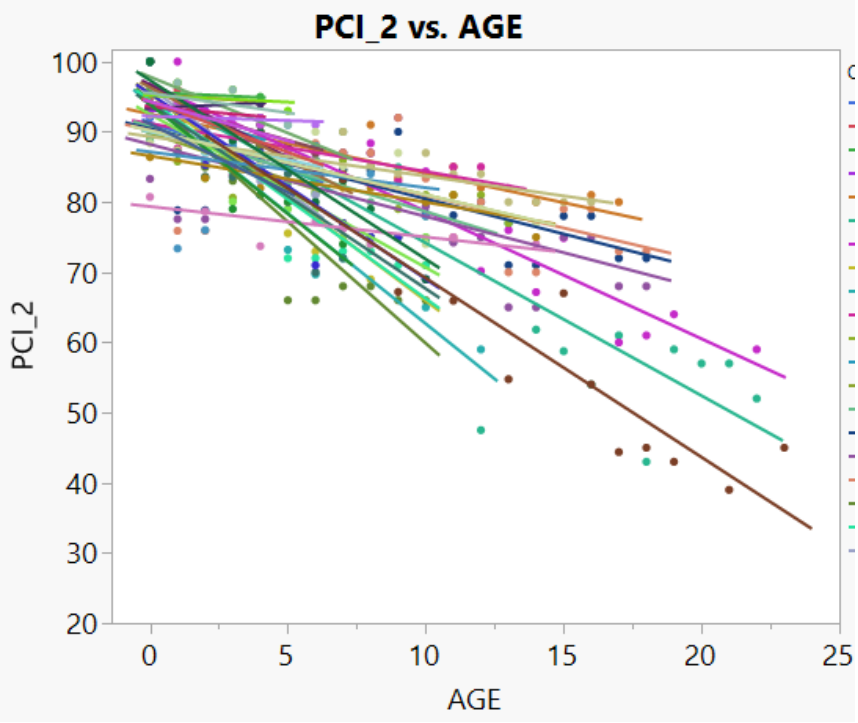

Figure 2-35. Linear fits of PCI_2 versus age

2.10.2. Correlation between Independent and Dependent Variables

To perform a multivariate analysis, correlation coefficients between distress indices, traffic variables, pavement thickness, and structural data first needed to be calculated.

A correlation occurs when a relationship exists between two variables in a dataset, such that altering the first variable leads to a corresponding change in the second variable and vice versa. Correlations can be either positive or negative, depending on the relationship they share in the dataset. A positive correlation indicates that an increase in one variable leads to an increase in the other variable. On the other hand, a negative correlation indicates that an increase in one variable leads to a decrease in the other. A strong correlation has a correlation coefficient close

to +1 or -1, while a weak correlation has a correlation coefficient near zero. The advantage of calculating correlations is that doing so simplifies the process of identifying independent variables in a multivariate analysis, since likely significant effects can be predetermined by examining the correlations between the independent and dependent variables.

Table 2-10 presents the correlation coefficients among the distress indices for CIR pavements of all ages in the PMIS. Correlation coefficients with a magnitude greater than 0.5 are considered to have a greater magnitude of significance than coefficients with a magnitude less than 0.5 and are highlighted with bold numbers. Any correlation with a magnitude less than 0.2 is not considered to be statistically significant. Positive correlations greater than 0.20 are denoted in blue, while negative correlations less than 0.20 are denoted in red.

Table 2-10. Correlation coefficients among PMIS variables for sections of all ages (0–20 years)

Row	PCI slope	PCI_2	CRACK_INDX	IRI (in./mi)	RUT (in.)
PCI slope	**1.00**	0.08	0.15	0.00	-0.04
PCI_2	0.08	**1.00**	**0.87**	**-0.71**	**-0.80**
CRACK_INDX	0.15	**0.87**	**1.00**	-0.41	**-0.60**
IRI (in./mi)	0.00	**-0.71**	-0.41	**1.00**	**0.50**
RUT (in.)	-0.04	**-0.80**	**-0.60**	**0.50**	**1.00**
STRUC80	0.04	0.09	0.00	-0.07	0.10
STRUCAV	0.03	0.09	-0.02	-0.04	0.12
ADT	-0.31	-0.04	-0.01	0.01	0.21
TRUCKS	-0.08	0.06	0.03	-0.10	0.14
PAVTHICK (in.)	-0.06	0.20	0.11	-0.04	-0.11
SURTHK (in.)	0.37	-0.18	-0.08	0.29	-0.02
BASTHK1 (in.)	0.31	-0.24	-0.13	0.28	0.12
SUBTHK1 (in.)	0.27	-0.03	-0.05	-0.05	0.02
AGE	0.12	**-0.74**	**-0.72**	0.48	**0.64**

The correlation coefficients in Table 2-10 show that the PCI_2 values of the CIR sections have correlations with distress variables such as IRI, rut depth, and cracking index. This is to be expected because the value of PCI_2 is derived from the values of these individual distress indices. There is also a correlation between PCI_2 and age, and since older pavements tend to have lower PCI_2 values, the correlation is negative. There is a weak correlation between PCI_2 and the thickness of pavement base layers. There are no significant correlations between PCI_2 and traffic variables such as the number of trucks or ADT or between PCI_2 and structural variables such as surface, subgrade (CIR layer), and overall pavement thickness, since correlation coefficients are derived from an analysis of data from pavements of all ages after CIR construction, i.e., 0- to 20-year-old sections. This could indicate that PCI_2 does not correlate with these structural variables over a broad spectrum of ages, but correlations might be observed if a smaller timeframe were considered. However, the slope of the PCI curve shows weak correlations with the pavement layer (surface, CIR layer, and base) thickness variables as well as

with ADT, indicating that performance trends across the life of the pavement might be modestly influenced by layer thickness and traffic.

Table 2-11 shows correlation coefficients over a narrower range of pavement ages (6 to 10 years). While the PCI slope has correlations with variables similar to those observed in Table 2-10, more variables seem to correlate with PCI_2 in Table 2-11. These include structural and traffic variables, while surface and subgrade (CIR) layers also show correlations with PCI_2. These correlations appear strongest within this range of pavement ages, indicating a potential timeline in which the structure, traffic level, and layer thicknesses of CIR sections begin to have an impact on overall performance. In simpler terms, significant differences between CIR pavements having good performance and those having poor performance are likely to be noticed in this time window.

Table 2-11. Correlation coefficients among PMIS variables for sections with ages between 6 and 10 years

Row	PCI slope	PCI_2	CRACK_INDX	IRI (in./mi)	RUT (in.)
PCI slope	**1.00**	**0.66**	**0.62**	-0.36	**-0.51**
PCI_2	**0.66**	**1.00**	**0.88**	**-0.65**	**-0.67**
CRACK_INDX	**0.62**	**0.88**	**1.00**	-0.39	**-0.51**
IRI (in./mi)	-0.36	**-0.65**	-0.39	**1.00**	0.28
RUT (in.)	**-0.51**	**-0.67**	**-0.51**	0.28	**1.00**
STRUC80	-0.14	-0.22	-0.23	0.13	0.46
STRUCAV	-0.12	-0.26	-0.27	0.21	**0.52**
ADT	-0.40	**-0.57**	-0.36	0.41	**0.73**
TRUCKS	-0.10	-0.16	-0.08	0.08	0.47
PAVTHICK (in.)	-0.16	-0.12	-0.18	0.11	0.24
SURTHK (in.)	0.41	0.22	0.24	0.08	-0.45
BASTHK1 (in.)	0.25	0.00	0.11	0.18	-0.11
SUBTHK1 (in.)	0.38	0.32	0.37	-0.21	-0.29

An analysis of variance (ANOVA) was performed, and the results presented in Table 2-12 can provide insight into the factors influencing CIR performance and bolster inferences from the case studies considered in the survival analysis. The significance level, alpha, was set to 0.05.

Table 2-12. Parameter estimates for model fit

Equation Term (x_n)	Regression Coefficient (a_n)	Prob>|t|
Intercept (k)	1.368	0.0388
ADT	-8.23×10^{-5}	0.1430
SURTHK	1.695	**0.0013**
BASTHK1	-1.050	0.0403
SUBTHK1	-0.438	**<.0001**
ADT x SURTHK	0.000	0.6999
ADT x BASTHK1	-0.001	0.1587
ADT x SUBTHK1	0.000	0.0302
SURTHK1 x BASTHK1	-10.504	**0.0001**
SURTHK1 x SUBTHK1	3.349	**0.0031**
BASTHK1 x SUBTHK1	-3.580	**0.0003**

Table 2-12 indicates that the individual pavement layer thicknesses are likely significant for the pavement distress factor. ADT shows its influence on the pavement distress factor through interactions with the CIR layer thickness (SUBTHK1). Other possibly significant interactions are observed between individual layer thicknesses.

Figure 2-36 shows a three-dimensional plot of CIR thickness (i.e., SUBTHK1), ADT, and the pavement distress factor.

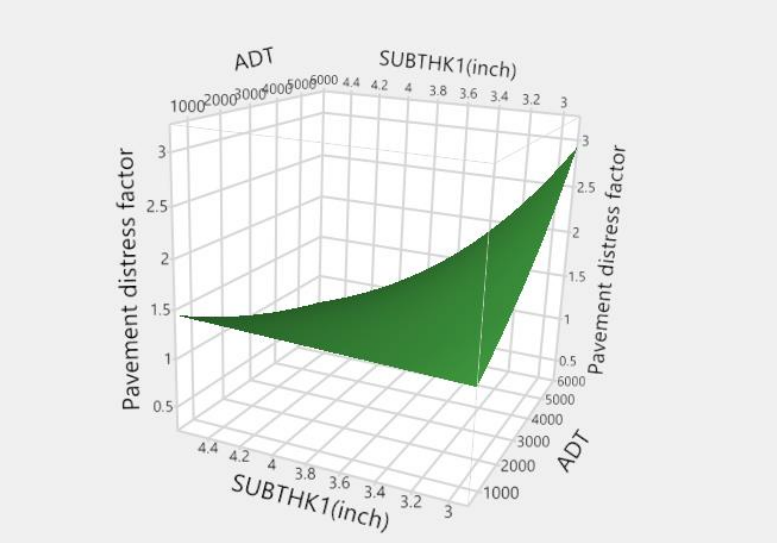

Figure 2-36. Surface plot of CIR thickness (SUBTHK1), ADT, and pavement distress factor

For low ADT values, the pavement distress factor does not change considerably across CIR thickness values. However, at high ADT values, a decrease in CIR thickness causes an increase in the pavement distress factor, indicating more distress. This inference backs up observations made in the case studies in the previous chapter comparing well performing with poorly

performing CIR sections, where the 4 in. thick CIR sections generally performed better than the 3 in. thick sections. This inference also highlights the significant interaction between ADT and CIR thickness. CIR thickness influences pavement performance more at higher traffic levels than at lower traffic levels, and 4 in. of CIR seems to provide better support and stress relief than 3 in. of CIR. The case studies of individual projects described in the previous chapter tend to agree with this hypothesis, where 4 in. thick CIR sections had lower amounts of recorded distress compared to 3 in. thick CIR sections. It is also important to note that the base thickness is a significant factor. An adequate existing pavement structure is important for successful CIR projects.

Unlike the PCI slope values, the PCI_2 values of pavement sections are age dependent. Therefore, an age parameter was added to the model in addition to the independent variables listed above. The fit model for PCI_2 is shown in Figure 2-37.

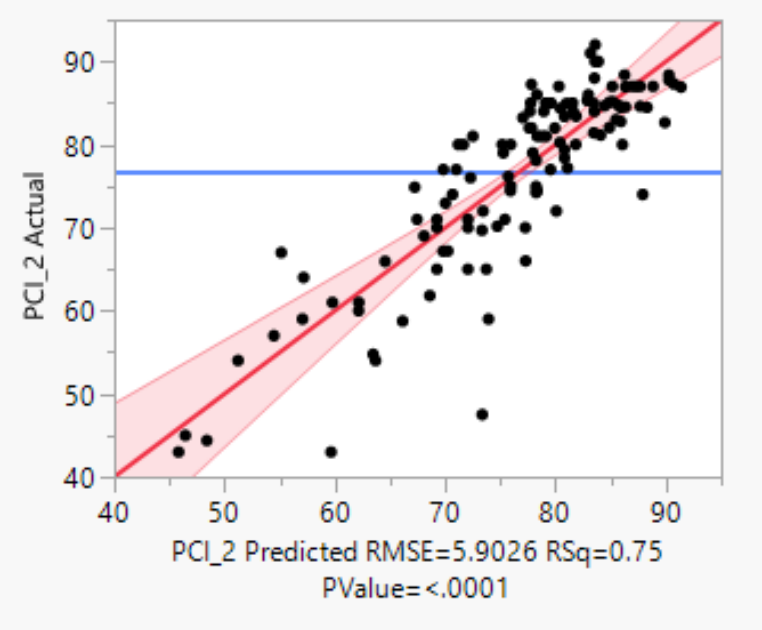

Figure 2-37. Actual versus predicted PCI_2 values for a second-degree polynomial fit

Age values were constrained to 6 years or older, since insufficient data on younger pavement sections could unfavorably skew the data. The R^2 value for the fit increased from 0.66 to 0.75 after constraining the section age values to between 6 and 20 years. The list of significant model effects along with the regression coefficient estimates are shown in Table 2-13.

Table 2-13. Model effects summary for PCI_2

Independent Variable	Regression Coefficient	Prob>|t|
Intercept	155.80	**<.0001**
ADT	-4.24×10^{-3}	**<.0001**
SURTHK	-30.10	**<.0001**
SUBTHK	-0.99	0.5819
AGE	-1.69	**<.0001**
ADT x SURTHK	-0.017	**<.0001**
ADT x SUBTHK	5.2×10^{-3}	**<.0001**
ADT x AGE	-2.6×10^{-4}	0.2552
SURTHK x SUBTHK	9.53	0.2588
SURTHK x AGE	-7.07	**<.0001**
SUBTHK x AGE	-2.19	**<.0001**

From Table 2-13, it appears that ADT and pavement layer thicknesses have a direct effect on PCI_2. We can assume that higher ADT volumes cause lower PCI_2 levels irrespective of age, seeing that the interaction between ADT and age is not significant. Traffic volume as well as pavement age have significant interactions with surface thickness and CIR thickness.

Figure 2-38 graphically depicts the relationship between ADT and CIR thickness. At high traffic levels, an increase in CIR thickness lends itself to higher PCI_2 values, indicating that thicker CIR sections perform better than thinner CIR sections. However, this trend is reversed at low ADT levels, where an increase in CIR thickness tends to correspond with reduced PCI_2 ratings. This trend appears to be the opposite at an ADT of 2,000, as seen in Figure 2-38(c). One explanation for this trend is that sections with lower ADT volumes had insufficient subgrade support to begin with, and it is possible that the load of a CIR train on these sections reduced the structural integrity of the base layers, leading to poorer performance. While this might not necessarily explain the variation in PCI_2 values across CIR thickness levels, the PCI_2 values for sections with lower ADT volumes are lower than those at higher ADT volumes, which strengthens the claim that adequate base support is required for good CIR performance. Another point of note is that no data exist for CIR thicknesses other than 3, 4, and 4.5 in., making it challenging to predict a surface connecting these points. In this regard, the surface plot should only be used for understanding the relationship between variables of interest and PCI_2 and not for predicting intermediate values or any values that are not in the project dataset.

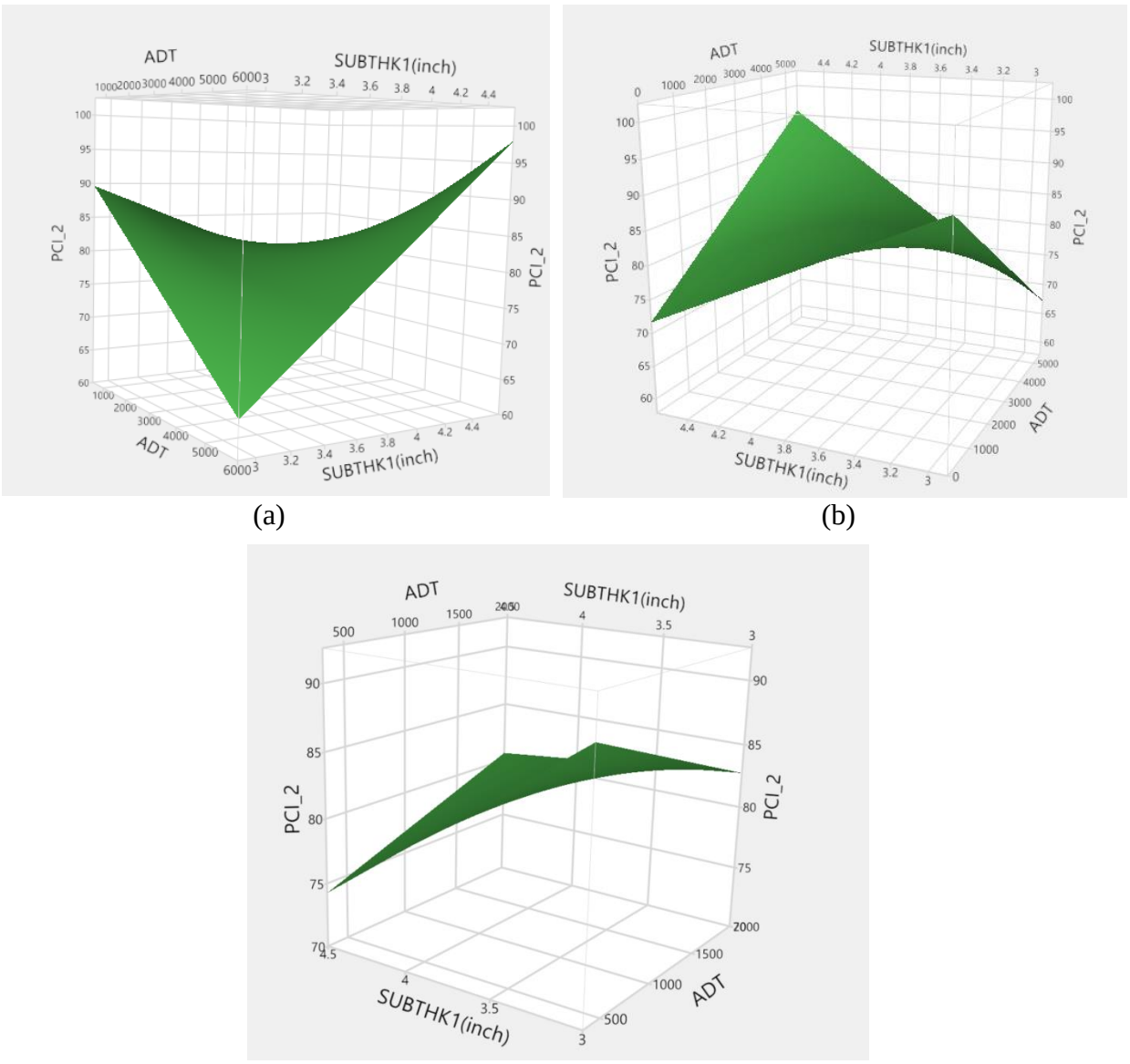

Figure 2-38. Graphical representation of the interaction of CIR thickness (SUBTHCK1) and ADT with PCI_2: (a) high ADT volumes, (b) low ADT volumes, and (c) ADT volumes between 400 and 2,000

3. ANALYSIS OF HMA/CIR CORES FROM US 34

To investigate the underlying characteristics of CIR, field cores were collected from CIR/HMA overlay sections on US 34 in Mills and Wapello Counties, Iowa, on November 16, 2021. The cores were evaluated to determine the cracking resistance, binder contents, and gradations of both the CIR and HMA layers. A total of 16 cores with 6 in. diameters were collected from 8 locations at one-mile intervals along US 34. Two cores were collected at each location, one in the wheel path and one between wheel paths. The process used to obtain the CIR cores is shown in Figure 3-1.

Figure 3-1. Process of collecting cores from US 34

3.1. Thicknesses of CIR and HMA Layers

The HMA and CIR layers were distinguished by a difference in color, with the CIR layer darker than the HMA layer. The thicknesses of both the HMA and CIR layers were measured from each core and are summarized in Table 3-1. Cores were labeled with the milepost number followed by either "RWP," which indicates that the core was collected from the pavement's right wheel path, or "¼ pt," which indicates that the core was collected from between the pavement's wheel paths.

Table 3-1. Thicknesses of HMA and CIR cores from US 34

Core	HMA (in./cm)	CIR (in./cm)	Total (in./cm)
12.3 RWP	5.9/15	3.5/9	9.4/24
12.3 ¼ pt	5.9/15	3.5/9	9.4/24
13.2 RWP	2.4/6	2.4/6	4.7/12
13.2 ¼ pt	2.8/7	3.1/8	5.9/15
14 RWP	2.4/6	3.1/8	5.5/14
14 ¼ pt	1.6/4	5.4/13	6.7/17
15.3 RWP	1.4/3.5	5.3/13.5	6.7/17
15.3 ¼ pt	1.6/4	5.1/13	6.7/17
18.4 RWP	1.6/4	3.9/10	5.5/14
18.4 ¼ pt	1.6/4	3.5/9	5.1/13
19.3 RWP	1.4/3.5	3.5/9	4.9/12.5
19.3 ¼ pt	1.4/3.5	5.3/13.5	6.7/17
20.3 RWP	1.6/4	3.5/9	5.1/13
20.3 ¼ pt	1.6/4	3.5/9	5.1/13
181.4 RWP	2.6/6.5	3.7/9.5	6.3/16
181.4 ¼ pt	2.4/6	3.9/10	6.3/16

3.2. Semicircular Bending Test Results

Semicircular bending (SCB) tests have been used to evaluate both fatigue cracking and low-temperature cracking. The flexibility index (FI) resulting from this test has been reported to have the capability to capture some of the critical changes in mixture variables. Lower FI values indicate that the asphalt mixture is more brittle and has a higher crack growth rate.

SCB tests were performed according to AASHTO TP 124 on the cores taken from US 34. As shown in Figure 3-2, samples for SCB testing were prepared by cutting the cores into semicircular specimens, each with a diameter of 150 mm and a maximum thickness of 50 mm (with some samples thinner because field core samples have various thicknesses). A notch 15 mm long and 1.5 mm wide was made on the flat side of each semicircular specimen to induce cracking. All specimens were conditioned at 25ºC for 2 hours before performing SCB testing.

Figure 3-2. Cuts made to prepare a semicircular specimen with a thickness of 50 mm

The SCB test setup and the dimensions of the test specimens are illustrated in Figure 3-3. To induce cracking in the middle of the specimens, a 15 mm notch was created in each.

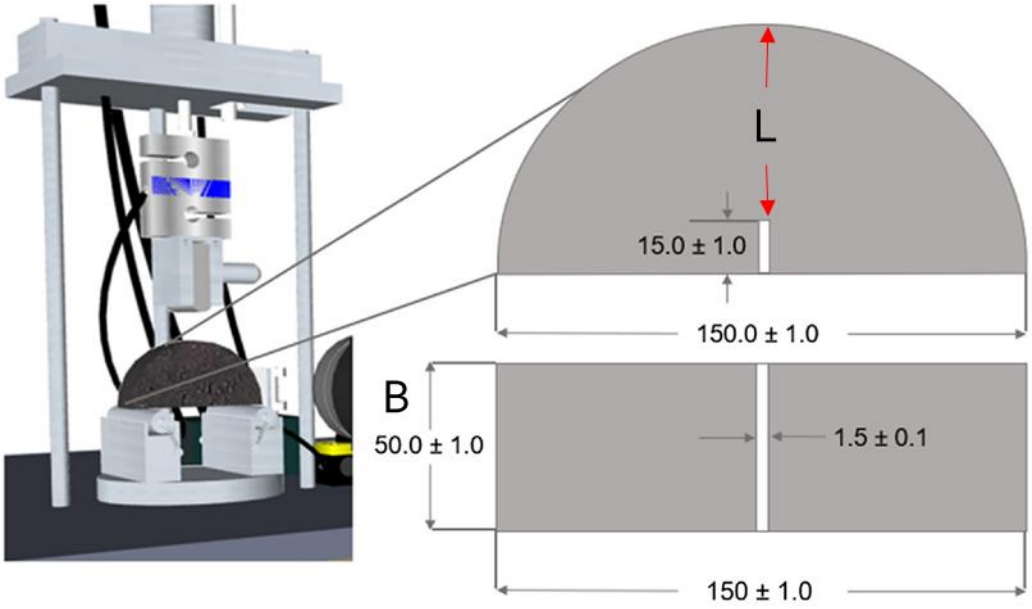

Figure 3-3. SCB test setup (left) and dimensions of the test specimen (right)

A typical force-displacement curve from an SCB test is illustrated in Figure 3-4, which shows the work of fracture (W_F) as the area under the curve and the post-peak slope (m) at the inflection point after the peak point. These parameters were used to calculate fracture energy (G_F) using Equation 3-1 and FI using Equation 3-2.

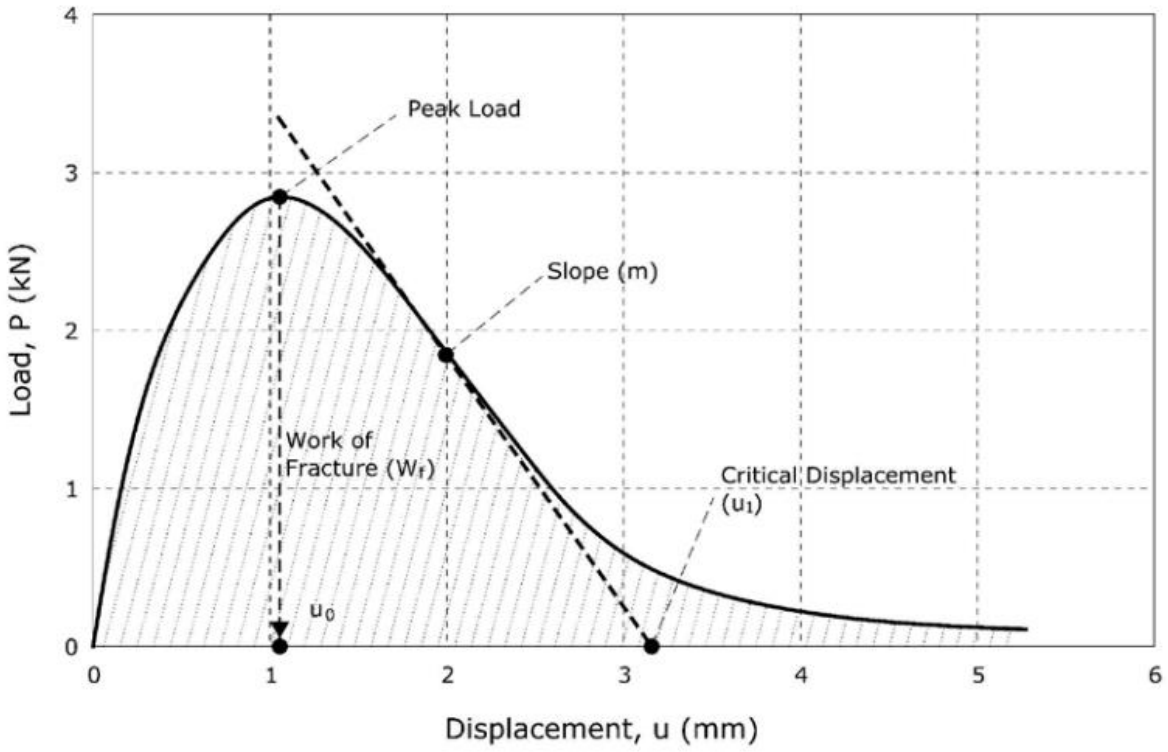

Figure 3-4. Typical force-displacement curve from an SCB test and parameters for evaluation

Fracture energy (G_F) can be calculated using the equation below:

$$G_F = \frac{W_F}{B \times L} \tag{3-1}$$

where W_F is the work of fracture, B is the specimen thickness, and L is the ligament length.

FI can be calculated using the equation below:

$$FI = \frac{G_F}{|m|} \times A \tag{3-2}$$

where G_F is the fracture energy calculated by dividing the work of fracture by the ligament area, m is the post-peak slope at the inflection point after the peak point, and A is a unit conversion from field to laboratory (0.01).

A total of 79 tests were conducted. The SCB test results are summarized in Tables 3-2 to 3-9. Compared to the CIR layer, the HMA layer provided a lower fracture energy with a higher post-peak slope, which resulted in a lower FI value compared to that of the CIR layer. It is postulated that, overall, that the CIR layer has more cracking resistance than the HMA layer.

Table 3-2. SCB test results for MP 12.3

Location	Layers	Mixtures	Test	Peak Load (KN)	Fracture Energy (J/m^2)	Post-Peak Slope (kN/mm)	FI
12.3_1/4pt	1	HMA	1	4.10	625.46	-7.59	0.82
			2	5.52	1038.29	-8.81	1.18
	Average			4.81	831.88	-8.20	1.00
	2	HMA	1	3.47	760.39	-7.22	1.05
			2	3.23	1096.20	-4.34	2.53
	Average			3.35	928.30	-5.78	1.79
	3	CIR	1	2.66	1251.98	-2.68	4.66
			2	2.78	978.75	-3.50	2.80
	Average			2.72	1115.37	-3.09	3.73
	4	CIR	1	2.22	988.37	-1.92	5.16
			2	2.30	1311.55	-1.79	7.32
	Average			2.26	1149.96	-1.85	6.24
12.3_RWP	1	HMA	1	4.53	870.30	-7.07	1.23
			2	3.84	579.63	-7.17	0.81
	Average			4.19	724.97	-7.12	1.02
	2	HMA	1	3.06	1586.78	-2.93	5.41
			2	3.03	1276.11	-3.15	4.05
	Average			3.05	1431.44	-3.04	4.73
	3	CIR	1	1.84	783.81	-1.82	4.30
			2	1.80	721.11	-0.79	3.97
	Average			1.82	752.46	-1.31	4.13
	4	CIR	1	1.92	1256.27	-1.36	9.24
			2	1.65	836.63	-1.30	6.44
	Average			1.78	1046.45	-1.33	7.84

Table 3-3. SCB test results for MP 13.2

Location	Layers	Mixtures	Test	Peak Load (KN)	Fracture Energy (J/m^2)	Post-Peak Slope (kN/mm)	FI
13.2_1/4pt	1	HMA	1	3.41	620.78	-5.84	1.06
			2	3.09	565.02	-5.44	1.04
	Average			3.25	592.90	-5.64	1.05
	2	CIR	1	1.94	1324.57	-1.25	10.61
			2	2.25	1638.10	-1.46	11.23
	Average			2.09	1481.33	-1.35	10.92
13.2_RWP	1	HMA	1	4.64	737.77	-7.59	0.97
			2	4.53	762.60	-8.74	0.87
	Average			4.58	750.18	-8.16	0.92
	2	CIR	1	2.58	1124.87	-2.99	3.77
			2	2.57	1378.85	-2.21	6.23
	Average			2.57	1251.86	-2.60	5.00

Table 3-4. SCB test results for MP 14.0

Location	Layers	Mixtures	Test	Peak Load (KN)	Fracture Energy (J/m^2)	Post-Peak Slope (kN/mm)	FI
14.0_1/4pt	1	HMA	1	2.68	596.45	-5.01	1.19
			2	2.33	504.10	-5.12	0.99
	Average			2.50	550.28	-5.06	1.09
	2	HMA	1	2.36	346.62	-5.81	0.60
			2	2.06	332.88	-4.87	0.68
	Average			2.21	339.75	-5.34	0.64
	3	CIR	1	2.16	482.91	-3.57	1.35
			2	1.88	663.45	-2.33	2.85
	Average			2.02	573.18	-2.95	2.10
14.0_RWP	1	HMA	1	3.04	428.85	-5.83	0.74
			2	3.23	498.89	-7.01	0.71
	Average			3.14	463.87	-6.42	0.72
	2	CIR	1	2.55	1128.68	-3.01	3.75
			2	2.12	852.76	-2.28	3.73
	Average			2.33	990.72	-2.65	3.74

Table 3-5. SCB test results for MP 15.3

Location	Layers	Mixtures	Test	Peak Load (KN)	Fracture Energy (J/m^2)	Post-Peak Slope (kN/mm)	FI
15.3_1/4pt	1	HMA	1	4.23	876.05	-6.98	1.26
	2	HMA	1	3.09	1186.38	-4.76	2.50
			2	2.86	915.08	-4.74	1.93
	Average			2.97	1050.73	-4.75	2.21
	3	CIR	1	1.92	813.41	-2.01	4.04
			2	1.47	741.39	-1.20	6.17
	Average			1.70	777.40	-1.61	5.11
15.3_RWP	1	HMA	1	2.41	456.37	-5.88	0.78
			2	2.13	385.15	-4.98	0.77
	Average			2.27	420.76	-5.43	0.77
	2	HMA	1	2.25	417.48	-3.90	1.07
			2	3.01	538.79	-6.12	0.88
	Average			2.63	478.13	-5.01	0.98
	3	CIR	1	2.27	1021.29	-2.23	4.58
			2	2.41	1074.51	-2.09	5.15
	Average			2.34	1047.90	-2.16	4.86

Table 3-6. SCB test results for MP 18.4

Location	Layers	Mixtures	Test	Peak Load (KN)	Fracture Energy (J/m^2)	Post-Peak Slope (kN/mm)	FI
18.4_1/4pt	1	HMA	1	3.06	779.16	-5.48	1.42
			2	2.35	565.35	-4.28	1.32
	Average			2.70	672.25	-4.88	1.37
	2	HMA	1	2.14	515.45	-3.80	1.36
			2	2.28	473.03	-3.89	1.22
	Average			2.21	494.24	-3.84	1.29
18.4_RWP	1	HMA	1	2.93	922.72	-4.47	2.06
			2	2.90	651.53	-8.02	0.81
	Average			2.92	787.13	-6.25	1.44
	2	HMA	1	2.66	695.40	-4.01	1.73
			2	2.54	573.77	-4.07	1.41
	Average			2.60	634.59	-4.04	1.57

Table 3-7. SCB test results for MP 19.3

Location	Layers	Mixtures	Test	Peak Load (KN)	Fracture Energy (J/m^2)	Post-Peak Slope (kN/mm)	FI
19.3_1/4pt	1	HMA	1	1.56	368.22	-3.15	1.17
			2	1.87	428.57	-3.89	1.10
	Average			1.72	398.39	-3.52	1.14
	2	HMA	1	1.98	552.56	-2.68	2.06
			2	2.33	591.04	-3.77	1.57
	Average			2.16	571.80	-3.23	1.81
	3	CIR	1	2.12	679.26	-2.48	2.74
			2	1.88	684.55	-1.52	4.51
	Average			2.00	681.90	-2.00	3.62
19.3_RWP	1	HMA	1	2.78	585.91	-5.65	1.04
			2	2.59	649.48	-4.38	1.48
	Average			2.68	617.69	-5.02	1.26
	2	HMA	1	2.83	884.91	-3.76	2.35
			2	2.85	709.63	-4.29	1.66
	Average			2.84	797.27	-4.02	2.00

Table 3-8. SCB test results for MP 20.3

Location	Layers	Mixtures	Test	Peak Load (KN)	Fracture Energy (J/m^2)	Post-Peak Slope (kN/mm)	FI
20.3_1/4pt	1	HMA	1	2.50	514.06	-4.51	1.14
			2	2.89	537.93	-5.49	0.98
	Average			2.69	525.99	-5.00	1.06
	2	HMA	1	2.36	572.95	-3.60	1.59
			2	2.32	531.37	-3.89	1.37
	Average			2.34	552.16	-3.74	1.48
20.3_RWP	1	HMA	1	2.85	623.85	-5.47	1.14
			2	1.53	287.42	-4.37	0.66
	Average			2.19	455.64	-4.92	0.90
	2	HMA	1	3.35	789.15	-6.38	1.24
			2	3.44	953.73	-5.20	1.83
	Average			3.39	871.44	-5.79	1.54

Table 3-9. SCB test results for MP 181.4

Location	Layers	Mixtures	Test	Peak Load (KN)	Fracture Energy (J/m^2)	Post-Peak Slope (kN/mm)	FI
181.4_1/4pt	1	HMA	1	3.46	1263.36	-5.28	2.39
			2	3.10	898.75	-4.82	1.87
	Average			3.28	1081.05	-5.05	2.13
	2	CIR	1	1.63	509.90	-1.90	2.69
			2	1.48	374.77	-2.04	1.83
	Average			1.56	442.34	-1.97	2.26
181.4_RWP	1	HMA	1	4.23	893.29	-6.44	1.39
			2	4.01	727.38	-7.10	1.02
	Average			4.12	810.34	-6.77	1.21
	2	CIR	1	2.26	906.85	-2.34	3.87
			2	2.09	655.64	-3.22	2.04
	Average			2.17	781.24	-2.78	2.95

3.3. Asphalt Contents and Aggregate Gradation

To evaluate the asphalt contents and aggregate gradations of the cores, a total of 40 burn-off tests were conducted. After the burn-off tests were conducted, each sample was sieved according to AASHTO T 248.

The AC contents and aggregate gradations for each location (milepost) are summarized in Tables 3-10 to Table 3-21 and illustrated in Figures 3-5 to 3-12, respectively.

Table 3-10. Burn-off test results and aggregate gradation for MP 12.3_1/4pt

MP		12.3_1/4pt_1st_HMA			12.3_1/4pt_2nd_HMA			12.3_1/4pt_3rd_CIR			12.3_1/4pt_4th_CIR		
Sieve Size (in., mm)		Agg. Weight (g)	% Remain	% Passing	Agg. Weight (g)	% Remain	% Passing	Agg. Weight (g)	% Remain	% Passing	Agg. Weight (g)	% Remain	% Passing
3/4 in.	19.0	0.0	0.0	100.0	0.0	0.0	100.0	0.0	0.0	100.0	0.0	0.0	100.0
1/2 in.	12.5	52.8	2.6	97.4	32.3	2.0	98.0	70.8	4.5	95.5	49.6	2.9	97.1
3/8 in.	9.5	92.4	4.6	92.8	83.3	5.0	93.0	100.9	6.4	89.1	43.0	2.5	94.6
#4	4.75	335.0	16.6	76.2	376.2	22.8	70.2	394.5	25.1	64.0	310.0	18.1	76.4
#8	2.36	531.9	26.4	49.8	344.0	20.8	49.4	306.4	19.5	44.6	340.0	19.9	56.5
#16	1.18	260.7	12.9	36.8	216.4	13.1	36.2	185.0	11.8	32.8	242.2	14.2	42.4
#30	0.6	284.4	14.1	22.7	198.8	12.0	24.2	196.8	12.5	20.3	236.6	13.8	28.5
#50	0.3	298.0	14.8	7.9	221.3	13.4	10.8	207.0	13.2	7.1	233.8	13.7	14.8
#100	0.15	127.5	6.3	1.6	110.6	6.7	4.1	71.3	4.5	2.6	173.0	10.1	4.7
#200	0.075	18.0	0.9	0.7	25.8	1.6	2.5	17.0	1.1	1.5	50.4	2.9	1.8
Pan	0	13.7	0.7	0.0	41.6	2.5	0.0	24.1	1.5	0.0	30.3	1.8	0.0
AC		5.5			5.7			5.4			8.8		

Table 3-11. Burn-off test results and aggregate gradation for MP 12.3_RWP

MP		12.3_RWP_1st_HMA			12.3_RWP_2nd_HMA			12.3_RWP_3rd_CIR			12.3_RWP_4th_CIR		
Sieve Size (in., mm)		Agg. Weight (g)	% Remain	% Passing	Agg. Weight (g)	% Remain	% Passing	Agg. Weight (g)	% Remain	% Passing	Agg. Weight (g)	% Remain	% Passing
3/4 in.	19.0	0.0	0.0	100.0	0.0	0.0	100.0	0.0	0.0	100.0	0.0	0.0	100.0
1/2 in.	12.5	58.5	3.1	96.9	71.6	4.5	95.5	71.1	4.6	95.4	45.2	2.9	97.1
3/8 in.	9.5	87.8	4.6	92.3	106.6	6.7	88.9	126.6	8.1	87.3	72.5	4.7	92.5
#4	4.75	321.6	16.9	75.4	352.2	22.0	66.9	345.8	22.2	65.2	281.4	18.1	74.4
#8	2.36	451.8	23.7	51.7	336.7	21.0	45.8	316.0	20.3	44.9	327.6	21.0	53.4
#16	1.18	322.6	16.9	34.8	192.5	12.0	33.8	178.1	11.4	33.5	223.5	14.3	39.1
#30	0.6	253.7	13.3	21.5	164.0	10.2	23.5	156.8	10.1	23.4	232.0	14.9	24.2
#50	0.3	222.4	11.7	9.8	222.0	13.9	9.7	217.0	13.9	9.5	162.5	10.4	13.7
#100	0.15	116.1	6.1	3.7	120.6	7.5	2.1	116.1	7.4	2.1	167.6	10.8	3.0
#200	0.075	27.3	1.4	2.3	16.3	1.0	1.1	15.5	1.0	1.1	29.0	1.9	1.1
Pan	0	43.0	2.3	0.0	17.6	1.1	0.0	16.7	1.1	0.0	17.7	1.1	0.0
AC		5.5			5.3			5.5			9.6		

Table 3-12. Burn-off test results and aggregate gradation for MP 13.2

MP		13.2_1/4pt_1st_HMA			13.2_1/4pt_2nd_CIR			13.2_RWP_1st_HMA			13.2_RWP_2nd_CIR		
Sieve Size (in., mm)		Agg. Weight (g)	% Remain	% Passing	Agg. Weight (g)	% Remain	% Passing	Agg. Weight (g)	% Remain	% Passing	Agg. Weight (g)	% Remain	% Passing
3/4 in.	19.0	0.0	0.0	100.0	0.0	0.0	100.0	0.0	0.0	100.0	0.0	0.0	100.0
1/2 in.	12.5	77.6	4.4	95.6	55.0	3.4	96.6	111.5	5.1	94.9	32.6	2.1	97.9
3/8 in.	9.5	70.4	4.0	91.6	60.6	3.7	92.9	129.3	5.9	89.1	64.0	4.1	93.8
#4	4.75	336.0	19.1	72.5	275.3	16.8	76.1	361.4	16.4	72.7	248.6	15.9	78.0
#8	2.36	401.4	22.8	49.8	312.8	19.1	57.0	492.7	22.4	50.3	326.4	20.8	57.1
#16	1.18	278.2	15.8	34.0	226.2	13.8	43.2	329.0	14.9	35.3	266.7	17.0	40.1
#30	0.6	238.7	13.5	20.4	237.0	14.5	28.8	293.6	13.3	22.0	244.8	15.6	24.5
#50	0.3	205.5	11.7	8.8	237.6	14.5	14.2	275.5	12.5	9.5	203.3	13.0	11.5
#100	0.15	99.4	5.6	3.1	156.4	9.5	4.7	134.0	6.1	3.4	104.8	6.7	4.8
#200	0.075	23.5	1.3	1.8	50.0	3.1	1.6	28.8	1.3	2.1	45.0	2.9	1.9
Pan	0	31.4	1.8	0.0	27.0	1.6	0.0	46.2	2.1	0.0	30.1	1.9	0.0
AC		5.5			9.9			5.5			9.8		

Table 3-13. Burn-off test results and aggregate gradation for MP 14.0_1/4pt

MP		14.0_1/4pt_1st_HMA			14.0_1/4pt_2nd_HMA			14.0_1/4pt_3rd_CIR		
Sieve Size (in., mm)		Agg. Weight (g)	% Remain	% Passing	Agg. Weight (g)	% Remain	% Passing	Agg. Weight (g)	% Remain	% Passing
3/4 in.	19.0	0.0	0.0	100.0	0.0	0.0	100.0	0.0	0.0	100.0
1/2 in.	12.5	67.1	5.0	95.0	77.0	4.6	95.4	54.0	3.2	96.8
3/8 in.	9.5	60.8	4.6	90.4	104.2	6.2	89.2	86.2	5.1	91.8
#4	4.75	194.2	14.6	75.8	374.0	22.3	66.9	338.8	19.9	71.9
#8	2.36	355.3	26.7	49.1	311.3	18.6	48.3	320.0	18.8	53.1
#16	1.18	235.1	17.7	31.4	212.2	12.7	35.7	218.4	12.8	40.2
#30	0.6	157.2	11.8	19.5	212.5	12.7	23.0	234.0	13.7	26.5
#50	0.3	166.0	12.5	7.1	215.3	12.8	10.1	218.6	12.8	13.7
#100	0.15	53.4	4.0	3.0	98.5	5.9	4.3	99.2	5.8	7.8
#200	0.075	16.0	1.2	1.8	29.6	1.8	2.5	53.2	3.1	4.7
Pan	0	24.5	1.8	0.0	42.0	2.5	0.0	80.3	4.7	0.0
AC		5.4			5.6			8.0		

Table 3-14. Burn-off test results and aggregate gradation for MP 14.0_RWP

MP		14.0_RWP_1st_HMA			14.0_RWP_2nd_CIR		
Sieve Size (in., mm)		Agg. Weight (g)	% Remain	% Passing	Agg. Weight (g)	% Remain	% Passing
3/4 in.	19.0	0.0	0.0	100.0	0.0	0.0	100.0
1/2 in.	12.5	128.2	7.0	93.0	51.9	3.5	96.5
3/8 in.	9.5	81.6	4.4	88.6	74.9	5.1	91.4
#4	4.75	293.2	16.0	72.6	268.7	18.3	73.1
#8	2.36	451.6	24.6	48.0	292.7	19.9	53.2
#16	1.18	295.7	16.1	31.9	201.3	13.7	39.5
#30	0.6	233.7	12.7	19.1	222.5	15.1	24.3
#50	0.3	207.3	11.3	7.8	194.8	13.3	11.1
#100	0.15	121.1	6.6	1.2	83.2	5.7	5.4
#200	0.075	13.2	0.7	0.5	48.5	3.3	2.1
Pan	0	0.0	0.0	100.0	0.0	0.0	100.0
AC		5.2			8.3		

Table 3-15. Burn-off test results and aggregate gradation for MP 15.3_1/4pt

MP		15.3_1/4pt_1st_HMA			15.3_1/4pt_2nd_HMA			15.3_1/4pt_3rd_CIR		
Sieve Size (in., mm)		Agg. Weight (g)	% Remain	% Passing	Agg. Weight (g)	% Remain	% Passing	Agg. Weight (g)	% Remain	% Passing
3/4 in.	19.0	0.0	0.0	100.0	0.0	0.0	100.0	0.0	0.0	100.0
1/2 in.	12.5	59.0	4.7	95.3	0.0	0.0	100.0	108.2	6.6	93.4
3/8 in.	9.5	56.0	4.4	90.9	81.8	6.1	93.9	63.5	3.9	89.5
#4	4.75	182.4	14.5	76.4	328.1	24.6	69.3	306.5	18.8	70.7
#8	2.36	353.2	28.0	48.4	260.6	19.5	49.8	276.0	16.9	53.9
#16	1.18	245.0	19.4	28.9	156.6	11.7	38.1	190.6	11.7	42.2
#30	0.6	165.0	13.1	15.8	188.2	14.1	24.0	208.2	12.7	29.5
#50	0.3	113.0	9.0	6.9	196.7	14.7	9.3	228.6	14.0	15.5
#100	0.15	60.5	4.8	2.1	64.8	4.9	4.4	174.6	10.7	4.8
#200	0.075	12.2	1.0	1.1	25.0	1.9	2.6	55.5	3.4	1.4
Pan	0	13.7	1.1	0.0	34.2	2.6	0.0	22.8	1.4	0.0
AC		6.3			6.7			8.4		

Table 3-16. Burn-off test results and aggregate gradation for MP 15.3_RWP

MP		15.3_RWP_1st_HMA			15.3_RWP_2nd_HMA			15.3_RWP_3rd_CIR		
Sieve Size (in., mm)		Agg. Weight (g)	% Remain	% Passing	Agg. Weight (g)	% Remain	% Passing	Agg. Weight (g)	% Remain	% Passing
3/4 in.	19.0	0.0	0.0	100.0	0.0	0.0	100.0	0.0	0.0	100.0
1/2 in.	12.5	41.6	2.3	97.7	101.0	5.6	94.4	34.2	2.0	98.0
3/8 in.	9.5	150.4	8.2	89.5	151.7	8.4	86.1	55.0	3.2	94.8
#4	4.75	475.4	25.9	63.7	356.6	19.7	66.4	314.6	18.2	76.7
#8	2.36	379.0	20.6	43.0	316.5	17.5	48.9	348.7	20.1	56.5
#16	1.18	205.1	11.2	31.9	230.0	12.7	36.2	255.6	14.8	41.8
#30	0.6	199.0	10.8	21.0	227.3	12.5	23.7	255.5	14.8	27.0
#50	0.3	207.9	11.3	9.7	251.8	13.9	9.8	233.3	13.5	13.5
#100	0.15	77.2	4.2	5.5	110.4	6.1	3.7	137.6	8.0	5.6
#200	0.075	34.6	1.9	3.6	24.6	1.4	2.3	58.2	3.4	2.2
Pan	0	66.6	3.6	0.0	42.0	2.3	0.0	38.0	2.2	0.0
AC		5.1			5.3			9.0		

Table 3-17. Burn-off test results and aggregate gradation for MP 18.4

MP		18.4_1/4pt_1st_HMA			18.4_1/4pt_2nd_HMA			18.4_RWP_1st_HMA			18.4_RWP_2nd_HMA		
Sieve Size (in., mm)		Agg. Weight (g)	% Remain	% Passing	Agg. Weight (g)	% Remain	% Passing	Agg. Weight (g)	% Remain	% Passing	Agg. Weight (g)	% Remain	% Passing
3/4 in.	19.0	0.0	0.0	100.0	0.0	0.0	100.0	0.0	0.0	100.0	0.0	0.0	100.0
1/2 in.	12.5	32.7	2.9	97.1	53.8	3.2	96.8	69.0	4.6	95.4	100.4	6.0	94.0
3/8 in.	9.5	47.0	4.2	93.0	105.0	6.3	90.5	67.3	4.4	91.0	123.0	7.4	86.6
#4	4.75	176.2	15.6	77.4	376.8	22.6	67.9	212.0	14.0	77.0	313.6	18.8	67.9
#8	2.36	193.4	17.1	60.3	330.7	19.8	48.1	407.0	26.8	50.2	338.6	20.2	47.6
#16	1.18	250.4	22.1	38.1	207.8	12.4	35.7	274.0	18.1	32.1	204.4	12.2	35.4
#30	0.6	167.3	14.8	23.3	201.0	12.0	23.6	190.2	12.5	19.6	187.0	11.2	24.2
#50	0.3	138.8	12.3	11.0	231.9	13.9	9.7	161.6	10.7	8.9	254.4	15.2	9.0
#100	0.15	87.4	7.7	3.3	103.5	6.2	3.5	101.0	6.7	2.2	111.7	6.7	2.3
#200	0.075	24.0	2.1	1.2	22.3	1.3	2.2	25.0	1.6	0.6	18.3	1.1	1.2
Pan	0	13.5	1.2	0.0	36.5	2.2	0.0	9.0	0.6	0.0	20.9	1.2	0.0
AC		5.6			5.4			5.5			5.5		

Table 3-18. Burn-off test results and aggregate gradation for MP 19.3_1/4pt

MP		19.3_1/4pt_1st_HMA			19.3_1/4pt_2nd_HMA			19.3_1/4pt_3rd_CIR		
Sieve Size (in., mm)		Agg. Weight (g)	% Remain	% Passing	Agg. Weight (g)	% Remain	% Passing	Agg. Weight (g)	% Remain	% Passing
3/4 in.	19.0	0.0	0.0	100.0	0.0	0.0	100.0	0.0	0.0	100.0
1/2 in.	12.5	65.4	6.0	94.0	69.1	4.2	95.8	61.8	3.3	96.7
3/8 in.	9.5	57.8	5.3	88.6	110.2	6.8	89.0	90.0	4.8	91.9
#4	4.75	130.7	12.0	76.6	351.3	21.6	67.4	358.8	19.0	72.9
#8	2.36	291.6	26.9	49.7	307.6	18.9	48.5	330.0	17.5	55.4
#16	1.18	198.8	18.3	31.4	201.5	12.4	36.1	244.0	13.0	42.4
#30	0.6	133.3	12.3	19.1	194.5	12.0	24.1	252.1	13.4	29.0
#50	0.3	111.8	10.3	8.8	250.2	15.4	8.7	230.8	12.3	16.8
#100	0.15	72.5	6.7	2.1	109.3	6.7	2.0	123.0	6.5	10.2
#200	0.075	12.4	1.1	1.0	16.7	1.0	1.0	68.9	3.7	6.6
Pan	0	10.4	1.0	0.0	16.0	1.0	0.0	124.1	6.6	0.0
AC		5.2			5.4			9.3		

Table 3-19. Burn-off test results and aggregate gradation for MP 19.3_RWP

MP		19.3_RWP_1st_HMA			19.3_RWP_2nd_HMA		
Sieve Size (in., mm)		Agg. Weight (g)	% Remain	% Passing	Agg. Weight (g)	% Remain	% Passing
3/4 in.	19.0	0.0	0.0	100.0	0.0	0.0	100.0
1/2 in.	12.5	86.7	6.4	93.6	111.0	7.1	92.9
3/8 in.	9.5	46.0	3.4	90.2	130.0	8.3	84.6
#4	4.75	178.8	13.2	77.0	330.2	21.1	63.5
#8	2.36	368.1	27.2	49.7	285.1	18.2	45.3
#16	1.18	236.5	17.5	32.2	178.2	11.4	34.0
#30	0.6	168.7	12.5	19.7	222.1	14.2	19.8
#50	0.3	145.5	10.8	9.0	193.5	12.4	7.4
#100	0.15	96.6	7.1	1.8	69.5	4.4	3.0
#200	0.075	11.5	0.9	1.0	22.2	1.4	1.6
Pan	0	13.2	1.0	0.0	24.5	1.6	0.0
AC		5.7			5.4		

Table 3-20. Burn-off test results and aggregate gradation for MP 20.3

MP		20.3_1/4pt_1st_HMA			20.3_1/4pt_2nd_HMA			20.3_RWP_1st_HMA			20.3_RWP_2nd_HMA		
Sieve Size (in., mm)		Agg. Weight (g)	% Remain	% Passing	Agg. Weight (g)	% Remain	% Passing	Agg. Weight (g)	% Remain	% Passing	Agg. Weight (g)	% Remain	% Passing
3/4 in.	19.0	0.0	0.0	100.0	0.0	0.0	100.0	0.0	0.0	100.0	0.0	0.0	100.0
1/2 in.	12.5	75.7	4.6	95.4	70.2	3.9	96.1	38.9	2.7	97.3	71.8	4.3	95.7
3/8 in.	9.5	75.7	4.6	90.7	107.4	5.9	90.2	70.9	4.8	92.5	170.2	10.3	85.3
#4	4.75	199.3	12.2	78.5	330.3	18.2	72.0	187.6	12.8	79.7	311.0	18.8	66.5
#8	2.36	453.0	27.8	50.7	341.5	18.8	53.2	379.2	25.9	53.8	303.1	18.4	48.2
#16	1.18	315.0	19.3	31.4	276.0	15.2	38.0	299.3	20.4	33.3	220.7	13.4	34.8
#30	0.6	225.5	13.8	17.5	266.6	14.7	23.3	220.0	15.0	18.3	217.2	13.2	21.6
#50	0.3	197.7	12.1	5.4	260.6	14.4	8.9	150.0	10.2	8.1	220.3	13.3	8.3
#100	0.15	71.8	4.4	1.0	107.0	5.9	3.0	69.2	4.7	3.3	82.2	5.0	3.3
#200	0.075	10.6	0.7	0.3	30.6	1.7	1.3	21.0	1.4	1.9	22.8	1.4	1.9
Pan	0	5.7	0.3	0.0	24.0	1.3	0.0	28.0	1.9	0.0	32.0	1.9	0.0
AC		5.5			5.5			5.3			5.0		

Table 3-21. Burn-off test results and aggregate gradation for MP 181.4

MP		181.4_1/4pt_1st_HMA			181.4_1/4pt_2nd_CIR			181.4_RWP_1st_HMA			181.4_RWP_2nd_CIR		
Sieve Size (in., mm)		Agg. Weight (g)	% Remain	% Passing	Agg. Weight (g)	% Remain	% Passing	Agg. Weight (g)	% Remain	% Passing	Agg. Weight (g)	% Remain	% Passing
3/4 in.	19.0	0.0	0.0	100.0	0.0	0.0	100.0	0.0	0.0	100.0	0.0	0.0	100.0
1/2 in.	12.5	21.6	1.7	98.3	58.0	3.6	96.4	84.3	4.5	95.5	50.8	3.1	96.9
3/8 in.	9.5	100.0	7.6	90.7	63.6	4.0	92.4	165.4	8.7	86.8	71.3	4.3	92.6
#4	4.75	347.3	26.5	64.2	272.6	17.0	75.4	468.7	24.8	62.0	271.9	16.5	76.1
#8	2.36	278.0	21.2	42.9	285.2	17.8	57.6	364.2	19.3	42.8	274.5	16.6	59.5
#16	1.18	158.4	12.1	30.8	205.8	12.9	44.7	231.7	12.2	30.5	206.0	12.5	47.0
#30	0.6	141.4	10.8	20.0	223.7	14.0	30.7	184.1	9.7	20.8	237.0	14.4	32.7
#50	0.3	142.4	10.9	9.1	232.4	14.5	16.2	226.8	12.0	8.8	198.0	12.0	20.7
#100	0.15	51.6	3.9	5.2	139.4	8.7	7.5	72.1	3.8	5.0	124.5	7.5	13.2
#200	0.075	25.0	1.9	3.3	78.0	4.9	2.6	61.6	3.3	1.7	50.7	3.1	10.1
Pan	0	42.9	3.3	0.0	42.4	2.6	0.0	32.7	1.7	0.0	166.6	10.1	0.0
AC		6.4			7.4			6.4			7.4		

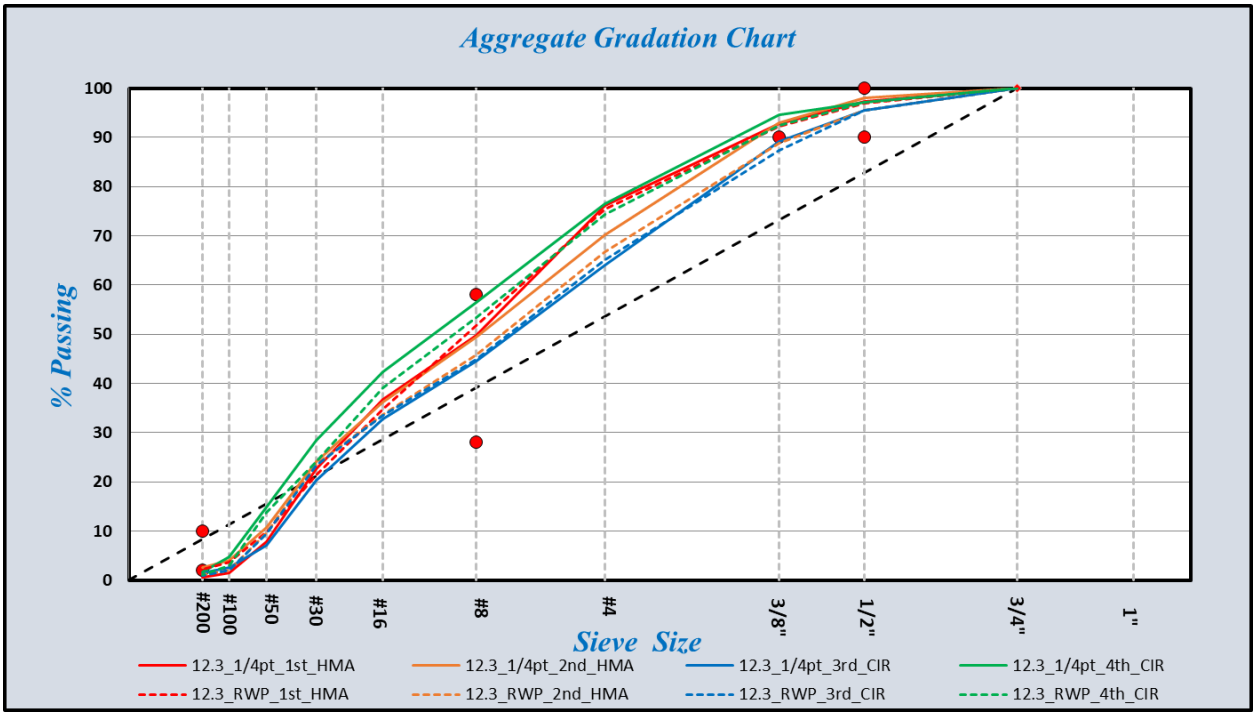

Figure 3-5. Aggregate gradation for MP 12.3

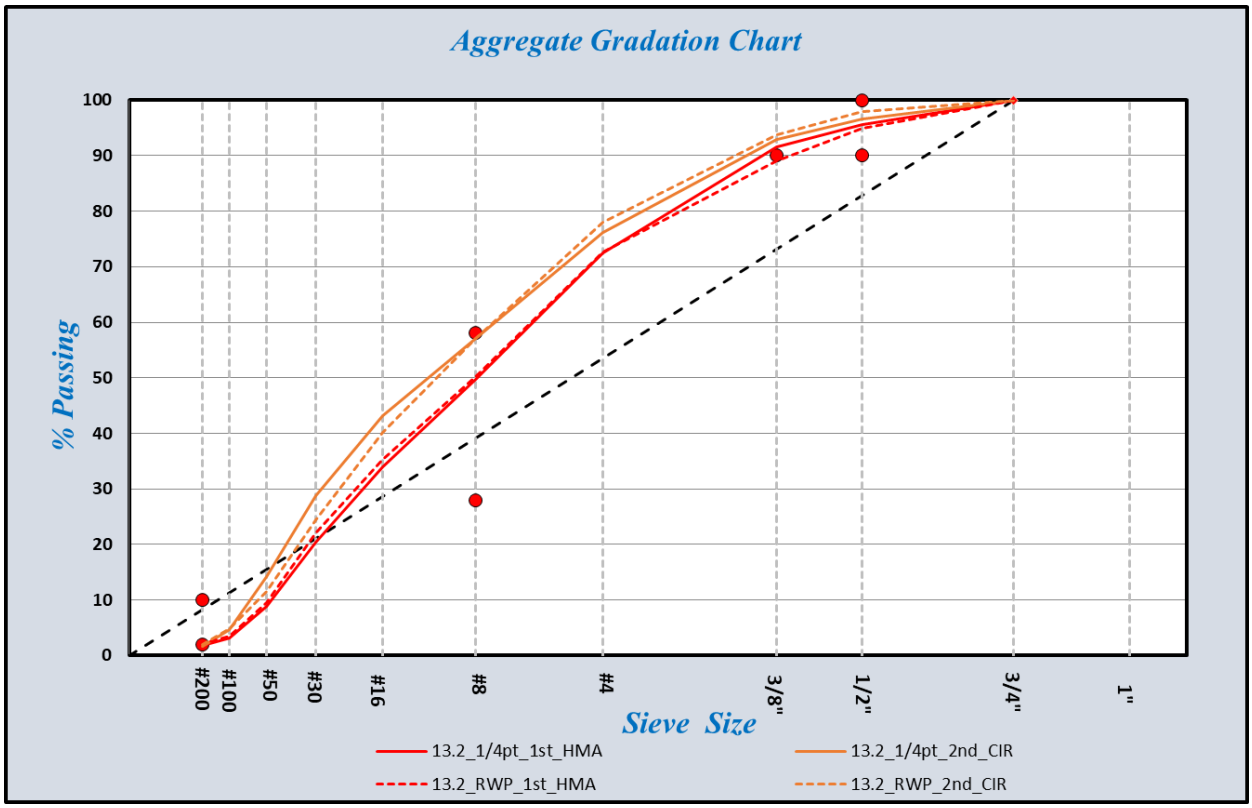

Figure 3-6. Aggregate gradation for MP 13.2

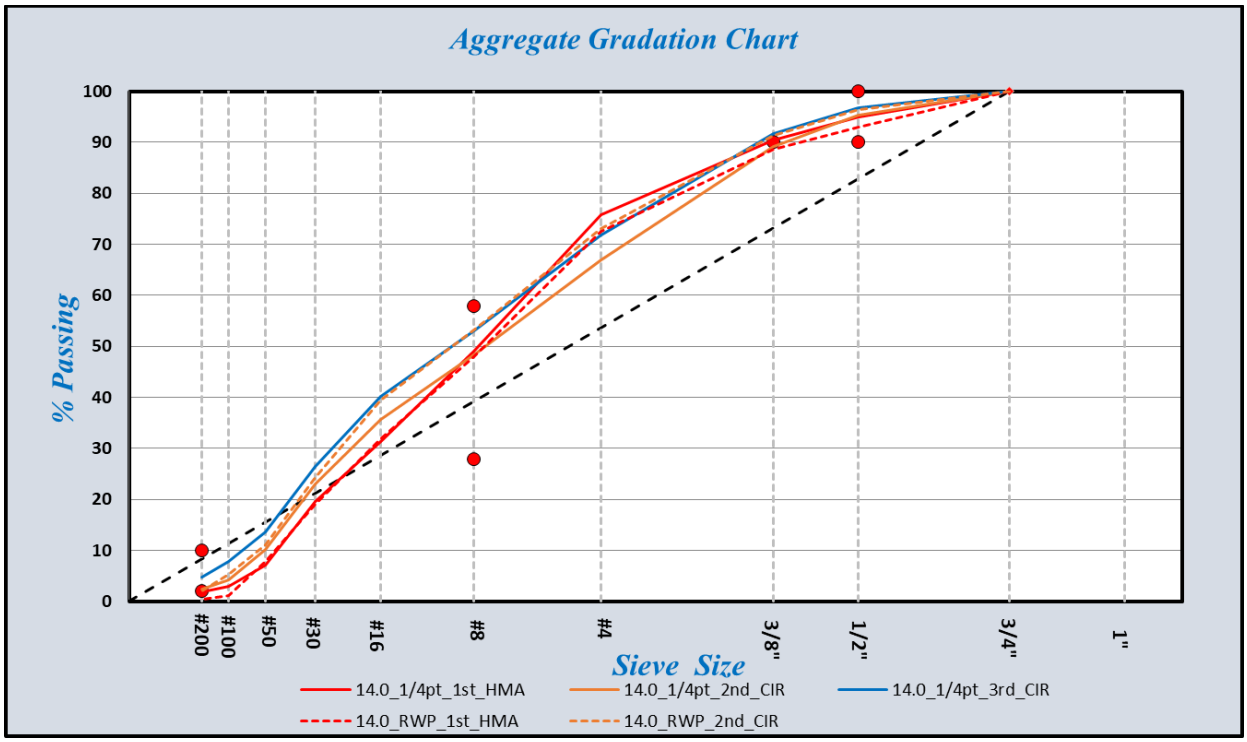

Figure 3-7. Aggregate gradation for MP 14.0

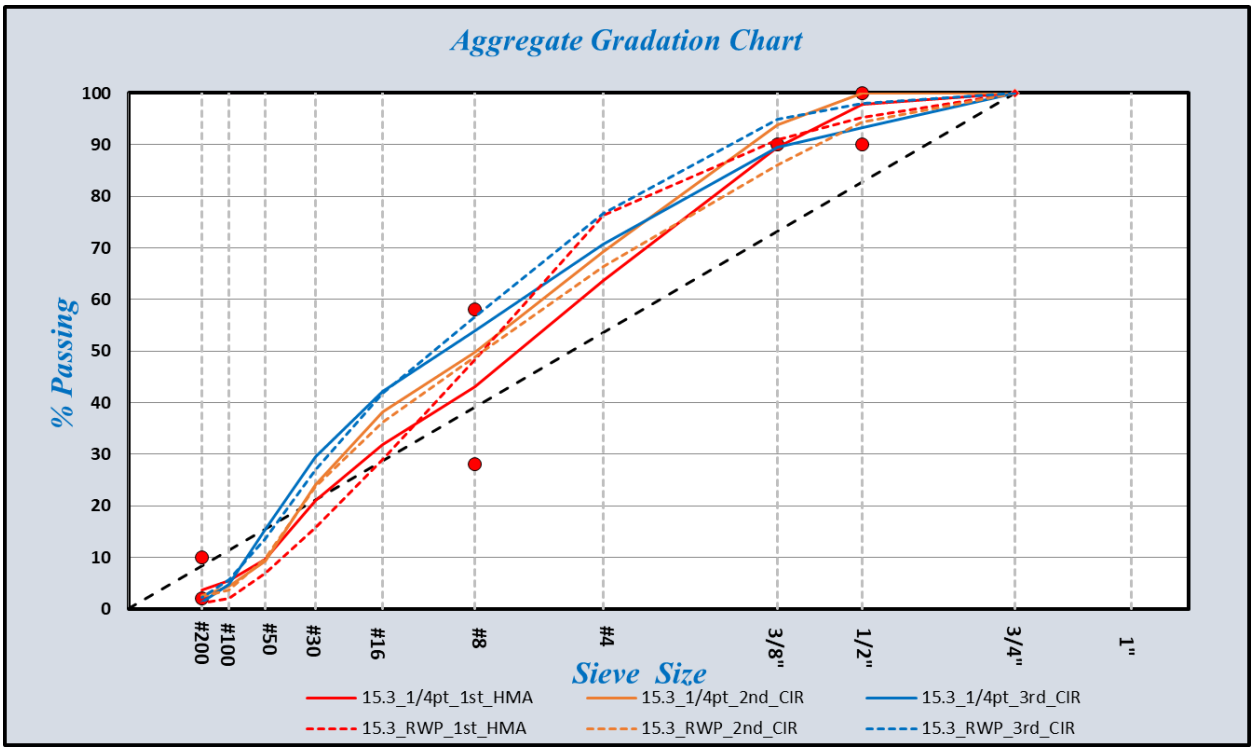

Figure 3-8. Aggregate gradation for MP 15.3

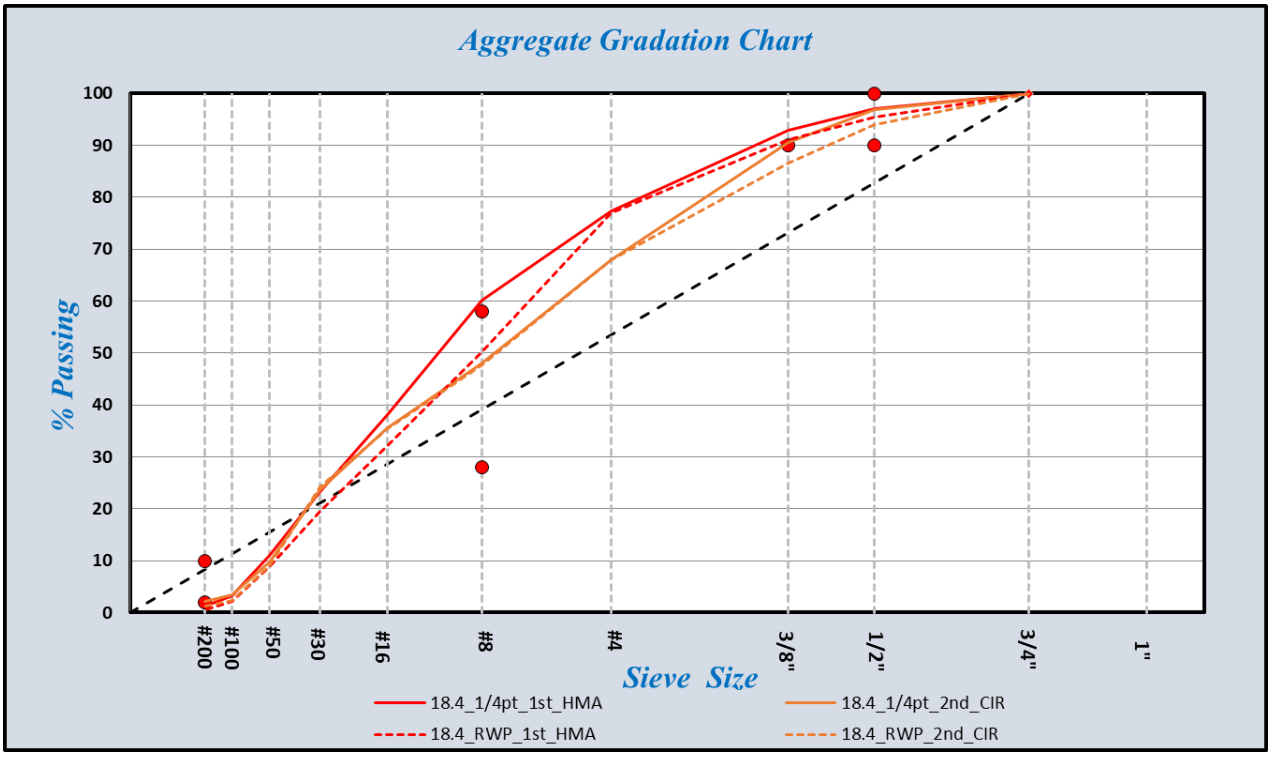

Figure 3-9. Aggregate gradation for MP 18.4

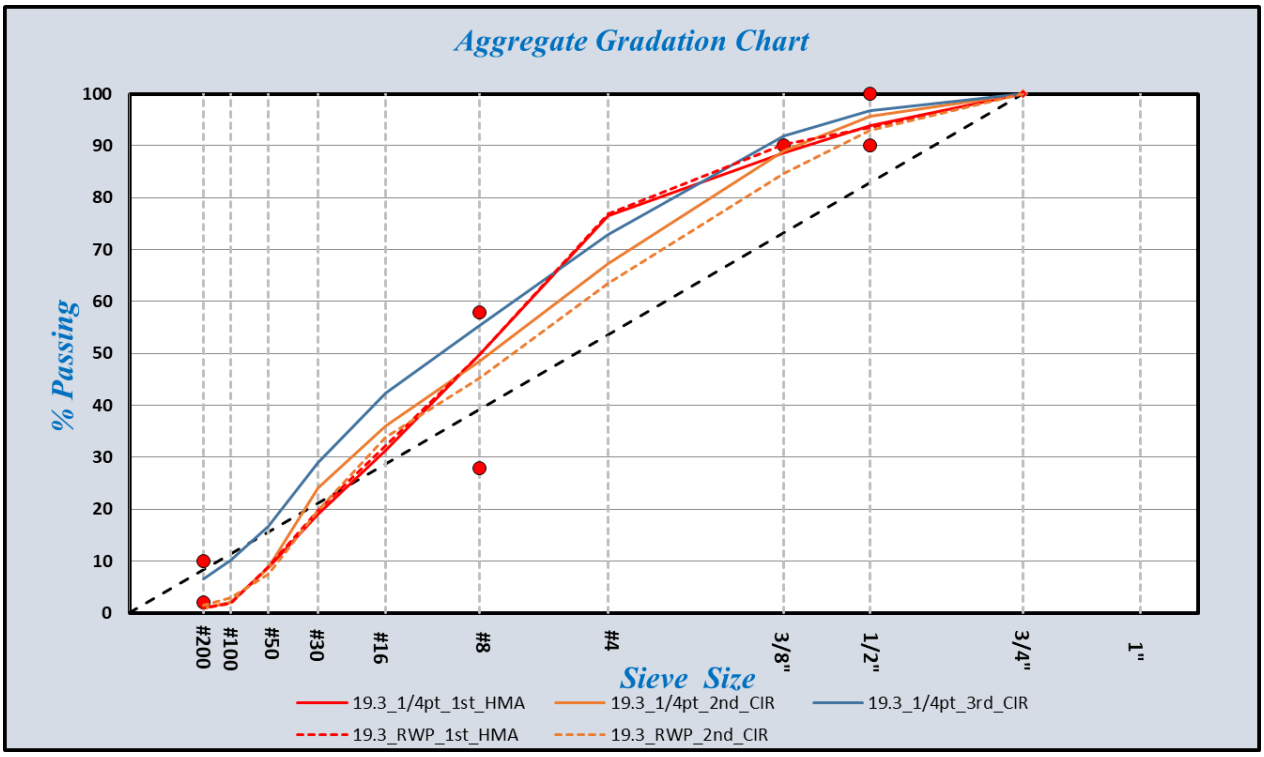

Figure 3-10. Aggregate gradation for MP 19.3

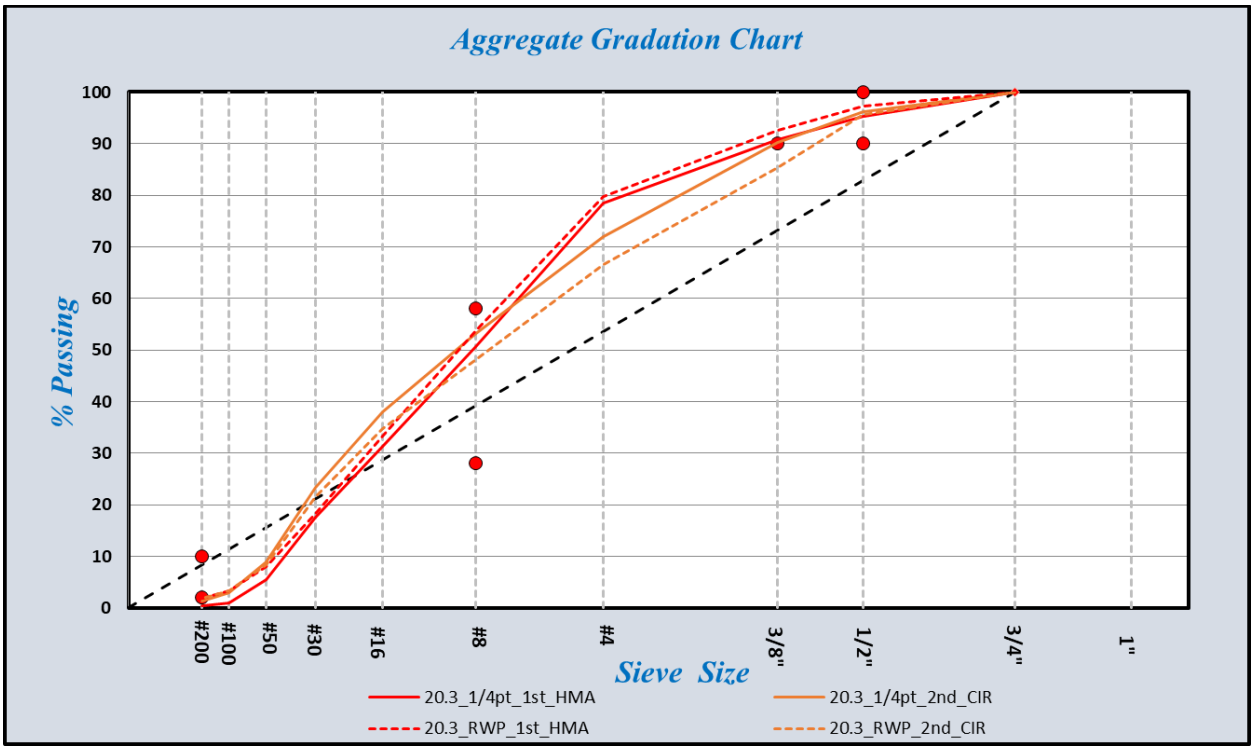

Figure 3-11. Aggregate gradation for MP 20.3

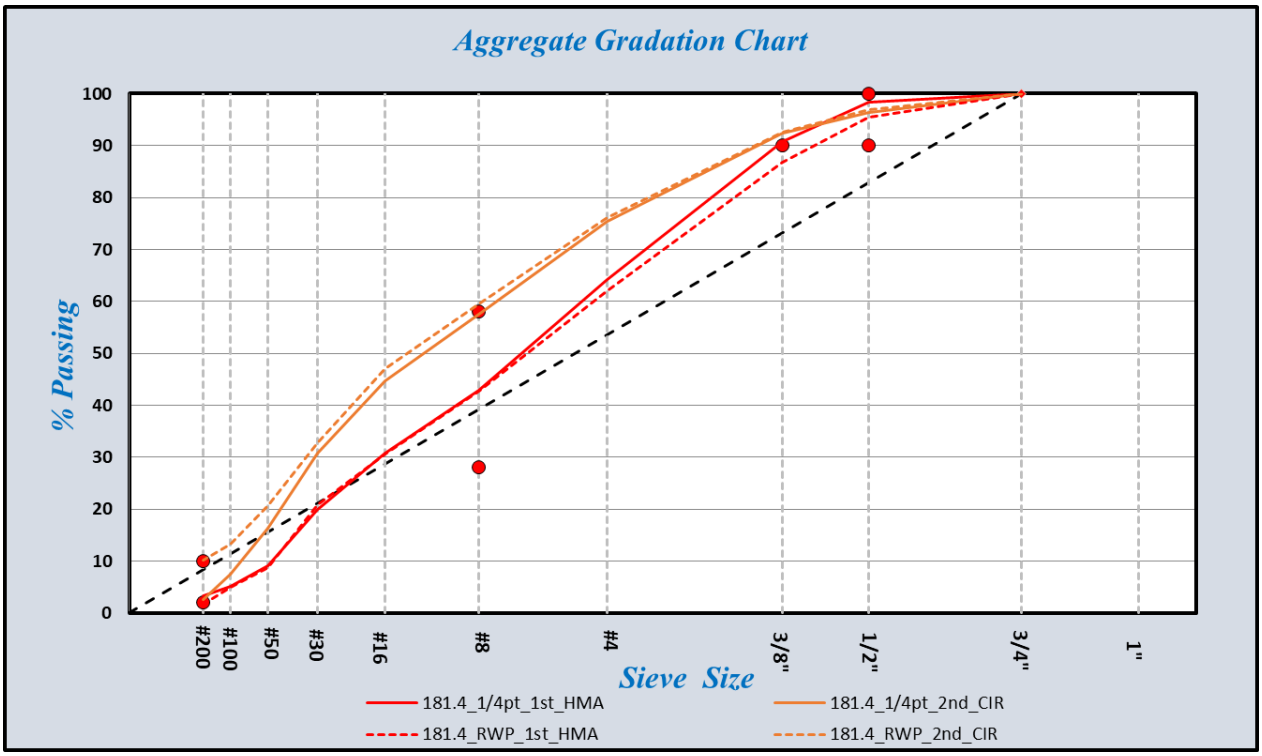

Figure 3-12. Aggregate gradation for MP 181.4

Based on the burn-off and sieve test results for the cores from all eight MP locations, the asphalt contents in the CIR layers were higher than those in the HMA layers and the aggregates of the CIR layers were finer than those of the HMA layers, as expected. However, there was no statistically significant difference in aggregate gradations and AC contents between the cores obtained from the right wheel path (RWP) and the cores obtained from between the wheel paths (¼ pt).

The FI values of both the CIR and HMA samples are plotted against binder contents in Figure 3-13. Based on the SCB test results of the CIR and HMA samples, increased binder contents produced higher FI values for both the CIR and HMA samples. However, the FI values of the CIR samples were significantly higher than those of the HMA samples. The average FI value of the CIR samples was 4.808, whereas that of the HMA samples was 1.422. It can be postulated that the HMA samples were aged more than the CIR samples, resulting in lower FI values and therefore the relative brittleness observed in the HMA samples.

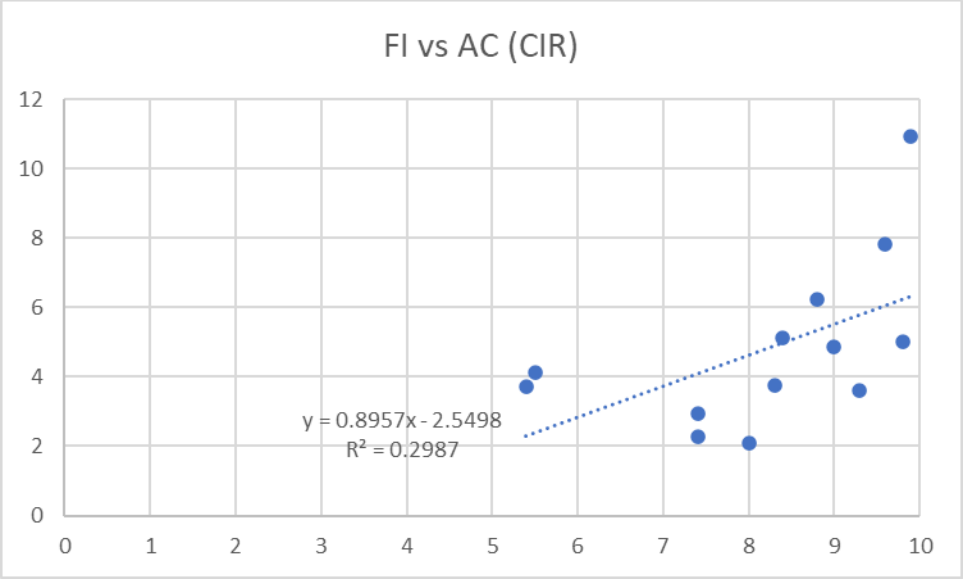

(a) FI values versus binder contents for CIR samples

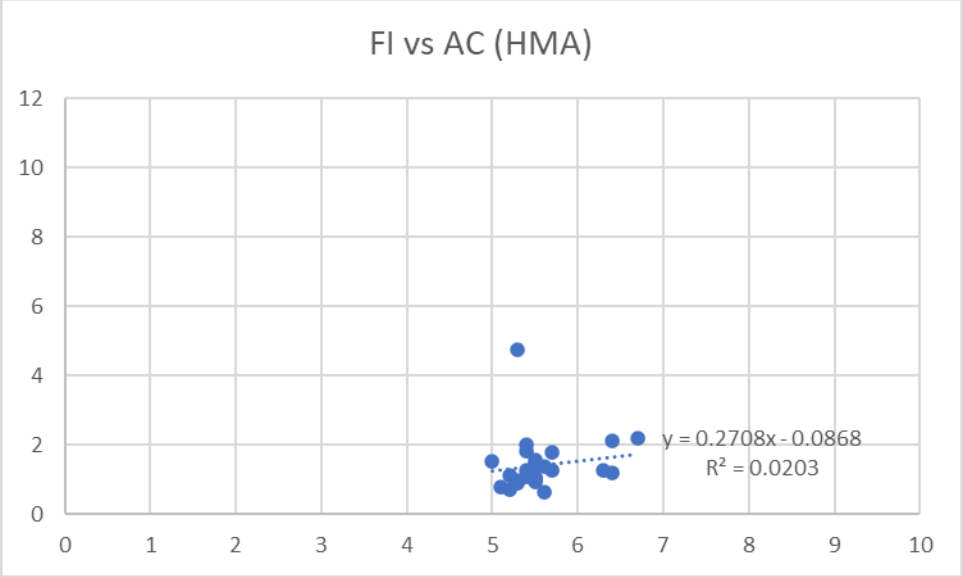

(b) FI values versus binder contents for HMA samples

Figure 3-13. Plots of FI values versus binder contents for (a) CIR and (b) HMA samples

4. FORENSIC INVESTIGATION OF CORES RECOVERED FROM CIR PROJECTS

This chapter documents the analysis of two poorly performing cold in-place recycled roadway sections in Iowa, one in Story County (R-38) and one in O'Brien County (L-36), and investigates why performance targets were not met. Field data for both projects were obtained from field cores as well as FWD testing. Cores were obtained from eight different locations in O'Brien County and seven in Story County (designated O1 through O8 for O'Brien County and S1 through S7 for Story County), while FWD data were obtained at 14 locations along the Story County project and 26 locations along the O'Brien County project. Design plan sets were obtained from the Iowa DOT and were used as a reference for the results obtained from the field.

The cores extracted from the two project locations were examined for compliance with the plan sets in terms of layer thickness, volumetrics, and gradations. Using project design thicknesses and core thicknesses, a pavement structural number was determined for the bound layers at each project location. This was compared with a structural number obtained from the FWD data. A structural strength index (SSI) was also calculated based on deflections obtained from the FWD data and compared to values that denoted the bounds for good and poor pavements. It was found that the FWD data indicated a much lower structural number than what was required by the traffic, subgrade support, and other design considerations; this could possibly be the cause of the premature failure observed for the two CIR projects.

The methodology used for this study and the results of the analysis are described in more detail in the following sections.

4.1. Examining Field Cores for Compliance with Plan Sets

The eight field cores from each project were visually inspected, and their volumetric properties were calculated in the laboratory and compared to the plan sets for any discrepancies. The samples were also inspected for damage and defects that could point to probable causes of pavement failure. Top-down cracking was noted on some of the samples, while others were broken along their length as a result of a crack that penetrated the entire depth of the core. Thicknesses were measured using Vernier calipers and compared to the design layer thickness in the plan sets. Discrepancies between actual field and plan set thicknesses were noted for the HMA lifts as well as the CIR layer. Visual inspection allowed for the detection of obvious signs of CIR failure and possibly its causes, such as cracking on samples with thinner HMA layers.

Samples were then tested for basic volumetric data, including the following:

- G_{mb} of the entire core
- G_{mm} and G_{mb} of the HMA layer
- G_{mm} and G_{mb} of the CIR layer
- Air void contents of the entire core and the individual layers
- Voids in mineral aggregate (VMA) values of the CIR and HMA layers
- Asphalt content and gradation

The cores were tested for the volumetric properties of the entire core and then cut at the boundaries of their respective layers to separate the CIR layers and the surface layers. The individual layers were then tested separately for volumetric properties, asphalt content, and gradation. Before the samples were broken up for the G_{mm} tests, indirect tensile strength tests were performed on the individual layers. Volumetric data obtained from the HMA layers are not displayed here because the HMA layers' volumetric properties were closely monitored both in the laboratory and in the field during construction and were eliminated as a contributing factor in the observed premature failure. In addition, daily reports from the HMA plant were examined to determine whether specifications were followed during placement. Of key interest was the volumetric and gradation data obtained from the CIR layers. Variability in the properties of the CIR layer has been known to cause performance problems, and hence examining the volumetric data for variability was relevant to this investigation.

4.2. Calculating Design Structural Number Based on AASHTO 1993 Design Equation

The second step in the analysis involved comparing the structural numbers obtained from the AASHTO 1993 design equation for the planned pavement thicknesses with those obtained from the FWD data from the field. Design calculations make use of the AASHTO 1993 design equation, which relates the number of 18 kip loads that a pavement will carry over its lifetime to the pavement structural number. The pavement structural number represents a pavement's load carrying capacity and depends on the thickness of the layers and the pavement material's layer coefficients. The pavement structural number is calculated as follows:

$$SN_{eff} = \sum_{i=1}^{n} a_i d_i \quad (4\text{-}1)$$

where a_i and d_i are the layer coefficient and the thickness of the i^{th} layer, respectively.

The AASHTO 1993 design equation for flexible pavements is as follows:

$$\log_{10} W_{18} = Z_r + S_o + 9.36 \times \log_{10}(SN+1) - 0.20 + \frac{\log_{10}(\frac{\Delta PSI}{4.2-1.5})}{0.40+\frac{1094}{(SN+1)^{5.19}}} + 2.32 \times \log_{10} M_R - 8.07 \quad (4\text{-}2)$$

The input variables for the AASHTO 1993 design equation are given in Table 4-1.

Table 4-1. Input variables for AASHTO 1993 design equation

Input Variable	Definition and Typical Value
Z_R	Standard normal deviation. Typically -1.64.
S_o	Combined standard error of prediction.
SN	Structural number. Total structural contribution of individual pavement layers.
ΔPSI	Change in the pavement serviceability index before rehabilitation is needed. Typically 1.7.
M_R	Subgrade resilient modulus.
W_{18}	Number of 18 kip ESALS that the pavement will be able to carry within its design life for a particular structural number, resilient modulus, and change in PSI.

The design comparison consisted of two steps, namely (1) the computation of an estimated structural number from PMIS data and the given plan sets and (2) the backcalculation of the required structural number based on the AASHTO 1993 design equation, which considers traffic, climatic, and soil data, as well as pavement design life and terminal conditions. While the traffic and performance data were sourced from the Iowa Pavement Management Program (IPMP) database and the pavement age and layer thicknesses were based on the individual project plan sets, the following reasonable assumptions for unknown data had to be made:

- The design life of the pavements was assumed to be 23 years, which is the typical life expectancy for CIR pavements in Iowa (Jahren and Chen 2007).
- The reliability for the project was assumed to be 75% due to the variable nature of CIR.
- The layer coefficients for the base layers were assumed to be 0.15 for a stone base, 0.26 for an asphalt-treated base, and 0.4 for the old HMA under the CIR layer, which are all reasonable best case scenarios; these assumptions were used to calculate the highest possible minimum structural number (AASHTO 1993).
- The standard deviation, S_o, for the AASHTO 1993 design equation was assumed to be 0.6 due to the large variability in CIR.
- The effective soil subgrade modulus was assumed to be 6,770 psi based on typical soils found in Iowa.

4.3. Using Pavement Resilient Modulus and Thickness Values Obtained from FWD Testing to Calculate a Structural Number for the Pavement

The FWD is a useful tool for the nondestructive evaluation of pavements. The FWD operates on the principle of correlating pavement deflections with the resilient moduli of both the bound layers and the subgrade. A fixed standard weight is dropped on the pavement, and sensors are located at fixed distances from the load to measure deflections. The resilient moduli of each pavement layer are iteratively backcalculated using the following process: the resilient moduli are first assumed and are then gradually changed to match the dimensions of the deflection basin

caused by a standard dropped weight with the dimensions of a theoretically calculated deflection basin.

FWD data were obtained for both roads, and the moduli of the bound layers and the subgrade were backcalculated. Other factors noted were the thickness of the bound layers, the ambient temperature, the temperature of the pavement, and the individual deflections under each sensor. The temperature data are relevant because they influence the analysis and interpretation of the FWD data.

The AASHTO 1993 design guidelines correlate the elastic modulus of the bound layers and their total thickness to the structural number of the pavement through the following equation:

$$SN_{eff} = 0.0045 \times D \times {E_p}^{0.333} \quad (4\text{-}3)$$

where SN_{eff} is the effective structural number of the bound layers, D is the total thickness of the bound layers above the subgrade, and E_p is the pavement modulus of all layers above the subgrade. The structural number of the pavement can be determined using the resilient modulus of the pavement layers based on the FWD data.

4.4. Developing an Equation for the Structural Number of the Pavement from FWD Deflections

Using a different approach, the structural number of the pavement layers can also be estimated from the structural index of the pavement (SIP). The SIP is the difference between the center deflection directly under the falling weight and the deflection measured at a distance of 1.5 times the depth D of the pavement, referred to in this methodology as $D_{1.5}$. Based on assumptions by past authors (Zhang et al. 2003), the deflections occurring at $D_{1.5}$ (which represent the measured deflection at 1.5 times the depth of the pavement as measured by the FWD) can be used to estimate the SIP of the pavement layers below a depth D from the surface. In contrast to obtaining the structural number from SSI and other deflection parameters, this correlation uses pavement thickness. In the present analysis, the calculated structural number from Equation 4-3 and the predicted structural number correlated from SIP and pavement depth were compared to the design structural number obtained from Equation 4-2. This methodology also attempted to quantify the layer coefficients of individual layers using the principles of SIP and the structural number obtained from this correlation. The SIP was calculated for the depth of a certain layer (AC), and the structural number and layer coefficients were then determined.

In a similar approach, Chang et al. (2002) proposed several parameters that could be indicators of pavement condition. Of particular interest was the curvature index $CI_i = D_i - D_{i+1}$, where D_i and D_{i+1} are deflections measured at consecutive sensors. The authors noted that the most important performance indicator for the upper pavement layers was the curvature index measured from the first two sensors, while the most important performance indicator for the base layers was the curvature index measured from the sensors located farthest from the weight, i.e.,

sensors 5 and 6. The curvature index is similar to the concept of the structural index of the pavement used in the calculation of the pavement structural number by Zhang et al. (2003).

The methodology used in the present analysis attempted to combine concepts from Zhang et al. (2003) and Chang et al. (2002) and propose an equation to calculate the structural number of the pavement as well as the respective structural contributions of the individual layers.

4.5. Results and Discussion

4.5.1. Visual Inspection and Preliminary Findings

The planned pavement sections for the two roadways featured in this analysis are shown in Figure 4-1.

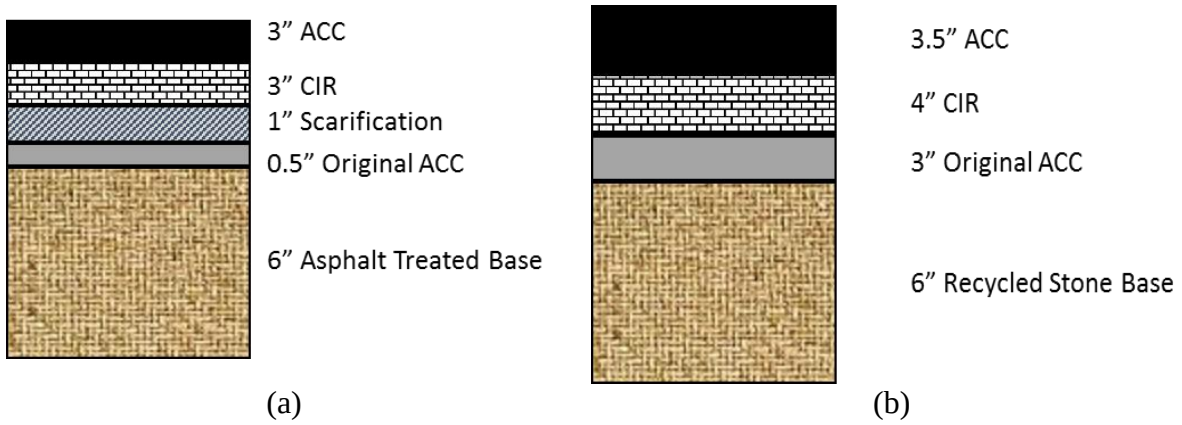

Figure 4-1. Typical cross sections for the (a) O’Brien County pavement and (b) Story County pavement

The plan sets for the Story County pavement section show a CIR depth of 4 in., while the plan sets for the O’Brien County pavement section show a 3 in. CIR layer. Examination of the cores revealed that all of the O’Brien County cores except O6 and O8 showed CIR thicknesses greater than or equal to the planned 3 in. thickness; however, all of the cores from Story County had CIR thicknesses less than the designed 4 in. thickness. Since CIR thickness has been shown to affect pavement performance (Pinto and Buss 2018), the designed thickness should be achieved in the field as accurately as possible. However, extenuating circumstances such as the risk of the recycling train breaking through the asphalt remaining after milling can sometimes limit the amount of existing asphalt that can be milled off, resulting in a rational decision to mill to a depth that is less than what was designed.

Table 4-2 compares the pavement layer thicknesses measured from the cores with the plan set requirements, along with notes on distresses. For O’Brien County, all cores that had HMA layers that were thinner than planned experienced top-down cracking. For Story County, the cores that had HMA layers that were more than 0.75 in. thinner than planned were cracked. Cores that have the notation “Core broken along length” broke before or during the extraction process.

Table 4-2. Compliance of cores with plan sets

Core No.	County	Core CIR Thickness (in.)	Design CIR Thickness (in.)	HMA Thickness (in.)	Design HMA Thickness (in.)	Core Remarks
O1	O'Brien	3.15	3	2.94	3	Top-down cracking
O2	O'Brien	3.7	3	2.88	3	Top-down cracking
O3	O'Brien	3.24	3	2.85	3	Top-down cracking
O4	O'Brien	3.47	3	3.50	3	
O5	O'Brien	3.13	3	3.38	3	
O6	O'Brien	2.8	3	2.93	3	Top-down cracking
O7	O'Brien	3.1	3	3.21	3	
O8	O'Brien	2.67	3	3.52	3	
S1	Story	3.85	4	3.25	3.5	
S2	Story	3.33	4	2.68	3.5	Core broken along length
S3	Story	3.24	4	3.24	3.5	
S4	Story	3.01	4	3.55	3.5	
S5	Story	3.62	4	2.57	3.5	Core broken along length
S6	Story	2.99	4	3.77	3.5	
S7	Story	4.04	4	2.58	3.5	Top-down cracking

Figures 4-2 to 4-4 show broken or cracked cores.

(a) (b)

Figure 4-2. Side view (a) and top view (b) of cracked O'Brien County core O3, which had a relatively thinner HMA lift thickness compared to cores with no distresses

(a) (b)

Figure 4-3. Story County core S2 broken along its length due to cracking

(a) (b)

Figure 4-4. Side view (a) and top view (b) of cracked Story County core S7, which had an insufficient HMA lift thickness

4.5.2. Volumetric and Material Properties of the Cores

The volumetric data for the cores are given in Table 4-3. Note that G_{mb} testing was executed in an open-top water bath, which may result in some inaccuracy. Also noteworthy is the relatively low air void content for the CIR layers of some of the cores. The air void content of CIR is typically in the range of 9% to 14% (Niazi and Jalili 2008).

Table 4-3. Preliminary volumetric data retrieved from the cores

Core No.	Location	G_{mb} (Whole Core)	Air Voids (CIR)	IDT (KPa)	CIR Thickness	HMA Thickness
O1	O'Brien	2.23	6.04	335.86	3.15	2.94
O2	O'Brien	2.26	8.98	458.80	3.70	2.88
O3	O'Brien	2.22	5.91	622.86	3.24	2.85
O4	O'Brien	2.23	4.68	311.51	3.47	3.50
O5	O'Brien	2.05	11.91	540.87	3.13	3.38
O6	O'Brien	2.09	8.18	390.39	2.80	2.93
O7	O'Brien	2.19	10.94	357.32	3.10	3.21
O8	O'Brien	2.29	12.97	449.09	2.67	3.52
S1	Story	2.42	5.83	310.78	3.85	3.25
S2	Story	Core broken			3.33	2.68
S3	Story	2.28	5.53	353.97	3.24	3.24
S4	Story	2.30	12.39	519.88	3.01	3.55
S5	Story	Core broken			3.62	2.57
S6	Story	2.33	5.65	232.42	2.99	3.77
S7	Story	2.03	5.37	274.02	4.04	2.58

The CIR layers in two of the cores from the Story County pavement broke after they were sawn to separate the CIR and other layers; therefore, G_{mb}, air void, and IDT measurements were not possible for these cores.

Target gradations were retrieved from the construction files for the two projects and compared to the gradations of the cores obtained from the field. The field gradations were obtained from the core samples after the asphalt content was determined with an asphalt analyzer provided by the Iowa DOT. Field gradations from the core samples from O'Brien County and Story County are given in Tables 4-4 and 4-5, respectively. Average field versus target gradations for O'Brien County and Story County are provided in Figures 4-5 and 4-6, respectively. Note that these gradations represent only the CIR layer of the core.

Table 4-4. Field gradation of samples from O'Brien County versus target gradation

Sieve No.	Field Gradation						Target
	O2	O3	O4	O5	O6	O7	
3/4 in.	100	100	100	100	100	100	100
1/2 in.	98	97	97	98	98	100	94
3/8 in.	94	94	92	95	95	97	83
#4	81	81	78	82	82	84	69
#8	65	65	65	66	66	68	57
#16	51	51	53	51	52	53	47
#30	38	38	41	38	39	39	32
#50	24	24	23	25	25	24	16
#100	16	16	13	17	17	16	5.6
#200	13	13	11	14	14	13	3.8

Table 4-5. Field gradation of samples from Story County versus target gradation

Sieve No.	Story County Actual					Target
	S1	S3	S4	S6	S7	
3/4 in.	100	100	100	100	100	100
1/2 in.	99	96	97	94	96	94
3/8 in.	96	91	92	86	92	89
#4	82	75	77	71	78	70
#8	66	62	65	59	65	53
#16	51	51	54	49	53	39
#30	39	40	42	38	41	24
#50	25	22	24	21	23	9.8
#100	17	14	14	10	14	5.1
#200	14	11	11	7.7	11	3.9

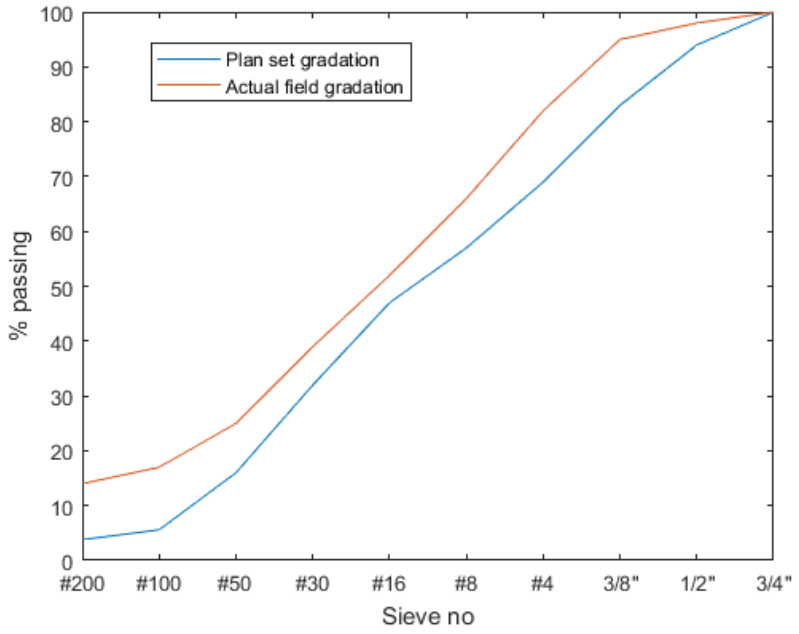

Figure 4-2. Average field versus target gradation for O'Brien County

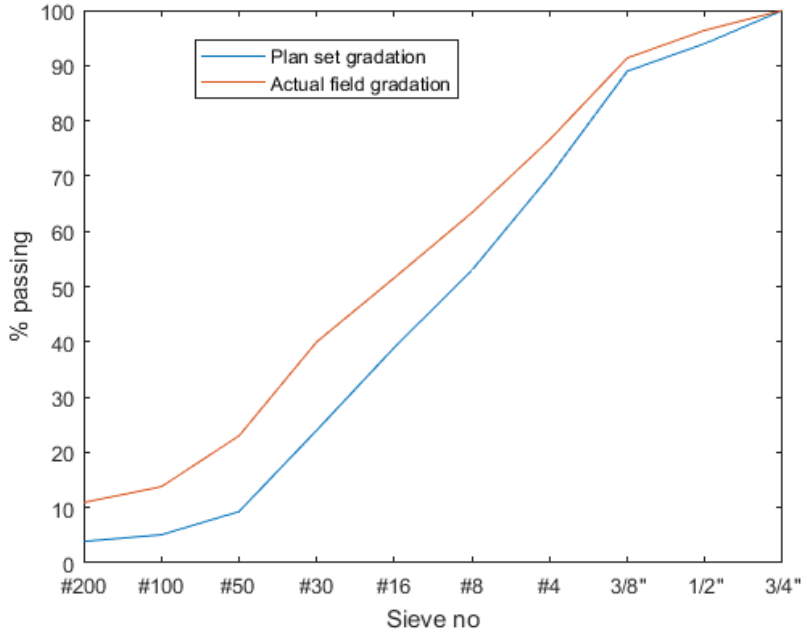

Figure 4-3. Average field versus target gradation for Story County

Table 4-4 shows a comparison of gradations between the field data from cores and the laboratory design guidelines for O'Brien County. There are noticeably more fines in the field gradation compared to the target, which is especially evident in Figure 4-5. The proportion of material passing the #200 sieve is as high as 13% for some cores, while the design maximum for this material is 3.8%. A high proportion of fines in a mix can be associated with a weaker CIR layer. Intended gradations for CIR are similar across most of Iowa and depend largely on the details of

milling, screening, and other mechanical processes used for CIR production. The gradation is also influenced to a large extent by the initial gradation of the aggregate that was used in the asphalt layer.

4.5.3. Design versus Observed Pavement Performance Using AASHTO 1993 Flexible Pavement Equations

The AASHTO 1993 flexible pavement design equation (Equation 4-1) makes use of the pavement structural number as the basis for validating a design thickness for an expected traffic loading. Recall that the structural number for a pavement is calculated by multiplying each pavement layer's thickness by the layer coefficient for each layer and summing the products. The design structural number of a pavement can be compared with the actual structural number by using the results of FWD tests. Because layer coefficients vary with the current pavement condition, for the sake of comparison typical layer coefficients found in the literature (hereafter referred to as "ideal" layer coefficients) were assumed in order to calculate an ideal structural number for each pavement section using the planned layer thicknesses for the pavement sections. For this analysis, the ideal layer coefficients for HMA and CIR were selected as 0.44 and 0.30, respectively. Layer coefficients of 0.1 were used for the base layers (AASHTO 1993). The ideal structural numbers along with the pavement thicknesses are shown in Table 4-6.

Table 4-6. Expected design structural number based on design thickness

County	HMA Layer 1	HMA Layer 2	CIR	HMA below Milled CIR	Base	Ideal SN	AADT	Log W18	Req SN
O'Brien	1.5	1.5	3	1.5	6	4.11	1,080	275621	2.73
Story	1.5	2	4	3	6	4.24	3,050	780551	3.25

For each pavement section, Table 4-6 compares the ideal structural number calculated based on the planned thicknesses with the minimum required structural number calculated from the AASHTO 1993 design equation, which considers traffic, subgrade resilient modulus, and reliability. The ideal structural number shown in Table 4-6 for each pavement section is larger than the minimum required structural number, and thus the planned thicknesses for both sections meet the AASHTO 1993 requirements for the expected loading. The ideal structural number for each pavement section is almost 30% to 50% higher than the required value. This additional margin in the structural number potentially mitigates concerns that would reasonably arise because actual layer thickness are less than those planned in some cases.

The AASHTO 1993 design equation also allows for backcalculation of structural numbers using FWD readings, the recorded pavement thicknesses, and the resilient moduli of the pavement layers. Using Equation 4-3, a structural number was calculated for each location where FWD testing was carried out. This structural number was compared to the minimum required structural number for the section based on the AASHTO 1993 flexible pavement design equation (Equation 4-2). The variation in structural numbers along both projects is shown in Figure 4-7, while Figure 4-8 shows the structural number verses the actual recorded pavement thickness obtained from FWD data.

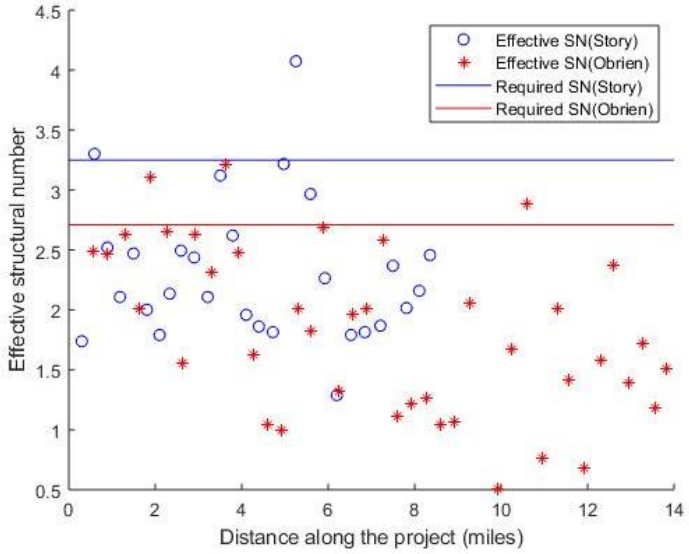

Figure 4-4. Effective pavement structural number versus distance along the project

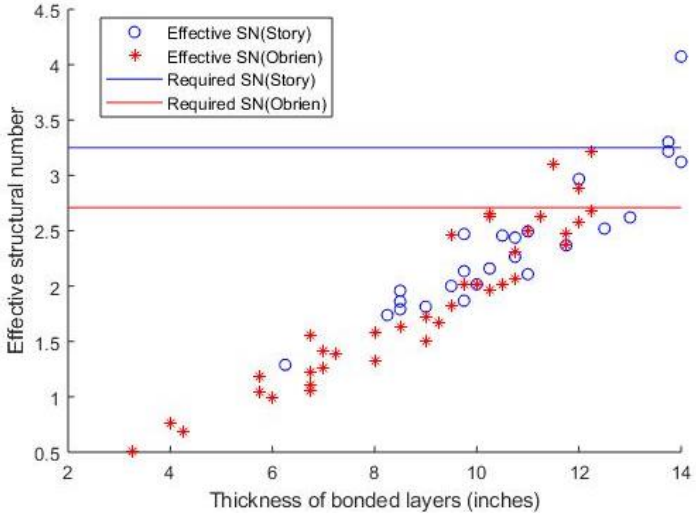

Figure 4-5. Effective structural number versus recorded pavement thickness

Figures 4-7 and 4-8 show that many sections along both CIR projects fail to meet the minimum required structural number and, in fact, are considerably lower than the required structural number calculated in Table 4-6. These results could indicate either layer thicknesses that were less than those required or a weak subgrade.

4.6. Conclusions

An investigation of pavement cores taken from both project locations led to a number of interesting observations, with the most obvious being the large discrepancy between the target and actual aggregate gradations. It was also noted that cores that exhibited top-down cracking or had broken along their length had insufficient HMA thickness. FWD analysis further backed the

hypothesis that the CIR layers did not meet design requirements due to a finer gradation than was desired. Based on the above observations, the following recommendations should be considered by local agencies when designing for CIR projects:

1. Take into consideration the original gradation of the HMA layer to be milled and recycled to ensure that the desired gradation can be achieved.
2. Ensure that pavement layer thicknesses are confirmed and that the required thicknesses on plans are followed.
3. Ensure that adequate support is available from subgrade/subbase layers.
4. A more detailed investigation into the effect of the materials used in CIR on the CIR layer coefficient is warranted in order to optimize CIR design. CIR may be achieved with a wide variety of stabilizers, which include lime, foamed asphalt, emulsified asphalt, portland cement, and a combination of cementitious and bituminous binders. A study that would tie the materials used in CIR to the end-product layer coefficient would be useful.
5. Visualizations comparing the effective versus required structural number can provide valuable insights into project performance. Figure 4-8 illustrates how actual thickness values from the field can impact structural number, which relates to pavement longevity.

Given the growing understanding of CIR design and construction, it can be expected that over time pavements rehabilitated with CIR will perform better as best practices for project selection improve. In working towards the goal of enhanced performance, it is important to understand why and how CIR pavements fail so that agencies can make better decisions and ensure better quality checks during cold in-place recycling projects.

5. GRADATIONS OF HIR AND CIR MILLINGS

In the last several decades, in-place recycling has been widely adopted for rehabilitating low-volume asphalt roads. Both hot in-place recycling (HIR) and CIR allow 100% reuse of reclaimed asphalt pavement. It is a common belief that, compared to CIR, HIR better retains the aggregate gradation of the original pavement without crushing the aggregates. However, no study has been performed that has compared the aggregate gradations of HIR millings against those of CIR millings.

For the investigation described in this chapter, HIR millings were collected from an HIR project on IA 22 in Wellman, Iowa. A total of four milling operations in sequence were performed, and 8 in. of the existing pavement was repaved. Loose HIR milling samples were collected after each milling and were sieved to determine whether the gradations differed among the four milling samples.

The aggregate gradations of the HIR millings were compared to those of CIR millings compiled from nine counties in Iowa (Kim et al. 2007, Kim et al. 2011).

5.1. Background

Asphalt recycling has become increasingly important because it is not only environmentally friendly but also more economical than traditional asphalt paving. In-place recycling involves removing and reusing the existing asphalt surface and repaving simultaneously. With the emphasis on fast pavement rehabilitation, both hot in-place and cold in-place recycling techniques have been widely used in the United States and around the world. HIR is normally used to correct surface distresses to a maximum of 2 in. deep. On the other hand, for CIR to be effective in mitigating reflective cracking, typically 4 in. of the existing asphalt pavement layer are normally recycled.

One of most important criteria for selecting pavements for in-place recycling is that the remaining pavement after milling must have a sufficient structural capacity to support the heavy recycling equipment used during construction. In-place recycling is not an appropriate rehabilitation strategy for pavements with major structural or base failures.

Chen et al. (2010) identified the optimum stiffness range of the CIR layer, as determined through FWD testing, for achieving long-term performance. Kim et al. (2010) evaluated CIR pavements in Iowa exhibiting long-term performance and estimated that they can last up to 25 years, which is significantly higher than the expected service life shown below for a typical CIR pavement with an HMA overlay.

Expected service lives for pavements treated with various HIR and CIR techniques are estimated in ARRA (2015). The expected service lives of various HIR techniques fall into the following ranges:

- HIR surface recycling with no surface treatment: service lives ranging from 2 to 4 years
- HIR surface recycling with surface treatment: service lives ranging from 6 to 10 years
- HIR remixing: service lives ranging from 7 to 14 years
- HIR remixing with HMA overlay: service lives ranging from 7 to 15 years
- HIR repaving: service lives ranging from 6 to 15 years

The expected service lives of various CIR techniques fall into the following ranges:

- CIR with surface treatment: service lives ranging from 6 to 8 years
- CIR with HMA overlay: service lives ranging from 7 to 15 years

5.2. HIR Project on IA 22 in Wellman, Iowa

A new hot in-place recycling system, MARS by Dustrol, was used to construct the HIR sections on IA 22 in Wellman, Iowa. A total of 12 mi of IA 22 were repaved using multiple-lift rejuvenation, where each lift was 2 in. thick. To recycle 8 in. of the existing pavement, four milling operations were performed. Loose milling samples were collected from each of the four milling piles and from the paver. To determine the extracted aggregate gradations, burn-off oven tests were performed on each milling sample. The resulting gradations of the extracted aggregates from each lift and the paver are plotted in Figure 5-1.

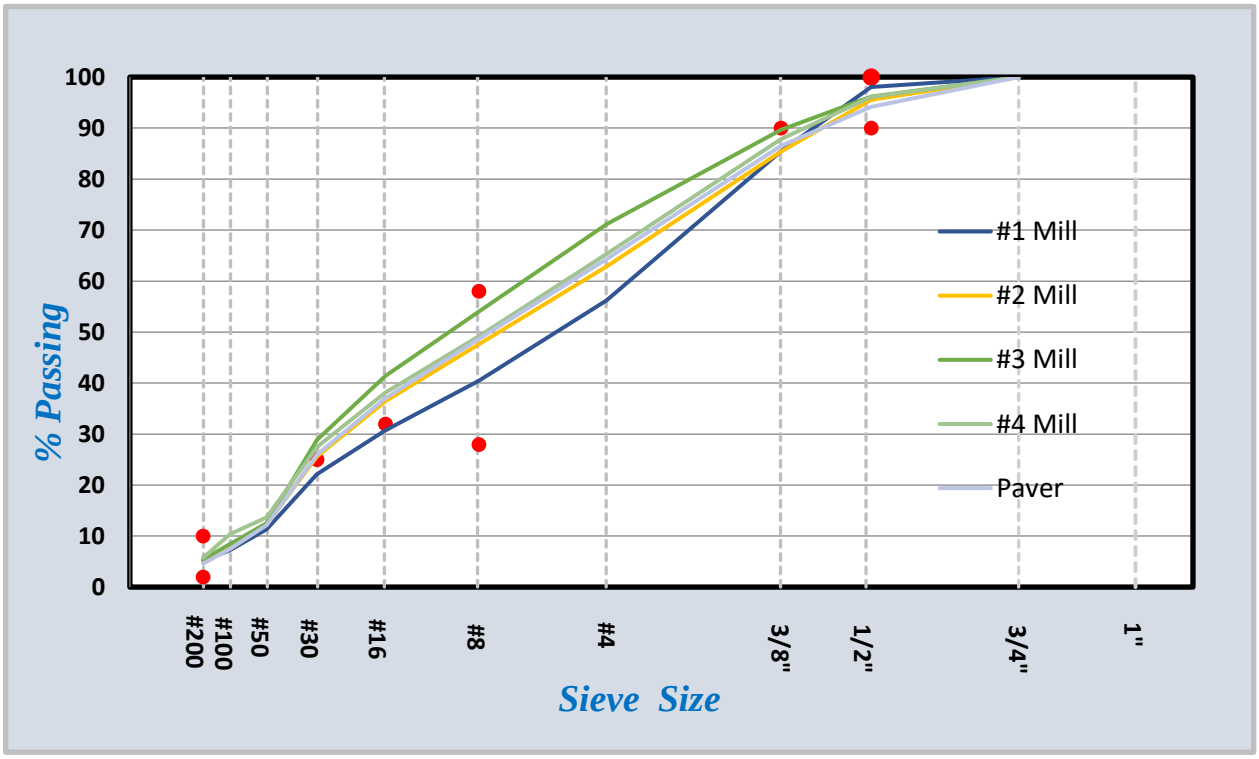

Figure 5-1. Gradations of four millings and the mixtures in the paver from the HIR section on IA 22

5.3. Comparison of CIR and HIR Aggregate Gradations

To compare the aggregate gradations of the HIR millings extracted from IA 22 against those of CIR millings, the gradations of CIR millings were compiled from previous research projects conducted in nine counties in Iowa (Kim et al. 2007, Kim et al. 2011). The gradations of these CIR millings are presented in Table 5-1, and the gradations of the HIR millings obtained from IA 22 are summarized in Table 5-2.

Table 5-1. Aggregate gradations of CIR millings from counties in Iowa

County in Iowa	25.0 mm	19.0 mm	12.5 mm	9.5 mm	4.75 mm	2.36 mm	1.18 mm	0.60 mm	0.30 mm	0.15 mm	0.075 mm
Muscatine	100	100	98	93	68	47	35	25	16	12	10.4
Webster	100	100	99	96	80	63	47	32	22	16	12.6
Hardin	100	100	98	93	75	62	50	37	21	12	9.7
Montgomery	100	100	99	96	80	61	47	35	22	15	12.7
Bremer	100	100	95	88	69	54	44	34	21	15	11.5
Lee	100	100	97	92	77	64	52	36	19	13	11.2
Wapello	100	100	98	91	69	50	39	29	18	14	11.2
Story	100	99.7	96.6	90.8	71.6	56.2	44.8	36.0	22.1	10.8	5.7
Clayon	100	100	97.3	92.9	74.0	59.4	45.5	34.6	23.0	12.5	4.4
Averages	**100**	**100**	**97.5**	**92.5**	**73.7**	**57.4**	**44.9**	**33.2**	**20.5**	**13.4**	**9.9**

Table 5-2. Aggregate gradations of HIR millings from IA 22

HIR Source	25.0 mm	19.0 mm	12.5 mm	9.5 mm	4.75 mm	2.36 mm	1.18 mm	0.60 mm	0.30 mm	0.15 mm	0.075 mm
IA 22 #1 milling	100	100	98	85.4	56.2	40.4	30.7	22.1	11.4	7.2	5.1
IA 22 #2 milling	100	100	95.6	85.4	62.9	47.6	36.4	25.6	12.3	7.5	5.1
IA22 #3 milling	100	100	96.2	89.7	71.2	54	41.4	28.9	12.5	8.5	5.4
IA 22 #4 milling	100	100	96.1	87.8	65.3	49.2	38.1	27.5	13.7	10.4	5.7
IA 22 paver	100	100	94.2	86.5	64.3	48.7	37	25.9	12.1	7.5	4.6
Averages	**100**	**100**	**96.0**	**87.0**	**64.0**	**48.0**	**36.7**	**26.0**	**12.4**	**8.2**	**5.2**

The average gradations of both the HIR and CIR millings are plotted in Figure 5-2. It should be noted that the percentage of fines passing the No. 200 sieve for the HIR millings was significantly less than the percentage for the CIR millings.

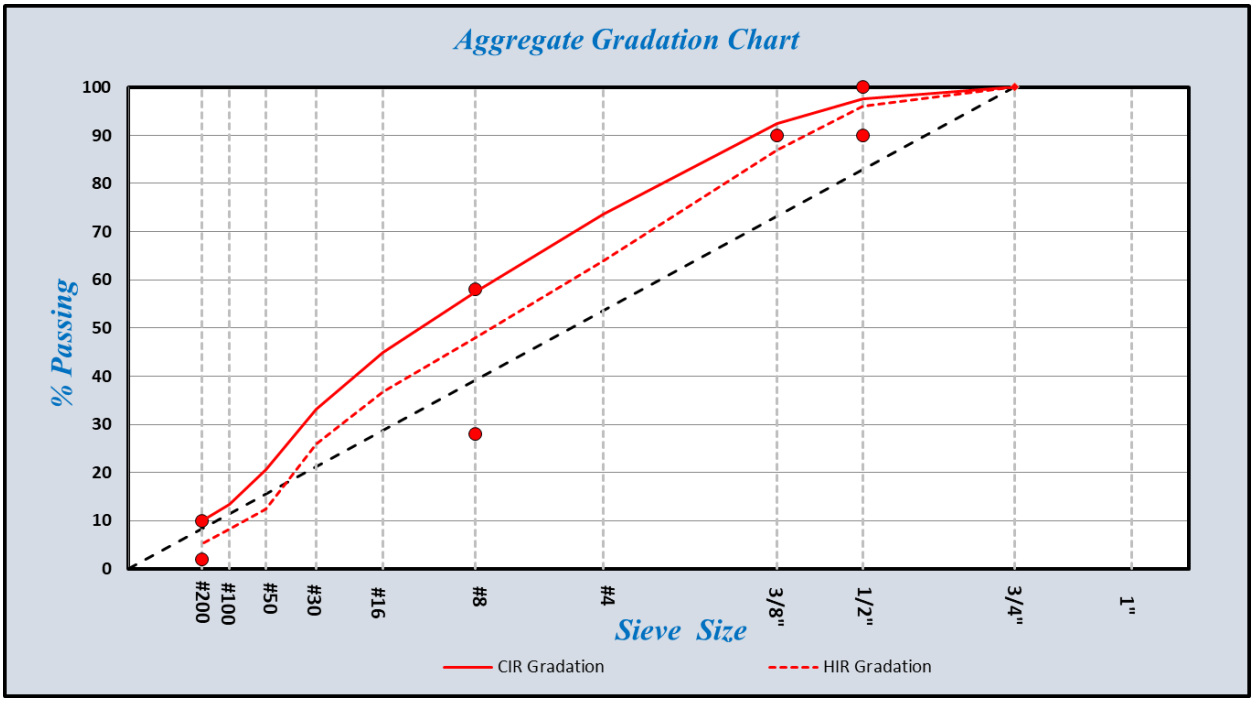

Figure 5-2. Average aggregate gradations of HIR versus CIR millings

5.4. Results of the Comparison of Aggregate Gradations from HIR and CIR Millings

The first part of this study investigated the gradation differences among milling samples obtained from an HIR recycling project on IA 22 in Wellman, Iowa. Based on the field samples collected after each lift of the rejuvenation treatment, no significant relationship was found among the different millings. To compare the gradations of HIR millings against those of CIR millings, CIR gradations from nine counties in Iowa were compiled from previous research projects (Kim et al. 2007, Kim et al. 2011). Overall, the average gradation of the HIR millings was coarser than that of the CIR millings.

6. SUMMARY, CONCLUSIONS, AND RECOMMENDATIONS

6.1. Summary

CIR is a useful rehabilitation strategy that has been in use for 30 to 40 years. Considerable knowledge has been documented in the literature regarding benefits, selection guidelines, mix design, construction, quality control, and quality assurance. This report documents a multifaceted investigation involving a data preparation procedure for the PMIS database, analysis of the PMIS database, field and laboratory testing to further investigate important results from the PMIS database analysis, a forensic case study of two low-volume roads to investigate why performance targets were not met, and an investigation comparing the aggregate gradations of millings from CIR and HIR projects.

Because the PMIS database has been incrementally developed over a number of years by various parties using various procedures, a data preparation effort was necessary. Data were converted to consistent units and excluded as necessary to facilitate analysis and to identify trends in pavement deterioration that would be helpful in drawing conclusions regarding pavement lifespans and common deterioration processes or in making recommendations for project selection. Exclusions were necessary to remove data that were recorded in years when observations were not made and to remove outliers that were likely caused by calibration, recording, or data processing errors. Further preparation was needed to separate pre- and post-construction data.

After the PMIS data were prepared, an initial analysis using descriptive statistics was conducted to identify overall trends. These trends suggested that in many cases noticeable deterioration occurred 10 to 15 years after CIR was performed. Rutting and cracking contributed the most to the deterioration. An analysis of traffic volumes showed considerable variation from year to year rather than a linear increase, which is often assumed for design. Statistical modeling was also conducted to obtain further insights. A survival analysis indicated that rutting was the distress that most quickly triggered concern for pavement condition. Further analysis presented in Figure 2-38 provided evidence that thicker CIR and HMA pavement layers in the pavement section were associated with less pavement distress for roads with higher traffic levels.

Laboratory testing was conducted on cores extracted from US 34 in Mills and Wapello Counties, Iowa. These cores were cut to isolate the HMA and CIR layers, and the resulting samples were fabricated into specimens for the semicircular bending test. The output of the test is a load versus displacement curve that can be processed to calculate the work of fracture; further calculations can be conducted to provide the flexibility index for each specimen. A higher flexibility index is expected to be associated with specimens that are more flexible and less likely to crack. When the HMA and CIR layers of the cores were compared, the HMA layers were found to have lower flexibility index values versus the CIR layers. This would suggest that for CIR projects with an HMA overlay, a more brittle HMA overlay layer covers a more flexible CIR layer. It was found that the asphalt contents among CIR cores varied noticeably and that CIR specimens with higher asphalt binder contents exhibited higher flexibility index values.

Combined with the knowledge obtained from the literature review for this project, the results of the core analysis suggest a possible deterioration process that can be proposed for pavements with CIR layers covered by HMA layers that have flexibility index values similar to those found in the laboratory study. Several references provide evidence that CIR layers have higher air void ratios and therefore act as a stress relieving layer and provide more flexibility compared to HMA. This flexibility mitigates crack propagation through the CIR layers, therefore making CIR a good treatment to address cracking distresses in pavements. While the higher air void content may enhance flexibility and mitigate crack propagation, it seems likely that a layer with a high air void content would also be susceptible to compaction rutting, especially when subjected to many heavy wheel loads. If covered with a less flexible HMA overlay, it would be expected that longitudinal cracks might form at the bottom of the wheel ruts as the HMA is forced to conform to the cross section of the now-rutted CIR layer. Members of the research team have noted longitudinal cracking in older CIR pavements that is consistent with the proposed deterioration process. This type of distress is especially noticeable at locations of likely end-of-load segregation for the surface layer. Although the proposed process is supported by the evidence gathered in this investigation, it should be noted that a causal relationship between the described process and CIR pavement deterioration has not been established with certainty.

The forensic case study of two low-volume CIR pavements provided three reasons why performance targets were not being met:

1. Pavement layer thicknesses were in many cases less than those required by the plans.

2. CIR gradations were finer than those specified by the plans or typical expectations in Iowa.

3. The pavement structure was inadequate given the likely strength of the subgrade.

The analysis of the field and laboratory study of cores obtained from US 34 led to the following observations:

1. Asphalt binder contents may vary significantly across a pavement's width due to a limited number of spraying nozzles and subsequent mixing operations for CIR with foamed asphalt.

2. Adding the correct amount of asphalt is important. Too much asphalt will the reduce air void content in the CIR layer, which will facilitate shearing of the pavement layer under heavy traffic loading. Too much asphalt will also reduce the aggregate-to-aggregate interlock, allowing aggregate particles to move past each other as they are separated by asphalt that shears under load. Too little foamed asphalt will increase the air void content in the CIR layer, which will cause wheel path cracking in the HMA overlay as compaction rutting of the CIR layer develops under heavy traffic loading.

The comparative analysis of CIR and HIR gradations was undertaken to investigate the common belief that HIR gradations are coarser than CIR gradations because less aggregate breakage occurs with HIR processing. In a meta-analysis of the gradations of HIR millings obtained from

IA 22 and CIR millings obtained from previous studies conducted in nine counties in Iowa, it was confirmed that the HIR millings were on average coarser than the CIR millings.

6.2. Conclusions

Conclusions are as follows:

- The analysis documented in Chapter 2 suggests the following:
    - Rutting is the deterioration mode that first causes concern regarding CIR pavement performance, with cracking being the second deterioration mode causing concern.
    - From an analysis standpoint, deterioration often becomes especially noticeable 10 to 15 years after CIR rehabilitation is performed.
    - Thicker CIR and HMA overlay layers have better performance outcomes compared to thinner ones.
- According to the field core recovery and laboratory testing results described in Chapter 3, the CIR layers are more flexible than the HMA overlay layers. This confirms other assessments in the literature.
- As discussed in Section 6.1, a possible reason for the observed distresses of rutting and wheel path cracking in the CIR layer is that the CIR layer has a relatively high air void content and differentially compacts in the wheel paths under heavy wheel loads. The less flexible HMA overlay layers longitudinally crack in the wheel paths as they are forced to conform to the CIR layers below.
- Based on the results from the forensic case studies of two low-volume roads discussed in Chapter 4, the roads did not meet performance expectations due to inadequate layer thicknesses, inadequate pavement structure given typical subgrade strengths, and CIR gradations that were finer than the target.

6.3. Recommendations

The following recommendations are made:

- Develop and provide researchers access to a tool encompassing the complete PMIS database with geospatially located data to facilitate future analysis efforts. A tool with prepared PMIS data from 1998 to the present would reduce data preparation efforts and provide a faster way for project data to be linked to performance data. Current data preparation efforts include converting units (metric versus imperial) to ensure uniform measurements, providing null

values for years when measurements were not made instead of repeating the values from the preceding year, and excluding obviously erroneous values. Input from likely users would be necessary to establish a procedure that will be valuable to a wide range of analysts, though it is likely that each analyst would nevertheless need to perform additional data preparation for each particular analysis.

- Consider project selection, design, construction, and maintenance strategies that address the proposed deterioration process described above, which is postulated to occur because the CIR layer is more flexible and compactable compared to the HMA overlay layer. Some possible strategies might include providing more flexible HMA layers that are less likely to crack, using rut filling treatments after ruts form, or limiting the use of CIR on roadways where heavy wheel loads might induce compaction rutting in the CIR layers.

- For low-volume roads where CIR is being considered as a rehabilitation strategy, increase predesign investigations of subgrade strength, increase quality control and quality assurance activities to ensure adequate pavement layer thickness, and adjust expectations for the structural strengths of CIR layers where milling gradations are finer than what is typically recommended.

- For HIR construction, investigate changes in project selection, design, and construction practices in light of the fact that HIR millings have been found to be on average coarser than CIR millings.

- For CIR using foamed asphalt, more evenly distribute and mix asphalt binder across the width of the pavement to ensure a more consistent asphalt binder content.

- Consider CIR and HIR mixture designs to optimize the binder content based on the actual anticipated gradation.

REFERENCES

AASHTO. 1993. *AASHTO Guide for the Design of Pavement Structures*. Vol. 1. American Association of State Highway and Transportation Officials, Washington DC.

Alkins, A., B. Lane, and T. Kazmierowski. 2008. Sustainable pavements: environmental, economic, and social benefits of in situ pavement recycling. *Transportation Research Record: Journal of the Transportation Research Board*, Vol. 2084, pp. 100–103.

ARRA. 2015. *Basic Asphalt Recycling Manual, 2nd Edition*. Asphalt Recycling and Reclaiming Association, Glen Ellyn, IL.

Berthelot, C., and R. Gerbrandt. 2002. Cold in-place recycling and full-depth strengthening of clay-till subgrade soils results with cementitious waste products in northern climates. *Transportation Research Record: Journal of the Transportation Research Board*, Vol. 1787, No. 1, pp. 3–12.

Buss, A., M. G. Mercado, and S. Schram. 2017. Long-term evaluation of cold-in-place recycling and factors influencing performance. *Journal of Performance of Constructed Facilities*, Vol. 31, No. 3.

Castedo, F., L. Humberto, and L. E. Wood. 1983. Stabilization with foamed asphalt of aggregates commonly used in low-volume roads. *Transportation Research Record: Journal of the Transportation Research Board*, Vol. 898, pp. 297-302.

Chang, J.-R., J.-D. Lin, W.-C. Chung, and D.-H. Chen. 2002. Evaluating the structural strength of flexible pavements in Taiwan using the falling weight deflectometer. *International Journal of Pavement Engineering*, Vol. 3, No. 3, pp. 131–141.

Chen, D., C. T. Jahren, H. "David" Lee, R. C. Williams, S. Kim, M. Heitzman, and J. "Joe" Kim. 2010. Effects of recycled materials on long-term performance of cold in-place recycled asphalt roads. *Journal of Performance of Constructed Facilities*, Vol. 24, No. 3, pp. 275–280.

Chen, C., R. C Williams, M. G. Marasinghe, J. C. Ashlock, O. Smadi, S. Schram., and A. Buss. 2015. Assessment of composite pavement performance by survival analysis. *Journal of Transportation Engineering*, Vol. 141, No. 9.

Cox, B. C., and I. L. Howard. 2015. Merits of asphalt concrete durability and performance tests when applied to cold in-place recycling. *2015 International Foundations Congress & Equipment Exposition (IFCEE)*, Vol. GSP 256, pp. 369–379.

Cox, B. C., and I. L. Howard. 2016. Cold in-place recycling characterization for single-component or multiple-component binder systems. *Journal of Materials in Civil Engineering*, Vol. 28, No. 11.

Cross, S. A., and Y. Jakatimath. 2007. *Evaluation of Cold In-Place Recycling for Pavement Rehabilitation of Transverse Cracking on US 412*. Oklahoma Department of Transportation, Oklahoma City, OK.

Cross, S. 1999. Experimental cold in-place recycling with hydrated lime. *Transportation Research Record: Journal of the Transportation Research Board*, Vol. 1684, pp. 186–193.

Croteau, J.-M., and J. K. Davidson. 2001. A twenty-year performance review of cold in-place recycling in North America. *Proceedings of the Annual Conference of the Canadian Technical Asphalt Association*, pp. 383–406.

Diefenderfer, B. K., and A. K. Apeagyei. 2014. *I-81 In-Place Pavement Recycling Project*. Virginia Department of Transportation, Richmond, VA.

Forsberg, A., E. Lukanen, and T. Thomas. 2002. Engineered cold in-place recycling project: Blue Earth County State Aid Highway 20, Minnesota. *Transportation Research Record: Journal of the Transportation Research Board*, Vol. 1813, pp. 111–123.

Hunsucker, D. Q., D. L. Allen, and R. C. Graves. 2017. *In-Place Recycling and Reclamation of Asphaltic Concrete Pavements in Kentucky*. KTC-17-25/SPR17-536-1F. Kentucky Transportation Cabinet, Frankfort, KY.

Iowa DOT. 2022. Section 2318. Cold In-Place Recycled Asphalt Pavement. Iowa Department of Transportation Standard Specifications with GS-15015 Revisions, October 18, 2022. https://iowadot.gov/erl/archiveoct2022/GS/content/2318.htm.

Jahren, C. T., B. Cawley, and K. Bergeson. 1999a. Performance of cold in-place recycled asphalt cement concrete roads. *Journal of Performance of Constructed Facilities*, Vol. 13, No. 3, pp. 128–133,

Jahren, C. T., B. Cawley, B. Ellsworth, and K. L. Bergeson. 1998. Review of cold in-place asphalt recycling in Iowa. *Crossroads 2000, August 19–20, Ames, IA*. Center for Transportation Research and Education, Ames, IA.

Jahren, C. T., B. J. Ellsworth, and K. Bergeson. 1999b. Constructability test for cold in-place asphalt recycling. *Journal of Construction Engineering Management*, Vol. 125, No. 5, pp. 325–329.

Jahren, C., and D. Chen. 2007. *Evaluation of Long-Term Field Performance of Cold In-Place Recycled Roads: Summary Report*. Institute for Transportation, Ames, IA.

Jahren, C. T., J. J. Yu, R. C. Williams. 2016. *Alternate Design Methods to Renew Lightly Traveled Paved Roads*. Minnesota Department of Transportation, St. Paul, MN.

Kim, Y., S. Im, and H. "David" Lee. 2011. Impacts of curing time and moisture content on engineering properties of cold in-place recycling mixtures using foamed or emulsified asphalt. *Journal of Materials in Civil Engineering*, Vol. 23, No. 5, pp. 542–553.

Kim, Y., and H. "David" Lee. 2006. Development of mix design procedure for cold in-place recycling with foamed asphalt. *Journal of Materials in Civil Engineering*, Vol. 18, No. 1, pp. 116–124.

Kim, Y., and H. "David" Lee. 2012. Performance evaluation of cold in-place recycling mixtures using emulsified asphalt based on dynamic modulus, flow number, flow time, and raveling loss. *KSCE Journal of Civil Engineering*, Vol. 16, pp 586–593.

Kim, Y., H. "David" Lee, and M. Heitzman. 2007. Validation of new mix design procedure for cold in-place recycling with foamed asphalt. *Journal of Materials in Civil Engineering*, Vol. 19, No. 11, pp. 1000–1010.

Kim, J. "Joe," H. "David" Lee, C. T. Jahren, M. Heitzman, and D. Chen. 2010. Long-term field performance of cold in-place recycled roads in Iowa. *Journal of Performance of Constructed Facilities*, Vol. 24, No. 3, pp. 265–274.

Lee, H. "David," Y. Kim, and S. Im. 2009. *Examination of Curing Criteria for Cold In-Place Recycling; Phase 2: Measuring Temperature, Moisture, Deflection and Distress from CIR Test Section*. Public Policy Center, University of Iowa, Iowa City, IA.

Mallela, J., H. L. Von Quintos, and K. L. Smith. 2006. *Performance Evaluation of Cold In-Place Recycling Projects in Arizona*. Arizona Department of Transportation, Phoenix, AZ.

Modarres, A., M. Rahimzadeh, and M. Zarrabi. 2014. Field investigation of pavement rehabilitation utilizing cold in-place recycling. *Resources, Conservation, and Recycling*, Vol. 83, pp. 112–120.

Moore, T., M. K. Farashah, M. Esenwa, S. Varamini, and A. S. Kucharek. 2017. *Twelve-Year Performance Review of Bloomington Road (York Region Road 40) Rehabilitation Using Cold In-Place Recycling and a 6.7 mm Fine Stone Mastic Asphalt*. Canadian Technical Asphalt Association, West Kelowna, BC.

Morian, D. A., J. Oswalt, and A. Deodhar. 2004. Experience with cold in-place recycling as a reflective crack control technique: Twenty years later. *Transportation Research Record: Journal of the Transportation Research Board*, Vol. 1869, pp. 47–55.

Niazi, Y., and M. Jalili. 2008. Effect of portland cement and lime additives on properties of cold in-place recycled mixtures with asphalt emulsion. *Construction and Building Materials*, Vol. 23, No. 3, pp. 1338-1343.

Pinto, I., and A. Buss. 2018. Layer coefficients of cold in-place recycled layers from performance data. *International Journal of Pavement Engineering*, Vol. 21, No. 3, pp. 304–310.

Prather, M., and J. Wielinski. 2016. The US 40 INDOT cold in-place recycling project. Purdue Road School, March 8, West Lafayette, IN. https://docs.lib.purdue.edu/roadschool/2016/presentations/16/.

Rogge, D. F., T. V. Scholz, and R. G. Hicks. 1990. *In-Depth Study of Cold In-Place Recycled Pavement Performance*. Vols. 1 and 2. FHWA-OR-RD-91-02 A&B. Oregon Department of Transportation, Salem, OR.

Sanjeevan, S., M. Piratheepan, E. Y. Hajj, and A. K. Bush. 2014. Cold in-place recycling in Nevada: Field performance evaluation over the past decade. *Transportation Research Record: Journal of the Transportation Research Board*, Vol. 2456, No. 1, pp. 146–160.

Scholz, T. V, R. G. Hicks, D. F. Rogge, and D. Allen. 1991a. Use of cold in-place recycling on low-volume roads. *Transportation Research Record: Journal of the Transportation Research Board*, Vol. 1291, pp. 239–252.

Scholz, T., D. F. Rogge, R. G. Hicks, and D. Allen. 1991b. Evaluation of mix properties of cold in-place recycled mixes. *Transportation Research Record: Journal of the Transportation Research Board*, Vol. 1317, pp. 77–89.

Sebaaly, P., G. Bazi, E. Hitti, D. Weitzel, and S. Bemanian. 2004. Performance of cold in-place recycling in Nevada. *Transportation Research Record: Journal of the Transportation Research Board*, Vol. 1896, pp. 162–169.

Stroup-Gardiner, M. 2012. Selection guidelines for in-place recycling projects. *Transportation Research Record: Journal of the Transportation Research Board*, Vol. 2306, pp. 3–10.

Thomas, T., and A. Kadrmas. 2003. Performance-related tests and specifications for cold in-place recycling: Lab and field experience. 82nd Annual Meeting of the Transportation Research Board, January 12–16, Washington, DC.

Wood, L. E., T. D. White, and T. B. Nelson. 1988. Current practice of cold in-place recycling of asphalt pavements. *Transportation Research Record: Journal of the Transportation Research Board*, Vol. 1178, pp. 31–37,

Woods, A., Y. Kim, and H. Lee. 2012. Determining timing of overlay on cold in-place recycling layer: Development of a new tool based on moisture loss index and in situ stiffness. *Transportation Research Record: Journal of Transportation Research Board*, Vol. 2306, pp. 52–61.

Zhang, Z., G. Claros, L. Manuel, and I. Damnjanovic. 2003. Evaluation of the pavement structural condition at network level using falling weight deflectometer (FWD) data. 82nd Annual Meeting of the Transportation Research Board, January 12–16, Washington, DC.

THE INSTITUTE FOR TRANSPORTATION IS THE FOCAL POINT FOR TRANSPORTATION AT IOWA STATE UNIVERSITY.

InTrans centers and programs perform transportation research and provide technology transfer services for government agencies and private companies;

InTrans contributes to Iowa State University and the College of Engineering's educational programs for transportation students and provides K–12 outreach; and

InTrans conducts local, regional, and national transportation services and continuing education programs.

IOWA STATE UNIVERSITY

Visit **InTrans.iastate.edu** for color pdfs of this and other research reports.